IOP Conference Series:
Earth and Environmental Science

2019 International Conference on Environment and Ocean Engineering (ICEOE 2019)

June 7-9, 2019
Xiamen, China

ISSN: 17551307
E-ISSN: 17551315

IOP Conf. Series: Earth and Environmental Science **369** (2019) 011001 doi:10.1088/1755-1315/369/1/011001

PREFACE

It is our great pleasure to welcome all of you to 2019 International Conference on Environment and Ocean Engineering (ICEOE 2019) which was held on June 7-9, 2019 in Xiamen Ocean Vocational College, Xiamen, China. ICEOE 2019 is dedicated to issues related to Environment and Ocean Engineering.

ICEOE 2019 is organized by Xiamen Ocean Vocational College and Xiamen University of Technology, assisted by International Society for Environmental Information Sciences (ISEIS), Hong Kong Chemical, Biological & Environmental Engineering Society (HKCBEES), Environment and Agriculture Society (EAS), Fujian Smart City Association.

ICEOE 2019 is highlighted by several professional speakers. Prof. Caterina Valeo from University of Victoria, Canada; Prof. Yongping Li from Xiamen University Of Technology, China; Prof. Lixiao Zhang form School of Environment, Beijing Normal University, China; Prof. Guangwei Huang from Sophia University, Tokyo, Japan; Prof. R. J. (Dick) Haynes from The University of Queensland, St Lucia, Queensland, Australia; Prof. Gordon Huang from University of Regina, Canada had attended the conference as keynote speakers.

There were five sub-sessions with different topics: Modeling of Environmental Systems, Environmental Pollution Control, Environmental Management and Planning, Workshop on Environment, Water and Energy, Forum on South-South Sustainable Development. It was a golden opportunity for students, researchers and engineers to interact with the experts and specialists to get their advice or consultation on technical matters, dissemination and marketing strategies.

This proceeding presents a selection from papers submitted to the conference from universities, research institutes and industries. It has five chapters with topic: Coastal Engineering, Deep Sea Engineering, Ship Engineering, Utilization of Marine Resources, Water Pollution Control. All papers were subjected to peer-review by conference committee members and international reviewers. The papers were selected based on high quality and relevancy to the conference scope.

We would also express our sincere gratitude to organizing committee and the volunteers who had dedicated their time and efforts in planning, promoting, organizing and helping the conference.

Changping Chen
Xiamen Ocean Vocational College, China
2019-09-20

IOP Conf. Series: Earth and Environmental Science **369** (2019) 011002 doi:10.1088/1755-1315/369/1/011002

Conference Committee

Conference Chair

Gordon Huang, International Society for Environmental Information Sciences

Yongping Li, Beijing Normal University; Xiamen University of Technology, China

Technical Program Committee

Chairs

Changping Chen, Xiamen Ocean Vocational College, China

R. J. Haynes, The University of Queensland, St Lucia, Queensland

Members

Vaid Bakshi Hardeep, Nanjing University of Information Science and Technology, China

Francesco Zirilli, Universita di Roma La Sapienza, Italy

Carlos Chastre, NOVA University of Lisbon, Portugal

Moshe Gophen, Migal-Galilee Technology Center, Israel

Srinivasan Chandrasekaran, Indian Institute of Technology Madras, India

Maria Rosa Mosquera Losada, Universidade de Santiago de Compostela, Spain

Jean-Pierre Hermand, Université libre de Bruxelles, Belgium

Gang Li, Chinese Academy of Sciences, China

Petchporn Chawakitchareon,Chulalongkorn University, Thailand

Jitendra Sangwai, Indian Institute of Technology Madras, India

Cheng Su, Zhejiang University, China

Myriam Lopes, Universidade de Aveiro, Portugal

Hugo G. Nami, Universidad de Buenos Aires, Argentina

Mohammad Reza Khosravi, Shiraz University of Technology, Iran

Kaveh Ostad-Ali-Askari, Islamic Azad University, Iran

Galina Baturova,Moscow Technological University (MIREA),Russia

IOP Conf. Series: Earth and Environmental Science **369** (2019) 011004 doi:10.1088/1755-1315/369/1/011004

Peer review statement

All papers published in this volume of *IOP Conference Series: Earth and Environmental Science* have been peer reviewed through processes administered by the proceedings Editors. Reviews were conducted by expert referees to the professional and scientific standards expected of a proceedings journal published by IOP Publishing.

Table of Contents

Chapter 1: Coastal Engineering

Chapter 2: Deep Sea Engineering

Chapter 3: Ship Engineering

Chapter 4: Utilization of Marine Resources

Chapter 5: Water Pollution Control

Chapter 1:
Coastal Engineering

IOP Conf. Series: Earth and Environmental Science **369** (2019) 012001 doi:10.1088/1755-1315/369/1/012001

WaveNet: learning to predict wave height and period from accelerometer data using convolutional neural network

Tong Liu[1], Yongle Zhang[1], Lin Qi[1*], Junyu Dong[1], Mingdong Lv[2], and Qi Wen[2]

1 Ocean University of China, Qingdao, China
2 Haiyan Electronics Co Ltd, Qingdao, China
E-mail: qilin @ouc.edu.cn

Abstract. Inertial sensors carried by buoys, such as accelerometers, are widely used in wave characteristics measurement. Traditional methods usually employ numerical integration on the accelerate data for wave height, where the "drifting" errors are intractable. In this paper we propose a novel method to predict wave height and period using machine learning approach, specially a convolutional neural network. The end-to-end 1D convolutional neural network named WaveNet predicts wave height and period from the raw acceleration data directly. We designed a simple device to simulate the motion of the buoy in the wave, and used it to collect data for training and testing our model. The results of the proposed method were compared with traditional numerical integration method and found that the proposed model outperforms existing method in outputting more accurate wave height and period.

1. Introduction

Wave characteristics are important in oceanography and coastal engineering research, such as wave energy exploitation, sediment movement measurements, port design and soil erosion. Traditionally, there are two kinds of method in wave prediction. One is based on the numerical model of wave generation and dissipation physical process. The development and research are carried out on the basis of wave theory, such as SWAN [1], [2], WAM [3], [4], Wave Watch III [5]. Recently, researchers have shown an increased interest in data-driven method for wave prediction, which is based on previous empirical models of real-time or quasi-real-time data for meteorological, wave data or online buoy[6], [7]. These methods include neural networks[8], [9], [10], [11], time series models, genetic algorithms[12], [13], [14], support vector machines[15], Decision tree [16] and model combining numerical model with neural network[17], [18], etc. The former kind of method is often used in regional prediction [19] while the later one is mainly used for point forecasting.

Atmospheric modes and wave numerical models need to solve complex physical equations, and the computational cost is large. The data-driven model uses the buoy online monitoring data for real-time updating. It is based on the analysis and research of different state parameters, which can be used to solve the nonlinear function problem of numerical prediction. Recently, with the construction of online buoy monitoring networks, researchers have shown an increased interest in data-driven model predictions.

However, in a series of models for wave prediction based on data-driven patterns, most of the research data focus on past meteorological and wave data. These wave data used in experimental research is usually needed to calculate from the complex numerical model. For example, a wave height prediction model based on a data-driven pattern uses wave height values from previous period of time to predict the wave height values for the next period of time.

In the numerical model, the majority of surface deployed wave buoys use three dimensional acceleration signals processed using a double integration method to derive wave statistics. Such marine instruments are highly accurate but can be prohibitively expensive in terms of the initial purchasing, deployment/retrieval costs and servicing. Field measurements of wave parameters are typically derived using either pressure sensors, wave radar, acoustic sensors or motion sensing wave buoys. Wave buoys derive wave statistics by tracking the surface of the water using accelerometers.

Recently, deep learning methods have received amazing success in pattern recognition and machine learning application domains due to their outstanding capability to learn complex and robust representations. Convolutional networks, also known as CNNs, are a specialized kind of network for processing data that has a known grid-like topology. Examples include time-series data, which can be thought of as 1D grid taking samples at regular time intervals, and image data, which can be thought of a 2D grid of pixels. They have been shown to produce state-of-the-art results in image processing, computer vision [23] and speech recognition [24]. In recent years, CNNs have been successfully applied to NLP and document classification problems[25][26]. The input to CNNs is a feature map which corresponds to the pixels in an image or words in a sentence or document, or characters in words. This feature map is scanned in CNNs one area at a time by filters, assuming that filters slide, or convolve, around the feature map. The way CNNs adjust their filter weights is through back propagation, which means that after the forward pass, the network is able to look at the loss function and make a backward pass to update the weights. The CNN layer is followed by a pooling layer that compresses or generalizes over the CNN representations. It reduces the dimensionality of the CNN layer by down sampling the output and taking the maximum value as the feature corresponding to each filter. The pooling layer is typically followed by a feed-forward fully connected layer that takes the features from the pooling layer and makes new combinations for further learning or final predictions.

For some sequence processing problems, one-dimensional convolutional neural networks has excellent performance and the computational cost is usually much smaller. Recently, one-dimensional convolutional neural networks have achieved great success in the fields of audio generation and machine translation. In addition to these specific achievements, one-dimensional convolutional neural networks can apply to these tasks such as text classification and time series prediction with fast speed. One-dimensional convolution can extract local one-dimensional sequence segments from the sequence and identify local patterns in the sequence. Since the same input transformation is performed for each sequence segment, the patterns learned at a certain position in the sentence can be identified at other locations, which makes the one-dimensional convolutional neural network have translation invariance. Moreover, the sequence data can be subjected to a one-dimensional pooling operation, extracting a sequence segment from the input, and then outputting its maximum value or average value. Like the two-dimensional convolutional neural network, this operation is also used to reduce the length of a one-dimensional input.

This paper explore the use of machine learning method to predict wave characteristics from sensor data. Since we are not sure whether the accelerometer is accurate in real sea conditions, it is likely that the data collected will not be accurate when the equipment is directly applied to the real sea conditions. In order to measure and correct the accuracy of sensor equipment, we have designed a specific device to simulate the buoy in the wave. We therefore can judge and correct the accuracy of accelerometers and can access more accurate and realistic data to carry out a series of research in the real experimental environment. Based on these data, we propose an end-to-end convolutional neural network named WaveNet to process the obtained sensor data and predict wave height and period. The study found that the WaveNet model outperforms numerical integration method in our experiment.

2. Data acquisition and preprocessing

2.1. Data acquisition

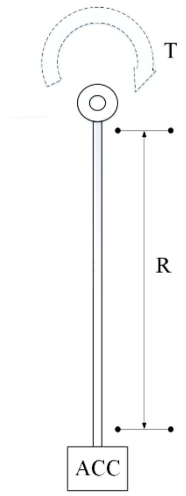

Figure 1. The illustration of the device used to generate simulation data of the accelerator in the buoy. "ACC" is the accelerator in the buoy.

According to the stochastic wave spectrum theory[20][21], waves are random because of the random changes in wind speed and pressure relative to position and time. Waves have random properties which are composed of many waves with different amplitude, frequency and phase, so we can use waveform curves to simulate the motion process of the buoy.

As shown in the **Figure 1**, the device simulates the movement of a buoy on the sea surface. the wave height equals twice of the distance R. After the device rotating, the acceleration sensor in the outputs a periodic acceleration signal moving, and a series of discrete vertical acceleration signals are collected through a certain sampling frequency to estimate the motion trajectory. By adjusting the distance between accelerator and the center of the rod and setting different periodic values, we can get multiple sets of data with different height values and period values. We use the data for research in the next experiment.

2.2. Data preprocessing

Data preprocessing are needed before feeding the data into the convolutional neural network for training or testing. Given the raw three-axis accelerator data, we first calculate the projected components on the vertical direction to the sea surface in the geographic coordinate system using the deflection angles.

We calculated the displacement by twice integrating the acceleration data. Then we used the cross-zero point to calculate the wave period and height. By comparing them with the ground truth, we can test the accuracy of methods. We also use these acceleration data to train the model and predict wave characteristics.

In the training data processing stage, we sampled the acceleration sequence data to compose training data. Each group of training data is 2048 continuous acceleration values, which belongs to one piece of an entire acceleration sequence data. After that we can form the final training data combined the sampled acceleration series data with the corresponding wave height value and periodic value.

3. Methodology

3.1 Numerical integration

Numerical integration was used to estimate the vertical movement of the buoy[22]. The zero-crossing point was used to locate the peak and trough. The average value of wave height and period can then be calculated.

3.2 Proposed Convolutional networks-WaveNet

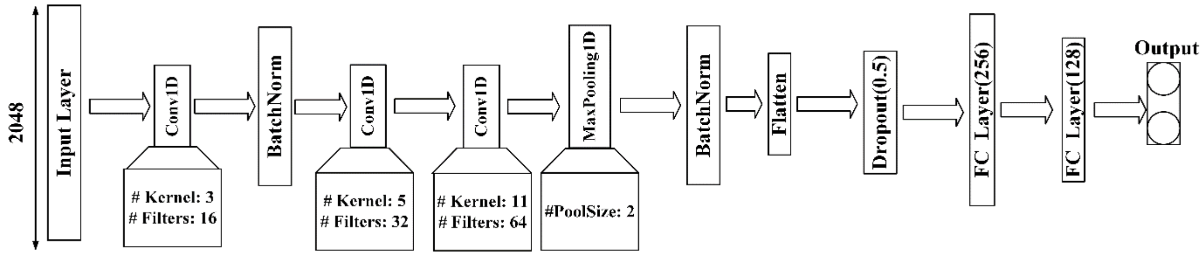

Figure 2. WaveNet architecture

As shown in **Figure 2**, Convolutional neural networks are selected here due to their capability to learning hierarchical representations. Especially, the input dimension of the samples is 2048 and output are height and period. We implemented WaveNet model using Keras based on Google Tensorflow. All experiments are conducted on a computer equipped with a NVIDIA GPU 8G.

3.3 Training methodology

After the data processing stage, we obtained the training data suitable for the model. In general, in order to evaluate the network while adjusting network parameters, we can divide the data into training sets and verification sets, but since the data points are few data points, the verification set is very small. Therefore, the verification score may fluctuate greatly depending on the verification set and test set selected. That is to say, the way the verification set is divided may result in a large variance in the verification score, so that the model cannot be reliably evaluated. Therefore, we can use the K-fold cross-validation to evaluate the model. In addition, after we divide the training data into a training set and a test set, the test set must not be used. Instead, the test set is used to test the performance of the model after adjusting various network parameters. As the neural network performs better on the training data, the model maybe overfitting and gets worse results on previously unseen data. Therefore an effective overfitting strategy is necessary. Deep learning model does not process the entire data set at the same time, but splits the data into small batches. We use these import strategies in our proposed model.

The specific training details of WaveNet model are as follows:

- Use BatchNorm to speed up the network learning rate
- Each layer uses the ReLu activation function in addition to the final output layer
- Optimize network parameters using the MSE loss function
- We take the ADAM stochastic optimization algorithm as the training algorithm
- Learning rate can use the default learning rate
- The batch size of the network training is 128
- Two-layer fully connected network in the Dense layer uses l2 regularization
- The value used in the dropout layer is 0.5
- We use five-fold cross validation to test the accuracy of the algorithm
- The early stopping strategy is used
- The number of iterations for the entire network on the training set is 200

4. Result and discussion

4.1. Evaluation metrics

We evaluated the performance of WaveNet using the mean absolute error (MAE) and the mean square error (MSE), which have been widely used. The smaller value, better performance.

$$MAE = \frac{1}{n}\sum_{i=0}^{n}|y_i - \hat{y}_i|$$

$$MSE = \frac{1}{n}\sum_{i=0}^{n}(y_i - \hat{y}_i)^2$$

4.2. Result and discussion

Table 1. Evaluation metric of WaveNet

	MAE	MSE
WaveNet	0.1537	0.1948

As shown in **Table 1**, the experimental results show that the performance of WaveNet on the MAE is 0.1537, and the the MSE is 0.1948. The MAE and MSE indicate the overall difference between the ground truth and the WaveNet prediction. It was suggested that the WaveNet model has better performance.

In the experiment, we use the correlation graph to compare he WaveNet prediction and the ground truth. As can be seen from **Figure 3**, the correlation coefficient between the true height and the height predicted by WaveNet is 0.97, the correlation coefficient between the true period and the period predicted by WaveNet is 0.99. The results show that prediction by WaveNet have a very strong correlation with the truth.

In the experiment, we set the height and period values using the device and collected corresponding experimental data. As shown in **Figure 4,** the velocity and displacement sequences are recovered by the numerical integration method using the acceleration. We chose ten groups of different data for comparison. **Table 2** show several sets of comparison values, including the ground truth, numerical integration results and WaveNet predictions.

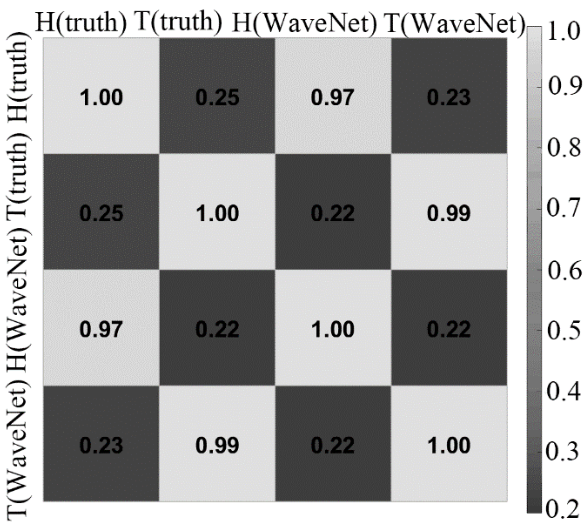

Figure 3. The correlation between and the truth and the predicted results using WaveNet

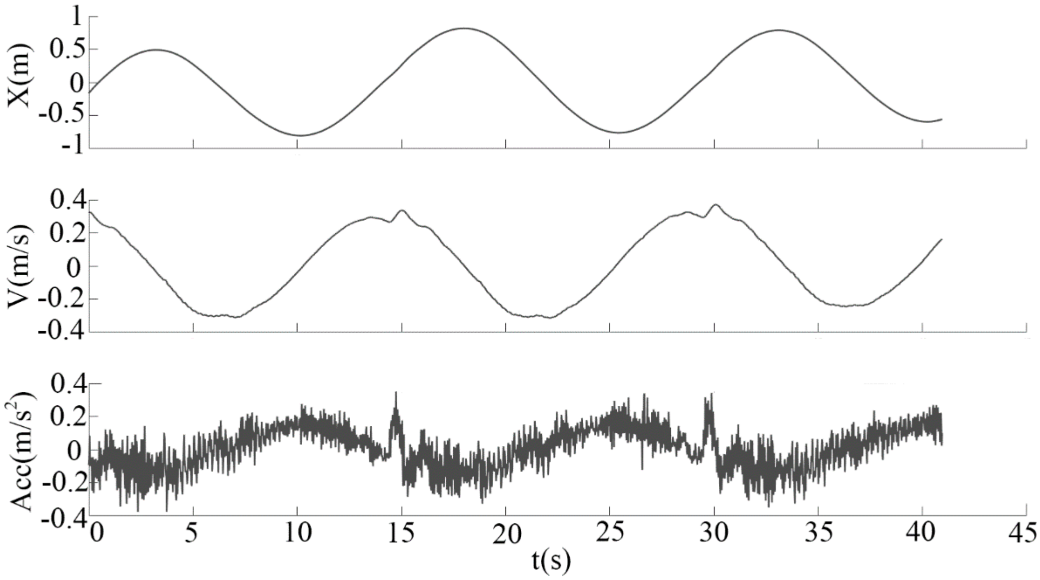

Figure 4. The velocity (2nd row) and the distance (1st row) recovered by numerical integration of the acceleration (3rd row). The ground truth wave height and the period is set to be 1.5m and 15s respectively on the device.

Table 2. Several sets of comparison results, including the ground truth, numerical integration results and WaveNet predictions.

Test No.	Wave Height (H) and Period (T)	Ground Truth	Numerical Integration	WaveNet
01	H(m)	1.5	1.44	**1.458**
	T(s)	15	14.41	**15.27**
02	H(m)	1.2	**1.12**	**1.2**
	T(s)	15	13.88	**14.55**
03	H(m)	1.0	1.04	**0.96**
	T(s)	15	10.07	**14.68**
04	H(m)	1.2	**1.22**	1.15
	T(s)	14	14.53	**13.88**
05	H(m)	1.1	1.09	**1.11**
	T(s)	12	14.41	**12.01**
06	H(m)	1.5	**1.56**	1.39

	T(s)	10	10.19	**10.05**
07	H(m)	1.0	**1.02**	1.15
	T(s)	10	10.12	**10.08**
08	H(m)	1.0	0.86	**0.93**
	T(s)	5	7.52	**6.11**
09	H(m)	1.0	**1.03**	1.05
	T(s)	6	6.23	**6.08**
10	H(m)	1.5	1.52	**1.48**
	T(s)	4	**4.00**	3.96

5. Conclusion

In this paper, an end-to-end 1D Convolutional network WaveNet was proposed to predict wave height and period from accelerator data of a buoy. We designed a device to simulate the movement of a buoy on the sea surface and collected accelerator data with different wave characteristics. Experiments show that the WaveNet successfully learns the wave pattern and outperforms traditional numerical integration method. Due to practical constraints, we didn't test with data from real conditions, which would be the future work.

6. References

[1]. Ou S-H, Liau J-M, Hsu T-W and Tzang S-Y 2002 Simulating Typhoon Waves by SWAN Wave Model in Coastal Waters of Taiwan *Ocean Eng* **29** 947-971.
[2]. Rogers W E, Kaihatu J M, Hsu L, Jensen R E, Dykes J D and Holland K T 2007 Forecasting and Hindcasting Waves with the SWAN Model in the Southern California Bight *Coastal Eng* **54** 1-15.
[3]. Hersbach H, Janssen P A E M 1999 Improvement of the short-fetch behavior in the Wave Ocean Model (WAM) *Journal of Atmospheric and Oceanic Technology* **16** 884-892
[4]. Monbaliu J, Padilla-Hernández R, Hargreaves J C, Albiach J C C, Luo W, Sclavo M and Günther H 2000 The spectral wave model, WAM, adapted for applications with high spatial resolution *Coastal Engineering* **41** 41–62
[5]. Mentaschi L, Besio G, Cassola F, and Mazzino A 2015 Performance evaluation of Wavewatch III in the Mediterranean Sea *Ocean Modelling* **90** 82–94
[6]. Mahjoobi J, Etemad-Shahidi A and Kazeminezhad M H 2008 Hindcasting of wave parameters using different soft computing methods *Ocean Res* **30** 28–36
[7]. Agrawal J D and Deo M C 2002 On-line wave prediction *Marine Structures* **15** 57–74
[8]. Deo M C, Jha A, Chaphekar A S and Ravikant K 2001 Neural networks for wave forecasting *Ocean Engineering* **28** 889–898
[9]. Gunaydın K 2008 The estimation of monthly mean significant wave heights by using artificial neural network and regression methods *Ocean Engineering* **35** 1406–1415
[10]. Deo M C and Naidu C.S 1999 Real time wave forecasting using neural networks *Ocean Eng* **26** 191–203.
[11]. Londhe S N and Panchang V 2006 One-day wave forecasts based on artificial neural networks *Journal of Atmospheric and Oceanic Technology* **23** 1593–1603.

[12]. Zanaganeh M, Mousavi S J and Etemad-Shahidi A 2009 A hybrid genetic algorithm–adaptive network-based fuzzy inference system in prediction of wave parameters *Engineering Applications of Artificial Intelligence* **22** 1194–1202
[13]. Canellas B, Balle S and Tintore J and Orfila A 2010 Wave height prediction in the western mediterranean using genetic algorithms *Ocean Engineering* **37** 742–748
[14]. Nitsure S P, Londhe S N and Khare K C 2012 Wave forecasts using wind information and genetic programming *Ocean Eng* **54** 61–69.
[15]. Mahjoobi J, Mosabbeb E A 2009 Prediction of significant wave height using regressive support vector machines *Ocean Engineering* **36** 339–347
[16]. Mahjoobi J and Etemad-Shahidi A 2008 An alternative approach for prediction of significant wave height based on classification and regression trees *Applied Ocean Research* **30** 172-177
[17]. O'Donncha F, Zhang Y, Chen B and James S C 2018 An integrated framework that combines machine learning and numerical models to improve wave-condition forecasts *Journal of Marine Systems* **186** 29–36
[18]. Berbić J, Ocvirk E, Carević D and Lončar G 2017 Application of neural networks and support vector machine for significant wave height prediction *Oceanologia* **59** 331–349
[19]. kumar N K, Savitha R and Mamun A A 2017 Regional ocean wave height prediction using sequential learning neural networks *Ocean Engineering* **129** 605–612
[20]. Massel S R 1996 Ocean surface waves: their physics and prediction *Advanced Series on Ocean Engineering*
[21]. Thomas T J and Dwarakish G S 2015 Numerical wave modelling – a review *Aquatic Procedia* **4** 443–448.
[22]. Massel S R 2001 Wavelet analysis for processing of ocean surface wave records *Ocean Engineering* **28** 957–987
[23]. Krizhevsky A, Sutskever I and Hinton G E 2017 ImageNet classification with deep convolutional neural networks *Communications of the ACM* **60** 84-90
[24]. Graves A, Mohamed A and Hinton G 2013 Speech recognition with deep recurrent neural networks *IEEE International Conference on Acoustics, Speech and Signal Processing*
[25]. Kim Y 2014 Convolutional Neural Networks for Sentence Classification *Proceedings of the 2014 Conference on Empirical Methods in Natural Language Processing (EMNLP)*
[26]. Johnson R and Zhang T 2015 Effective Use of Word Order for Text Categorization with Convolutional Neural Networks *Proceedings of the 2015 Conference of the North American Chapter of the Association for Computational Linguistics: Human Language Technologies*

Sandy coast erosion under the conditions of a storm surge combined with a spring tide

Shi Qian[1], Cai Aizhi[2], Qi Hongshuai[3]

1 School of Environmental Science and Engineering, Xiamen University of Technology, Xiamen 361024, China.
2 Department of Oceanography, Xiamen University, Xiamen 361005, China.
3Third Institute of Oceanography, SOA, Xiamen, 361005, China.
E-mail: shiq@xmut.edu.cn

Abstract. By comparing the changes of beaches and features in the southeastern coast of Xiamen Island before and after Typhoon No. 9914, the beach cycle and coast erosion processes under the condition of superimposed the spring tide of storm surge were discussed. The study showed that during Typhoon No. 9914, the coastal water level rose to 4.04m above the main sea level (MSL). The storm surge elevation was 1.43m. The stormy waves with 22m/s onshore winds brought overwash onto Huandao Road, up to the main sea level of more than 8.5m, depositing about 8-10cm of beach sands on the road. It caused the beach berm to disappear completely. The sand prism lying in the high tidal zone was scoured. Part of the sand of the prism was washed upward away from the beach, part of which was brought to the low tide zone. The bare shoreface without sand prism was scoured directly by waves and currents. Although the sandy sediment which was brought to the deeper zone by the storm can come back to the shoreface, but the overwash sand could not be returned after the storm, and the prime failed to return to its original condition for a long time, eventually leading to beach erosion and coast retreat.

1. Introduction

The beach cycle is an active and frequent geomorphological process of sedimentation in coastal zones. It is also researched around the globe within marine science. The theory was first introduced by D.W. Johson (1919), but it was an effort which required further research [1]. F.B. Phlegez, etc. (1972) researched the beach changes of the barrier-lagoon coasts in California with sedimentologic and hydrodynamic methods [2]. In the last half century, many experts have made great efforts to investigate and research the beach process. F.P. Shepard, a pioneer in marine geology, had performed long-term observations on Scrips Beach in California and collected many profile sketches in different beach cycles [3]. Furthermore, L.D. Immam (1953) and C.A.M. King (1959) further developed this theory with experiments [4, 5]. Recently, Morton, etc. (2003) have researched the beach and barrier change response to previous hurricanes in Mexico Bay and the Atlantic coast of America and proposed three storm morphological types [6]. Zhang, etc. (2005) compared the LIDAR data to analyze changes of a 4km-long beach along the Atlantic coast in the middle of Florida [7]. Switzer & Jonses (2008) twice studied the overwash sedimentology of different storms on the same coast in Australia [8]. Domestic researchers, such as Cai Aizhi (1989, 1995), Xia Yiming (1991) and so on, have primarily studied in this research field. They have been working on the researches about beach cycle under the action of storm in the Shandong Peninsula and Xiamen Island [9-12]. The response characteristics of different coastal geomorphological types to Typhoons were studied at the Cai Feng

IOP Conf. Series: Earth and Environmental Science **369** (2019) 012002 doi:10.1088/1755-1315/369/1/012002

etc. (2006) [13]. Kai Yin,etc. (2019) ，applying mathematical model to study the change of beach profile caused by storm surge, it is considered that high water level is more influential than wave impact[14].

However, their past researches on beach changes did not involved the beach erosion process and its essential conditions in the storm surge combined with a spring tide. This extreme condition and its process are the decisive factors leading to asymmetric beach circulation and coastal damage. In the 20 years since 1999, the southeastern sandy coast of Xiamen Island has experienced a frontal attack by the super-strong typhoons No.9914 (1999) and No.1614 (Meranti, 2016). Typhoon Meranti landed with a maximum wind speed of 52m/s, the strongest and most destructive typhoon in the last 60 years [15], but it was near a low tide at the time of landing and did not cause damage to the coast. Typhoon No. 9914 landed with a maximum wind speed of 34.2m/s, at the climax of the astronomical tide, causing unprecedented damage to the southeastern coast of Xiamen Island. It is clear that the hydrological conditions at the time of storm landing are critical to the impact of coastal erosion. Although nearly 20 years have passed since Typhoon No. 9914, it is still important to study its coastal erosion process and conditions for today's coastal protection.

2. Study Occasion and Methods

The severe typhoon attacked Xiamen on Oct 9, 1999. Although we got the prediction before its landfall, field observations could not be performed because of extreme weather and hydrodynamic conditions. The damaged conditions of original ground objects and constructions were the only useful evidence. Consequently, usable ground objects must be chosen before the storm, and how to select evidence after the typhoon with these ground objects should also be determined.

2.1. Severe damage of the seawall

We had anticipated that some unqualified coastal constructions would be destroyed in this storm. Therefore, we paid attention to these weak sites and took photos as evidence before the typhoon. We researched the coast immediately after the storm on the morning of October 10th. Unexpectedly, almost all of the seawall on the south and east coasts of Xiamen Island were destroyed except for two sections, Zhenzhu Bay and Taiyan Bay, altogether 900m long. Even those indestructible granite dams were also shattered in this storm.

The first research object we had chosen in advance was a 600m-long newly-built seawall between Baishi emplacement and Zengcuoan (Figure 1). Before construction of this seawall, we realized and brought to light two design flaws, the design elevation was not high enough and the foundation treatment was not suitable.

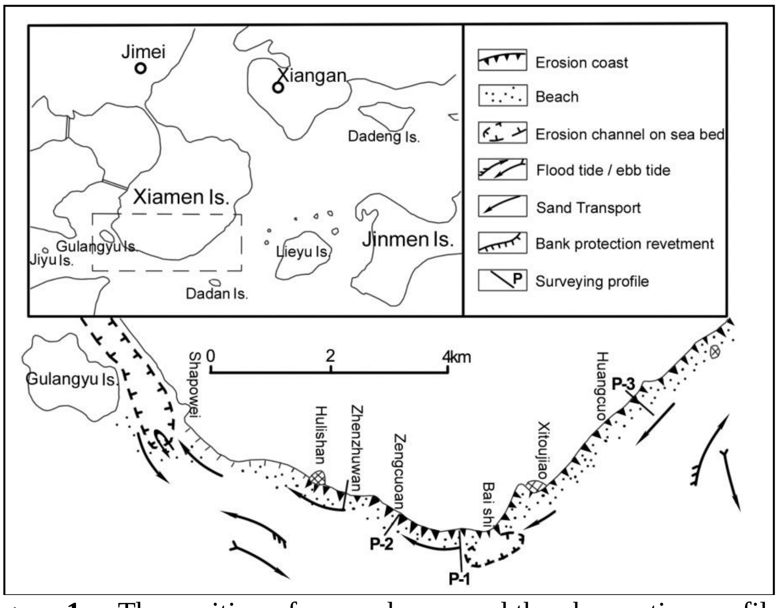

Figure 1. The position of research area and the observation profiles.

The seawall was attacked by this severe storm after the project was completed and it collapsed entirely (Figure 2, P-1).

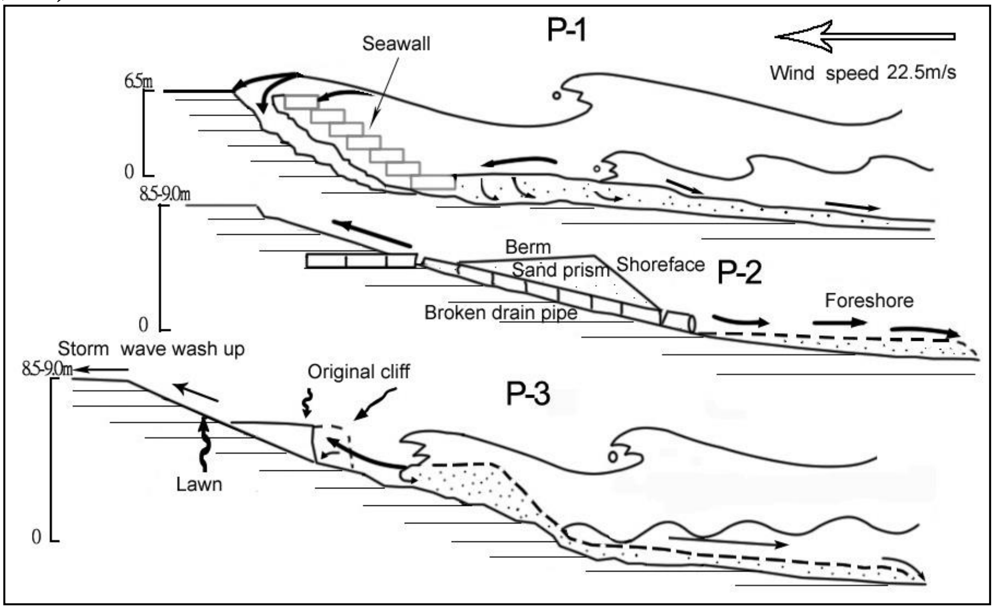

Figure 2. Wave wash over and erosion action under the beach cycles.

Profiles clearly show that the seawall's cement framework was still linked together after it collapsed. Because at the base of the seawall was loose sand, strong waves dredged the bottom of the seawall at low tide during the initial stage. With the water level rising and waves strengthening, dredging and erosion at the bottom became worse. Finally, the whole seawall collapsed by the momentum of the wave.

At the beginning of stage 2, the strong waves overtopped the seawall whose height was less than 6m, then impacted the cracked coastal soil behind the seawall, inducing 5-7m of coastal retreat (Figure 2, P-1).

2.2. Breakage of the sewage pipe buried in the beach

The 60cm diameter sewage pipe (Figure 2, P-2) broke as a result of the erosion and dredging of the energetic waves. The outlet on the slope break of shoreface was also damaged in the stormy waves. The sewage pipe buried in the beach also broke in many places under the impact of the stormy waves. The records reflect that the pipe was buried in the beach, but the prismatic sand washed away in stage II induced damage to the pipe.

3. Coastal Environmental Parameters

3.1. Combination of storm surge and spring tide

The predicted syzygial spring tide level was 2.1m above the main sea level(MSL) . During the landfall of the No.9914 typhoon, the storm surge was about 1.43m. The summated elevation was 4.04m upon the MSL.

3.2. Wind measurements

The wind speed measured by the Xiamen meteorological station was stronger because it is located on the top of Huwei hill (a.out 140m high). The Xiamen oceanographic station is located near the coast, so its wind data was more accurate and can be used in this study. The maximum wind speed measured by the oceanographic station was a 34.5m/s east wind and a 22.5m/s south wind. The severe anticlockwise wind duration was 5~6 hours.

3.3. Wave conditions
The incident wave direction mainly was east, southeast and south. The wave height (H) was 1.69~2.38m and wave rise (R) was 2.0~2.5m. The relationship between H and R depended on many factors, such as wind speed, bathymetric gradient and coastal strike. The value of R is inversely proportional to the backshore slope and roughness.

3.4. Beach geomorphology and sediment
The coast in the southeast of Xiamen Island has been retreating in the last few decades. Huangcuo beach, which runs northeast to southwest, has been left with a thin layer of sand, its berm only 30m wide and and its peak only reaching 3.9~4.6m above the main sea level. The shoreface gradient is 7.5~8.5°. The sediment is medium-fine sand (Mz=1.3~2.1φ,σ_1=1.1~1.5) in prismatic sand and well-sorted fine sand in foreshore (Mz=2.1~2.6φ, σ_1=0.5~0.8).

4. Hydrodynamic Energy Dissipation in the Beach Cycle

4.1 .Energy transmission of stormy waves in high water level
Waves are a carrier body which transport energy from the water to coasts. Under the same wave conditions, water depth is inversely proportionate to the dissipation of the seabed by friction. There are three hydrodynamic dissipation zones on the beach profile, including the nearshore shoal zone where water depth is less than half of the wavelength, the wave breaking zone lying between the lower slope and sand ridge, and the overwash zone and erosion scarp above the shoreface. However, hydrodynamic energy dissipation varies in the different zones. The dissipation proportion in the different zones changes with the maintenance time of water level and wave parameters. Water is deeper in the nearshore shoal zone and hydrodynamic energy will be transported to the overwash zone. To understand the relation between the beach cycle and energy dissipation and erosion, the energy dissipation (Figure 2) was divided into three stage: Stage 1, Stage 2 and Stage 3(Figure 3).

4.2. Beach cycle and erosion
As Figure 3 shows, the energy dissipated at the foreshore on the front of the seawalls at stage 1 resulted in washing and erosion on the beach. The erosion area moved up with the rising water level and the washing of the waves. The strong waves can wash all of the prismatic sand near Stage 2, and the hydrodynamic energy reached its peak in the middle of stage 2. With the stormy waves breaking, they can directly wash and erode the prismatic sand on the beach. The most sediment was brought down to the foreshore, while other sediment was brought up to the supralittoral zonen, even on Huan Dao Road during the overwash process. Meanwhile, the bare shoreface was impacted directly by the storm waves. At its peak, the water level rose to its highest, about 4.04m over the main sea level (MSL). Wave breakers induced huge energy dissipation on the eroded surface and caused overwash with the help of storm winds. At the same time, a powerful scour of scarp above the sand prism leaded to a retreat of the coastal line.

4.3. Overwash of beach sands
During the high water levels of stage 2, with the drive of wave breakers and strong winds (>20m/s), water-mixed sand currents caused overwash 7-8m over the main sea level or higher in places along the slope, even reaching the coastal road (8.5m over MSL). In some sites, the mixed current overwash ran through the lawns to the coastal road, depositing about 8-10cm of sand on the road (Figure 2, P-3) and 5cm of sand on the lawn. During stage 3, the water level and energy of the waves simultaneously decreased. The sediment transported to the foreshore moved back to the beach.

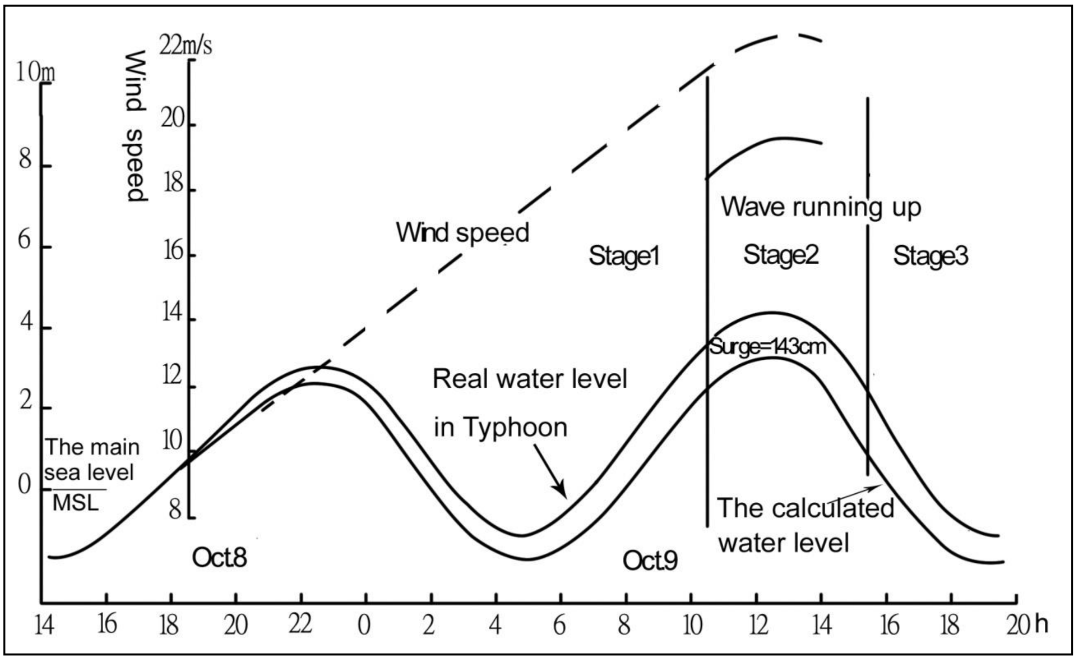

Figure 3. Hydrograph, wind speed and wave rise curve under the conditions of a storm surge combined with a spring tide in No.9914 typhoon

In the case of such a powerful typhoon and the high water level superimposed by the astronomical tide, the intensity and range of the wave to the coastal erosion are bound to expand. But two coastal seawalls , in Pearl Bay and Sun Bay, were not damaged because of their solid foundation and structure. The sea walls consists of the following parts, including: A. a foundation whose top is at the main sea level, B. a stone-made bottom slope whose elevation is from 0 to 2.5m, C. a trapezoidal slope whose elevation is from 2.5 to 5.5m , D. an arc retaining wall whose elevation is from 5.5 to 6.8m. During the storm surge, the foundation and bottom slopes successfully resisted the erosion of the storm, the trapezoidal slope efficiently dissipated waves, and the curved wall consumed the last part of the storm energy. It has been proved that the projects have achieved the dual effect of shore protection and beach preservation.

4.4. The asymmetry of the beach cycle

In stage 3, with the water level and waves gradually decreasing, the beach cycle turned to its recover stage. The sediment which had been transported to the low tidal zone gradually returned to the beach. Based on our subsequent observation, the height of the prismatic sand cannot be recovered completely. Mostly, this asymmetry of the beach cycle is presented as follows: it can recover to its approximate original height by moderate wave processes in several spring, neap tidal cycles. The lower water level during the spring tides and the moderate wave processes can help the sediment which was brought to the deeper zone by the storm come back to the shoreface and recover the beach.

But on some sandy coast such as Huangcuo beach, the huge waves washed some parts of the sand prism up to Huandao Road and the other parts back to the low tide zone. The naked beach would be washed directly by strong waves before they retreated. When the energetic waves calmed, the sediment which was transported to the low tidal zone would come back to the shoreface, but the sands of overwash couldn’t return. So the sand prism decreased and the coast retreated due to the overwash.

5. Conclusions

This storm surge combined with the spring tide resulted in abnormally high water levels. Due to this, more hydrodynamic energy was transferred to the coast. The sediment on the foreshore was washed away in the low water levels. The dredging and erosion at the foot of the seawall resulted in the firm seawall collapsing completely. At stage 2, the prismatic sand was washed away and the buried sewage pipe was broken by the stormy waves. The prismatic sand lying in the high tidal zone was scoured and induced offshore and onshore sediment transport. The bare shoreface which was originally covered by sand was directly washed by the stormy waves and currents, finally leading to coastal retreat. With the water levels and the energy of the waves increasing to a peak, the water-mixed sand current crossed the artificial slope run-up to a height of 8.5m above MSL, even encroaching onto the higher Huandao Road.

The strong waves impacted the protuberant erosion scarp and dissipated its energy through erosion. At the same time the coastal cliffs were retreating, the trees fell down, the sewage pipe was exposed and broke, and many structures were destroyed in the storm.

After stage 2, water levels and wave energy gradually decreased and entered the recovery stage, a slow beach process. Although the sediment which was brought to the deeper zone by the storm can return to the shoreface, the washover sediment never returned. Doubtless, the sediment lost in the storm from the beach and shoreface eroded and retreated. If there was no source to replace the sediment, the beach would decline, even disappear. Whether the beach berm can completely recover depends on sufficient sources of replacement sediment.

6. References

[1] Johnson D 1919 *Shore Processes and Shoreline Development* (New York: Wiley)p 784

[2] Phleger F and Ewing C 1962 Sedimentology and oceanography of coastal lagoons in Baja California *Geol. Soc.* Vol 73(2) (Mexico: Amer. Bull)pp 145-182.

[3] Shepard F 1973 *Submarine Geology, Third ed* (New York: Harper & Row)p 517.

[4] Inman D and Bognold R Littoral processes 1963 *In The Sea* vol 3 (New York: N.M. Hill, ed., Interscience) pp529-553.

[5] King C 1972 *Beaches and Coasts, 2nd ed* (London: Edward Arnold)pp 321-353.

[6] Robert A Morton and Asbury H Sallenger Jr 2003 Morphological Impacts of Extreme Storms on Sandy Beaches and Barriers *Journal of Coastal Research* vol 19(3)pp 560-573

[7] Zhang K and Whitman D 2005 Comparison of three algorithms for filtering airborne LIDAR data *Photogrammetric Engineering and Remote Sensing* vol 71(3)pp 313-324

[8] Switzer D and Jones G 2008 Setup, Deposition, and Sedimentary Characteristics of Two Storm Overwash Deposits, Abrahams Bosom Beach, Southeastern Australia *Journal of Coastal Research* vol 24(1)pp 189-200.

[9] Cai Aizhi 1989 Beach Cycle and Coast Engineering *The Ocean Engineering* vol 7(3)pp 57-64**.**

[10] Cai Aizhi 1995 Beach Resource and Protection in Xiamen Island. *Memoir of Resource for Xiamen Island* (Beijing: Ocean Press)pp 154-156

[11] Xia Yimin 1991 Study on the Engineering Means for Coastal Stability *The Ocean Engineering* vol 9(4)pp 45-58.

[12] Xue Hongchao Guo Da Pan Shaohua and Zhong Huzui 1991 Wave Rubup-Rundown Amplitude on Slope *The Ocean Engineering* vol 9(1)pp 39-46.

[13] Cai Feng Lei Gang and Su Xian Ze 2006 Study on process response of Fujian beach geomorphology to typhoon Aere *The Ocean Engineering* vol 24(1)pp 98-109.

[14] Kai Yin Sudong Xu Wenrui Huang Rui Li and Hong Xiao 2019 Modeling beach profile changes by typhoon impacts at Xiamen coast *Natural Hazards* vol 95(3)pp 783–804

[15] Chen Dehua Zhang Ling and Zhang Wei 2018 Structure characteristics and cause analysis of catastrophic wind caused by super typhoon Meranti *Transactions of Atmospheric Sciences* vol 41(5)pp 692-701

Chapter 2:
Deep Sea Engineering

IOP Conf. Series: Earth and Environmental Science **369** (2019) 012003 doi:10.1088/1755-1315/369/1/012003

Effects of seafloor topography on underwater acoustic channel

HUANG Hua[1], JIN Baogang[1], Cheng Rui[1,2], LIU Juan[1] and CHEN Jian[1]

1 Beijing Institute of Applied Meteorology, Beijing, China
2 State Key Laboratory of Geo-Information Engineering, Xian, china
E-mail: huang_hua_2000@163.com

Abstract. Sound wave is the main means of underwater communication at present. Focusing on effects of seafloor topography on underwater acoustic channel, some acoustic propagation models were compared and the BELLHOP method was chosen based on the experiment data of typical seafloor topography. Then the date of OFES model and SOM method were used to get the marine parameters of temperature, salinity, depth and sounding velocity along SS section near Diaoyu Island. At last, the acoustic propagations along the SS section in flat bottom and real seafloor topography were simulated using BELLHOP method. The comparison of acoustic propagation loss was presented. The results show that the BELLHOP method can be used to get authentic results of acoustic propagation under different seafloor topographies, and seafloor topography has a significient effect on acoustic propagation characteritics， which are also influenced by the depth of sound source and sound receiver.

1. Introduction

Seafloor topography is one of the boundaries, which has a very important impact on underwater acoustic propagation [1], which has been a hot topic in the field of acoustics research, and attracted great attention from researchers at home and abroad.

In California ocean experiment, Northrop found the "slope enhancement effect", that is, the loss of acoustic signal propagation will be reduced under the condition of continental shelf slope [2]. Tappert found that sound waves can travel down the slope of the continental shelf until near the axis of acoustics channel, i.e. the "mud flow effect" [3]. Subsequently, a series of underwater acoustic experiments were carried out in the United States, including AET, AST, ATOC, NPAL98, SLICE89, OWSP and so on. The effects of seamounts, slopes and other factors on acoustic propagation were studied [4]. In China, Zhao Xiaoqun studied the effect of seafloor topography on short-distance propagation of underwater acoustic channel in shallow sea area [5]. Pu Lianglong simulated the influence of typical seafloor topography, and found that sudden change of water depth would lead to rapid expansion of acoustics channel and increase propagation loss [6]. Based on the experimental results, Qin Jixing analyzed the "mud flow effect" of acoustic propagation in shallow sea area [7]. Those above studies mainly focus on the continental shelf slopes in shallow sea area, and there are few studies on acoustics propagation in deep sea and undulating terrain.

This paper focused on effects of seafloor topography on underwater acoustic channel using the data of OFES (OGCM for the Earth Simulator) model and SOM (Self Organizing Map) method, the parameters of ocean temperature, salinity, depth and sound velocity were obtained along the SS section near Diaoyu Island. Then the BELLHOP method was verified and used to simulate the acoustic propagation along SS section with flat bottom and underwater rugged terrain. While the path loss of underwater acoustic propagation were given, the effects of underwater rugged terrain were analyzed.

2. Selection of acoustic propagation methods

2.1. Acoustic propagation methods
Acoustics propagation in the ocean follows the wave equation, which can be solved under given boundary conditions and marine environment parameters. The common solving methods include normal wave theory and ray theory. Normal wave theory is perfect, which is suitable for low frequency situations, but the boundary conditions are difficult to deal with and the results are not intuitive. Ray theory is generally applicable in high frequency situations. It is easy to set boundary conditions, and can obtain ray propagation and acoustic path loss. As a general rule, the lowest working frequency of ray theory is f = 10c/H, H for depth and c for sound velocity. In this paper, the average sound velocity of marine environment is about 1500 m/s, the average depth is more than 500 m, then the lowest working frequency of ray model is 30 Hz, while the working frequency of sound source in this paper is 280 Hz. Therefore, it is appropriate to choose the ray theory. However, there are some shortcomings in the conventional ray theory. In 1987, Porter proposed the BELLHOP ray tracing method (BELLHOP method)[8]. Adding the Gauss intensity profile, we can successfully solve the problem of the conventional ray theory in sound film region and caustic region. BELLHOP method can also give key parameters such as acoustic propagation loss and sound ray, which are consistent with theoretical model and experimental data. It has gradually become one of the most widely used methods in underwater acoustic simulation.

2.2. BELLHOP method validation
Considering that the working frequency of sound source is 280Hz in this paper, and the influence of seafloor topography is mainly studied, the applicability and reliability of BELLHOP method should be investigated. It is validated based on the results of ocean acoustic experiment.

In this experiment of ocean acoustic propagation, the sound source (frequency 280 Hz) was in depth 50 m, while the receiver was in depth 50 m too. The propagation loss at different distances within 30 km was measured from near to far. Vertical sound velocity distribution and seafloor topography in the test area are shown in Fig. 1. Then BELLHOP method was used to simulate the acoustic propagation and the results were compared with the experimental data, as shown in Figure 2. With the increase of propagation distance, the propagation loss increased gradually, and had a large fluctuation. When we compared the experimental data with the simulation results, they basically coincided with each other, which shows that BELLHOP method has good applicability under underwater rugged terrain and could be used to predict the path loss of underwater acoustic propagation.

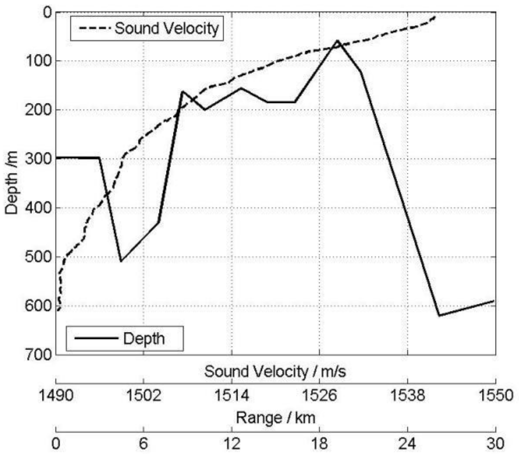

Figure 1. Marine Environment of Acoustic Experiment.

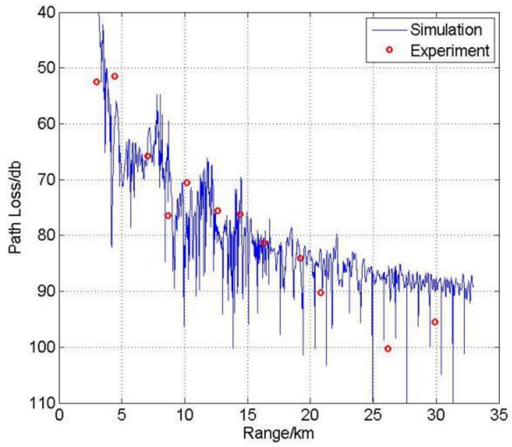

Figure 2. Verification of BELLHOP Method

BELLHOP method was used to simulation underwater acoustic channel and propagation path loss. The attenuation of acoustic propagation along this section is obtained as follows:

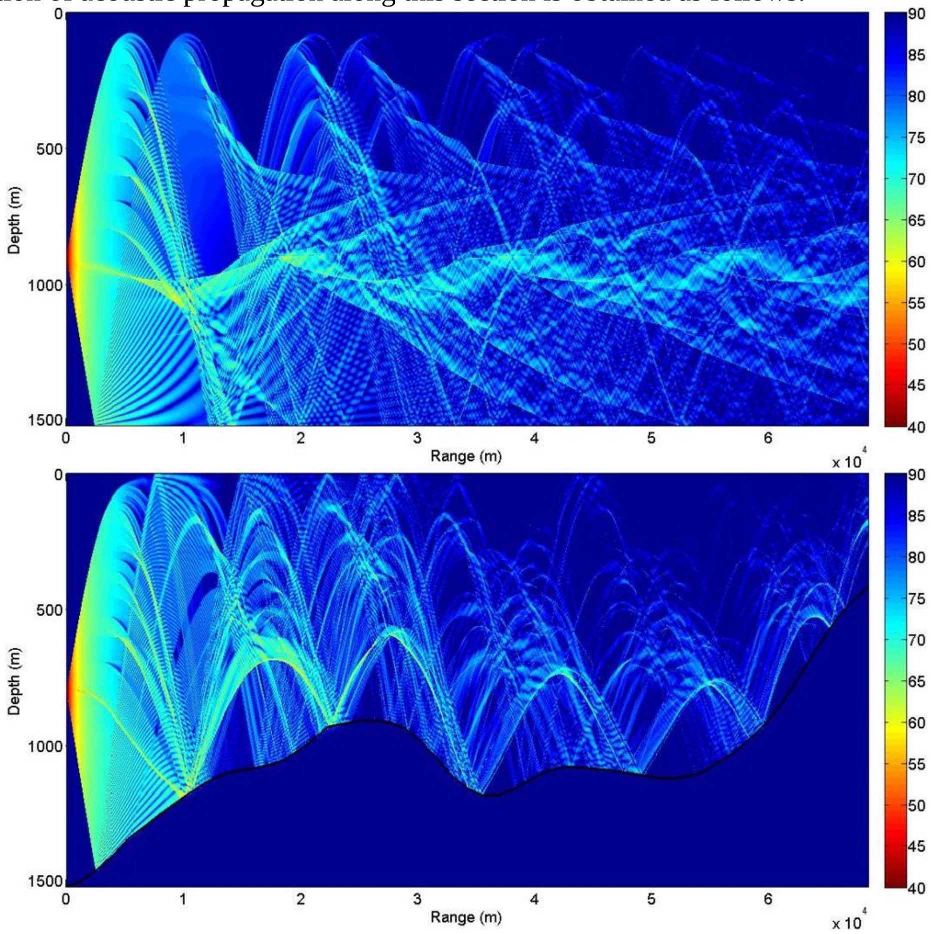

Figure 5. Path loss of acoustic propagation
(up: flat seafloor; down: real seafloor topography).

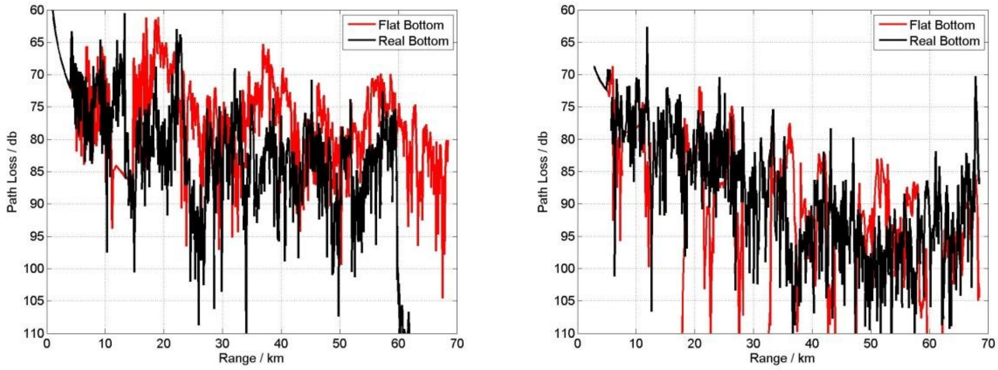

Fig. 6 Path loss of acoustic propagation in different depth (left: 900m; right: 200 m).

It can be seen from Fig. 5 and Fig. 6 that under the assumption of flat bottom, while the sound source is located at the axis of the channel (depth 800 m), the structure of acoustic propagating along the acoustic channel axis is clear and regular, the upper part of the acoustic channel is not affected by the reflection of the seafloor, including the convergence area and the acoustic shadow area. the lower part of the channel axis is affected by both the propagation along the channel and the reflection of the seafloor, and there is no obvious acoustic shadow area. But in the real seafloor terrain, the acoustic propagation along the acoustic channel axis is greatly affected by the reflection of seafloor terrain, the basic structure is destroyed, and there is no obvious acoustic channel propagation any more. Especially in the long distance, the elevation of the terrain basically blocked the acoustic channel axis; the upper part of the channel axis is also affected by the reflection of seafloor terrain, the acoustic shadow area disappears basically, and in the long distance, the propagation is affected by the elevation of the terrain, and the loss is slightly reduced. the lower part of acoustics channel axis is mainly controlled by the reflective effect of the undulating terrain, including the convergence area and the shadow area.

4. Conclusion

The BELLHOP method is used to simulate the acoustics propagation under ideal flat seafloor and real seafloor topography along SS section near Diaoyu Island. The path loss of acoustics propagation are given, and the effects of seafloor topography on acoustic channel are compared and analyzed. The results show that:

- The results of BELLHOP method are in good agreement with the experimental data. It has good applicability in the real seafloor terrain and can be used to predict the acoustic propagation characteristics.
- For the underwater acoustic channel, the complex terrain of the seafloor will have an obvious impact on the path loss along the acoustic channel.
- In different depths, the influence of seafloor topography is different for the acoustic propagation characteristics.

In the future, this method can be applied to underwater acoustic channel evaluation and application.

5. References

[1] Jensen F B, Kuperman W A, Porter M B, Schmidt H. Computational Ocean Acoustics (second edition)[M]. New York: Springer-Verlag, 2011.
[2] Northrop J, Lougbrid M S, Werner E W. Effects of near-source bottom conditions on long range sound propagation in the deep ocean[J]. J. Geophys. Res., 1968, 73(12): 3905-3908.
[3] Tappert F D, Spiesberger J L, Wolfson M A. Study of a novel range-dependent propagation effect with application to the axial injection of signals from the Kaneohe source[J]. J. Acoust. Soc. Am., 2002, 111 (2): 757-762.
[4] Chandrayadula T K. Mode Tomography using Signals from the Long Range Ocean Acoustic Propagation EXperiment (LOAPEX)[D]. George Mason University, 2009.
[5] ZHAO Xiaoqun，ZHANG Yang，ZHANG Kai. Effects of Seafloor Topographies on Short-range Shallow Water Acoustic Channels[J]. Military Communications Technology, 2011，32(4): 32-37
[6] DA Liang-long. Modeling and Application of Underwater Acoustic Environmental Effect[M]. Beijing, Science Press, 2012
[7] QIN, Jixing, ZHANG Renhe, LUO Wenyu，Two-dimensional sound propagation over a continental slope [J]. ACTA ACUSTICA，2014，39 (2): 145-153.
[8] Porter M B, Bucher H P. Gaussian beam tracing for computingocean acoustic fields [J]. Acoust Soc. Am, 1987,82(4):1349- 1359.
[9] Jin Baogang. Interactions between the North Pacific Western Boundary Current System and Mesoscale Eddy[D]，PLA University of Science and Technology Ph.D, 2011.6.
[10] http://www.ngdc.noaa.gov/mgg/global/relief/ETOPO1.

IOP Conf. Series: Earth and Environmental Science **369** (2019) 012004 doi:10.1088/1755-1315/369/1/012004

The error analysis of an underwater acoustic short baseline array detection and location system

QU Jia-sheng[1], QU Yuan-xin[2], YANG Shan-shan[3]

1 Senior Engineer, Dalian Scientific Test and Control Technology Institute, Dalian, China
2 Senior Engineer, Dalian Scientific Test and Control Technology Institute, Dalian, China
3 Engineer, Dalian Scientific Test and Control Technology Institute, Dalian, China
E-mail: honghu0711@163.com

Abstract. This paper briefly introduces the composition, working principle and the common installation method of the shipborne underwater acoustic short baseline array detection and positioning system. Based on the underwater acoustic direction measurement and location algorithm and the underwater acoustic short baseline array detection and positioning system, the error sources affecting the accuracy of the underwater acoustic direction and positioning are analysed in great detail, and the influence of each error source is quantitatively analysed. In this paper, through theoretical calculation and analysis, the influence factors and the influence degree of the error sources on the direction and location measurement are obtained, the technical indexes of direction measurement accuracy and positioning accuracy of the system are estimated. The results of the error analysis of short baseline array system in this paper provide a theoretical basis for the operation of related underwater acoustic location systems at sea, and has important guiding and practical significance for the underwater target detection and positioning system design.

1. Brief introduction of the acoustic short baseline array detection and positioning system

1.1 System composition and operational principle

The shipborne of the acoustic short baseline array detection and positioning system described in this paper is mainly composed of underwater acoustic short baseline array, electronic compass, Beidou/GPS, display and processing computer. In this system, the electronic compass is used to measure the ship's course, Beidou/GPS is used to measure the position of the ship, the underwater acoustic short baseline array includes 2-3 receiving hydrophone array elements which is used to receive the signal of the target, the display and control processing computer is used to process the array element signal, the electronic compass data, Beidou/GPS data and the necessary system parameters data, so as to obtain the direction and position of the target.

The principle of the system is: first to calculate the direction of the target relative to the underwater acoustic short baseline array by measuring the time difference between the 2 array elements of the target sound source. Then, combined the data of electronic compass and Beidou/GPS to obtain the direction of the target in the geodetic coordinate system. Finally, the two-direction and cross-location method is adopted to locate the target sound source.[1] In fact, the 2 array elements of the underwater short baseline array can measure the direction of the target. The third array element can eliminate the false direction in the course of target direction measurement which can make the result of direction measurement more accurate.[2]

1.2 System installation

In order to obtain accurate results, all parts of the system need to be fixed on the ship. As shown in figure 1 (a), it is assumed that two underwater acoustic short baseline arrays for target direction measurement are vertically mounted with the bow line. As shown in figure 1 (b), the perpendicular direction of the transducer array coincides with the bow direction of the ship, and the electronic compass direction coincides with the bow direction. Beidou/GPS is installed at the midpoint of transducer array. This installation diagram is for reference only. When this installation method is not adopted, the calculation method needs to be changed accordingly.

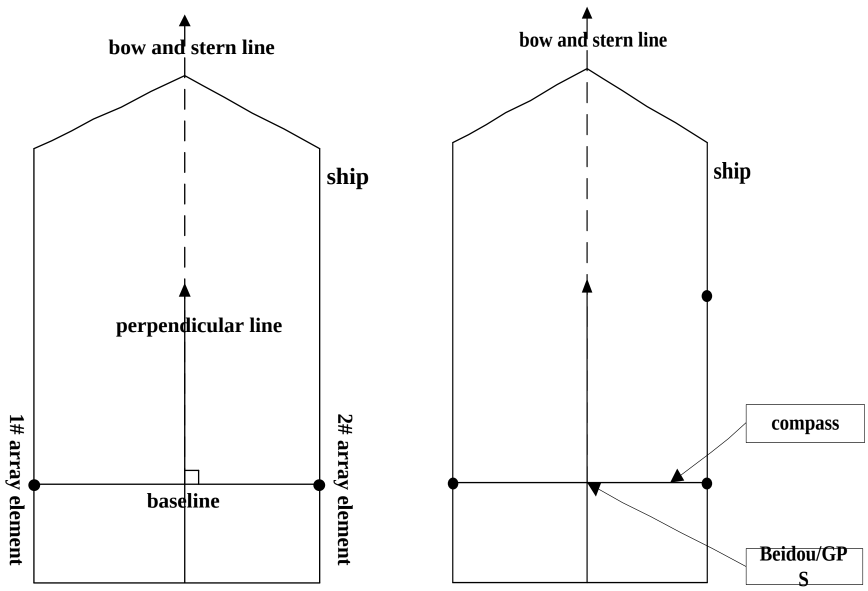

Figure 1. System installation diagram

2. System direction measurement accuracy analysis

2.1. The error source of the direction measurement

According to the direction measurement principle of the underwater acoustic short baseline array system, the main factors affecting the direction measurement error of the underwater acoustic short baseline array detection and positioning system introduced in this paper are as follows:[3]

(1) Assuming that the target is at infinite distance, the errors caused by the far-field approximate mathematical model;

(2) Errors caused by the measurement accuracy of the acoustic path difference;

(3) Errors caused by the measurement accuracy of electronic compass;

(4) Errors caused by the installation accuracy of short baseline array;

(5) Errors caused by the not parallel installation between the zero graduation of the electronic compass and the bow.

2.2. Errors caused by using far-field approximate mathematical model

According to the acoustic path difference between the target sound source and the two receiving array elements, the angle between the target and the baseline is calculated.[4] The mathematical model is shown in figure 2.

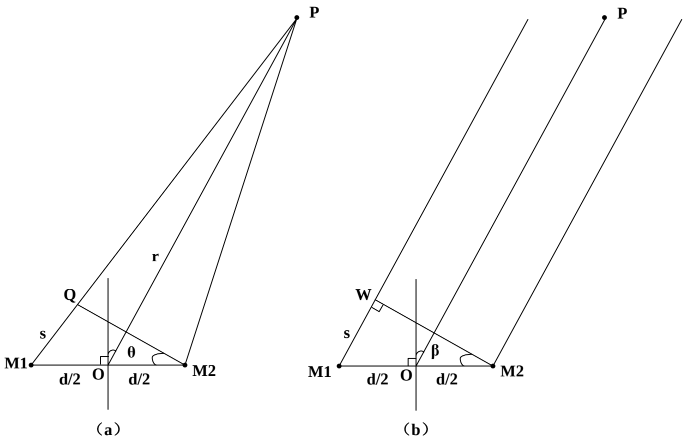

Figure 2. Mathematical model of the direction measurement by short baseline array

As is shown in the figure 2, the transducer receiving array is composed of hydrophone M1 and M2. And the distance between M1 and M2 is marked d; The midpoint of M1 and M2 is marked O; The target position is P, and the distance between P and O is r; Q is the point on t PM1 (or its extension line), PQ = PM2. The acoustic path difference from sound wave to M1 and M2 is s.
Figure 2 (a) is the relative bearing angle calculation model of near-field, PQ=PM2.
Figure 2 (b) is the relative bearing angle calculation model of far-field, WM2 ⊥ WM1.
The true location of the target is shown in figure 2 (a). Assuming that the distance between the target and O is R and the relative bearing angle of the target is θ, so the acoustic path difference s can be expressed as:

$$S = \sqrt{r \times r + d \times d / 4 + r \times d \times \cos(\theta)} - \sqrt{r \times r + d \times d / 4 - r \times d \times \cos(\theta)} \quad (1)$$

According to the approximate calculation model of the far-field model of figure 2 (b), the acoustic path difference s and the relative bearing angle β of the target can be obtained.[5] Then the relative bearing angle error of the target can be expressed as follows:

$$\theta_1 = \beta - \theta = \arcsin\frac{S}{d} - \theta \quad (2)$$

In the formula (2), θ is the real value of the target relative bearing angle, β is the calculation of the target relative bearing angle, S is the acoustic path difference, d is the length of the baseline.
Consider the following example, the range from the target sound source to the midpoint of the baseline is 50 meters and 1500 meters. The baseline length of short baseline array is 9 meters. The range of target relative bearing angle covers – 90 °~90 °. According to formula (2), the angle errors of direction measurement is calculated by the formula. Adopting the plotting method, the curves of the target direction measurement error and relative bearing angle change can be obtained, and which is shown in figure 3 and figure 4.

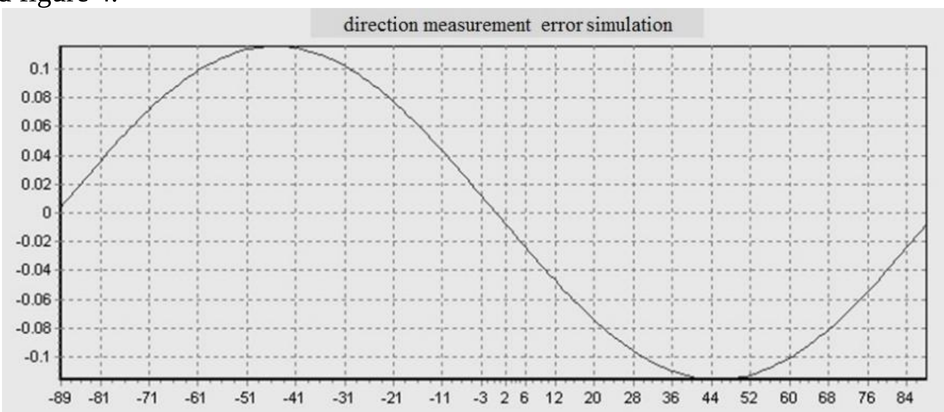

Figure 3. Measurement errors in all directions from the target to the center of the baseline at 50 meters

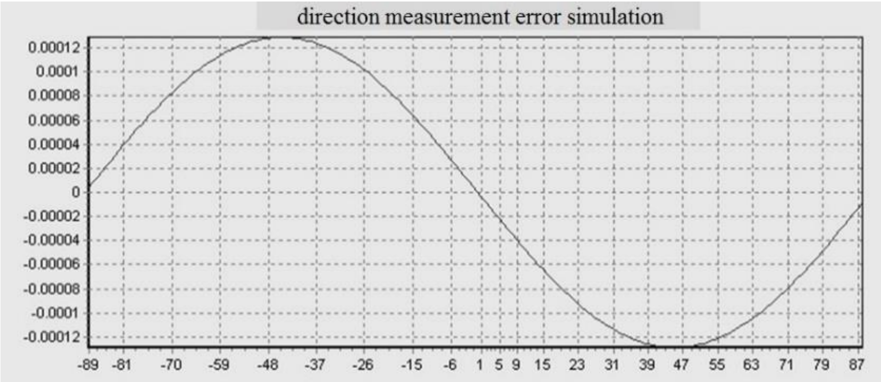

Figure 4. Measurement errors in all directions from the target to the center of the baseline at 1500 meters

For the target direction measurement error caused by the far-field approximate mathematical model, the following conclusions can be drawn:

(1) The farther the target sound source from the baseline, the smaller the error of direction measurement will be.

(2)When the distance of the target is fixed, the direction measurement error varies with the distribution of the target relative bearing angle according to the waveform of trigonometric function. The absolute value of the error is the largest when the target relative bearing angle is ±45 °and zero when the target angle is 0 °.

(3)When the distance of the target is 50 meters, the relative bearing angle is 45 °, the maximum direction measurement error introduced by the far-field approximate mathematical model is 0.116 °.

2.3. Errors caused by the accuracy of the acoustic path difference measurement

Due to the sound speed, the acoustic channel and the circuit delay, the errors marked Δs does exist in the process of the acoustic path measurement when the target signal arrives at the two receiving elements.[6] According to the mathematical model, the principle of the relative bearing angle error is shown in figure 5.

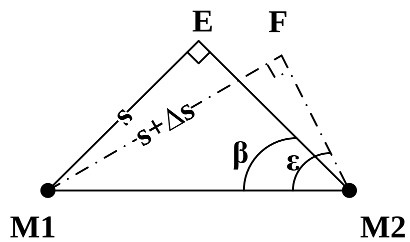

Figure 5. The influence of the test errors of the acoustic path difference on the calculation of the relative bearing angle

In the figure, EM1 is the true direction of the target, while FM1 is the measured target direction which is affected by the accuracy of the acoustic path difference measurement.[7]

According to the relative bearing angle formula, if the error of the acoustic path difference is s and the sound velocity is c, the direction measurement errors can be expressed as：

$$\theta_2 = \arcsin\frac{S+\Delta S}{d} - \arcsin\frac{S}{d} \tag{3}$$

From this formula, it can be seen that the accuracy of direction measurement of the equipment is related to S , d ,and ΔS . In the process of testing, parameter d is a fixed value, so parameter θ_2 varies with parameter S and ΔS .

Physically speaking, value S is determined by the target relative bearing angle, and value ΔS is determined by the accuracy of equipment acoustic path difference.

(1) Target relative bearing angle error analysis

Assuming that the measurement error of the path difference between two elements is 0.25 meters, the baseline length of the element is 9 meters, and the relative bearing angle of the target sound source relative to the baseline is from larboard-90 °to starboard-90 °, the resulting direction measurement error is shown in figure 6.

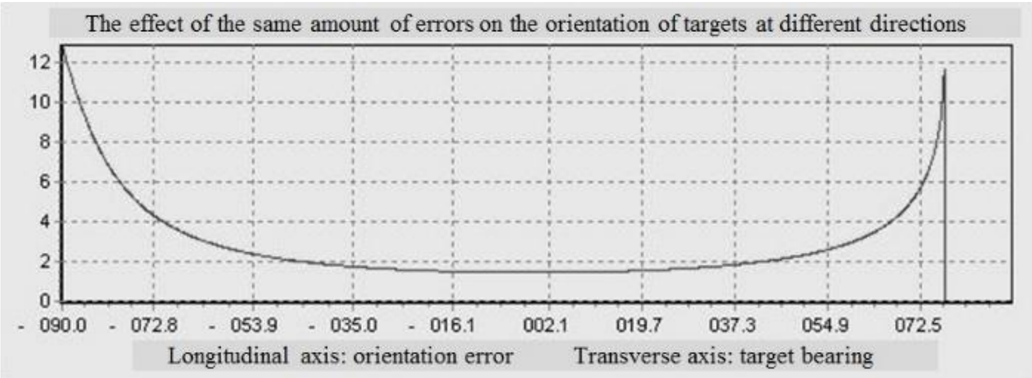

Figure 6. The direction measurement error caused by the acoustic path difference measurement error of 0.25 meters at different relative bearing angles

It can be seen from the figure that the measurement error of path difference lies the location near the stern line. That is, when the target relative bearing angle is 0 °, the direction measurement error is the smallest, and when the target angle is 90 °, the direction measurement error is the largest.

(2) The equipment measurement accuracy of the acoustic path difference analysis

The baseline length of the array element is 9m, the angle of the target is 45 °, and the measurement error of the path difference is 0-0.5ms. The relation between the direction measurement error and the path difference is shown in figure 7.

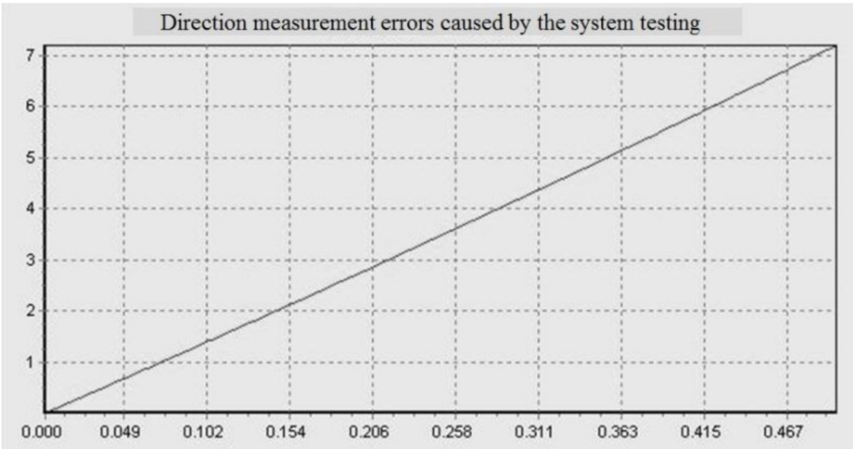

Figure 7. Direction measurement error caused by different acoustic path difference measurements in 45 °direction

(3) The joint effect of the target relative bearing angle and acoustic path difference on direction measurement

According to the operating parameters of the system, assuming that the range of the acoustic path difference is - 0.60 meters to 0.60 meters, the direction measurement errors caused by the target at different relative bearing angles are counted. The statistical results are shown in Table 1.

IOP Conf. Series: Earth and Environmental Science **369** (2019) 012004 doi:10.1088/1755-1315/369/1/012004

Table 1. Direction measurement error caused by the accuracy of the acoustic path difference measurement at different relative bearing angles

Acoustic path difference test error	Relative bearing angle				
	0	30 °	45 °	60 °	90 °
-0.60m	176.18	-4.32	-5.18	-6.93	-21.04
-0.45m	177.13	-3.26	-3.92	-5.31	-18.19
-0.30m	178.09	-2.18	-2.64	-3.62	-14.84
-0.15m	179.05	-1.10	-1.34	-1.86	-10.48
0.00m	0	0	0	0	0
0.15m	0.95	1.11	1.37	1.97	None
0.30m	1.91	2.23	2.77	4.07	None
0.45m	2.87	3.37	4.21	6.35	None
0.60m	3.82	4.52	5.69	8.86	None

"None" in the table represents the overflowed calculation which cannot get the target direction. The following conclusions can be drawn for the direction measurement errors caused by the measurement accuracy of the system's acoustic path difference:

(a)When the acoustic path difference is fixed, the direction measurement error of the target is the smallest when the relative bearing angle is 0 °, and the direction measurement error of the target is the largest when the relative bearing angle is 90 °.[8]

(b) When the target in the same relative bearing angle direction, the bigger the absolute value of path difference is, the bigger the absolute value of direction error will be.

(c) When the target angle is not more than 60 °and the measurement error of the acoustic path difference of the equipment is not more than 0.15 meters, the maximum direction locating error caused by the time measuring error of the equipment is about 1.97 °.

2.4. Errors caused by the precision of the electronic compass

As shown in figure 8, y' represents the true north direction, u represents the bow direction, γ represents the true course of the electronic compass, and the measurement error is $\Delta\gamma$, $\Delta\gamma = \gamma' - \gamma$. When calculating the direction of the target in geodetic coordinates, the heading measurement error caused by the accuracy of the electronic compass is Δγ.

$$\theta_3 = \gamma' + \beta - (\gamma + \beta) = \Delta\gamma \quad (4)$$

From this formula, we can see that the accuracy of electronic compass directly affects the direction measurement, the accuracy error of compass affects the error of direction measurement directly. Generally speaking, the measurement error of electronic compass is not more than 0.2 °.

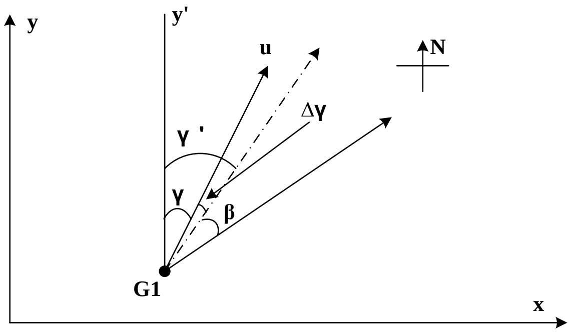

Figure 8. Direction measurement error caused by the accuracy of the electronic compass

2.5. Errors caused by the installation accuracy of the short baseline array

IOP Conf. Series: Earth and Environmental Science **369** (2019) 012004 doi:10.1088/1755-1315/369/1/012004

The array elements of the short baseline array in the system are independent of each other. After installation on the hull, it is necessary to measure the positions of every array elements. Because the measuring equipment and the algorithm is not absolutely accurate. The error of the direction measurement caused by the installation accuracy of transducer array elements are shown in figure 9 and figure 10.

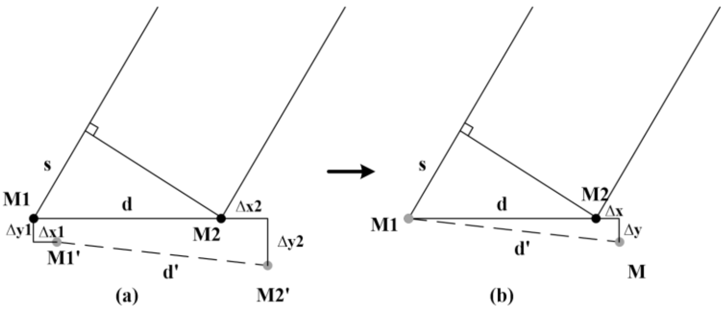

Figure 9. Measurement error caused by the accuracy of the transducer array installation

In figure 9 (a), M1 and M2 are the true positions of the transducer elements and $M1', M2'$ are the measured values of the position of the transducer elements. The errors between the measured values and the true values are x1, y1, x2, y2 respectively.
In order to simplify the error sources, the measurement errors are transformed, as shown in figure. 9 (b). Translating elements $M1'$ and $M2'$, coincide $M1'$ with M1, move M2 to M, then Δx=Δx2-Δx1, Δy=Δy2-Δy1.
As shown in figure. 10, the influence of single element position measurement error on direction measurement is simplified. M is the measured value of M2. The connection of M and M1 is perpendicular to the stern line, the spacing of the elements is d', and the angle between the elements and the baseline is φ.

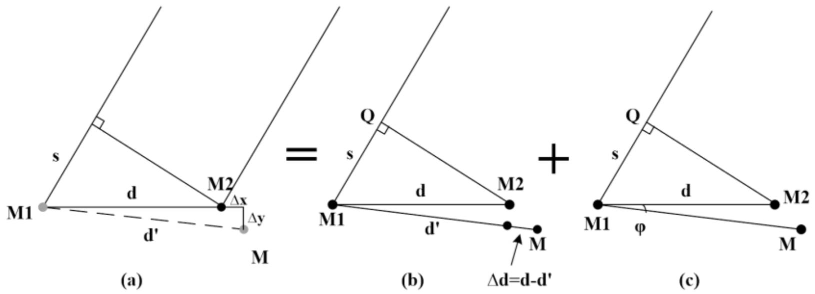

Figure 10. Measurement error caused by the installation of the accuracy of the single transducer array element

As can be seen from the figure, the error of orientation measurement caused by the accuracy of element installation is as follows:

$$\begin{aligned} \theta_4 &= \varphi + \arcsin\frac{s}{d+\Delta d} - \arcsin\frac{s}{d} \\ &= \varphi + \arcsin\frac{c \times t}{d+\Delta d} - \arcsin\frac{c \times t}{d} \end{aligned} \tag{5}$$

From this formula (5), we can see that:

(a) The baseline angle error caused by the transducer element installation is directly superimposed on the target direction.

(b) The system direction measurement error caused by the transducer element installation accuracy are determined by the acoustic path difference（s）, the baseline length measurement error （Δd） and the baseline length （Δd）.

As can be seen from formula (5), the transducer element installation error is divided into two parts, as shown in figure 5, Δd and φ. When the transducer array elements are installed at the keel of the hull, Δy usually is less than 1 cm, which is negligible. Next, the influence of direction measurement error （Δd） is analyzed as follows.

In the actual test process, the baseline length d is a fixed value, and the acoustic path difference s is determined by the target relative bearing angle.[9] The baseline length is 9 meters, the sound velocity is 1500 m/s, the error range of baseline length measurement is - 0.2 meters - 0.2 meters, and the relative bearing angle varies from 0 °to 90 °. The direction measurement error is concluded in Table 2.

Table 2. The influence of the installation accuracy of the short baseline installation on calculating the relative bearing angle

Transducer array installation error (m)	Direction measurement error（° ）				
	0 °	30 °	45 °	60 °	90 °
-0.2	0	0.75	1.32	2.34	None
-0.1	0	0.37	0.65	1.13	None
0	0	0	0	0	0
0.1	0	-0.36	-0.63	-1.07	-8.50
0.2	0	-0.72	-1.23	-2.09	-11.97

For the direction measurement error caused by the installation accuracy of short baseline, the following conclusions can be drawn:

(a) The bigger the absolute value of baseline length measurement error is, the bigger the direction measurement error will be.

(b) The direction measurement error caused by baseline length measurement error increase monotonously in the range of 0 °-90 °. The minimum is at 0 °and the maximum is at 90 °.

(c) In the range of 60 °relative bearing angle when the length measurement error of array elements is no more than 0.1m after installation, the maximum direction measurement error is about 1.13 °.

2.6. Errors caused by the installation accuracy of electronic compass

When the zero-degree direction of the electronic compass is parallel to the bow direction, the installation position of the electronic compass on the ship has no effect on the course measurement. When the zero-degree direction of the compass is not parallel to the bow direction, the error will be existed between the course value provided by the electronic compass and the true value. As shown in figure 11, y' is true north direction, u is bow direction, w is zero-degree direction of electronic compass, and ξ is angle difference between bow direction and zero-degree direction of electronic compass.

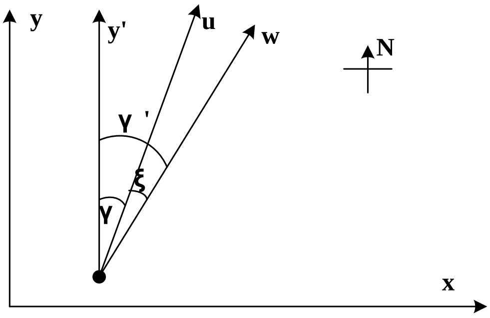

Figure 11. The influence of the installation accuracy of electronic compass on heading measurement

The data provided by electronic compass is γ', the true heading value is γ, and the introduced error of the direction measurement is as follows:

$$\theta_5 = \xi \tag{6}$$

After the installation of electronic compass, using compass data as the true value of course to compensate electronic compass data which can greatly reduce the error of course measurement caused by the installation of electronic compass.[10] This error is the compass reading error only, usually less than 0.1 °.

2.7. The comprehensive system direction measurement accuracy

According to the analysis results of the above errors, it can be seen that the measurement accuracy of the path difference and the array installation accuracy have great influence on the system direction measurement accuracy. Under the current technical conditions, the system direction finding error is no more than 3.5 °

3. System positioning accuracy analysis

3.1. Sources of system positioning errors

According to the positioning principle of underwater acoustic short baseline array, the positioning error is related to the following factors:

(1) Beidou/GPS measurement accuracy;

(2) System direction measurement accuracy.

3.2. Positioning error induced by Beidou/GPS

As shown in figure 12, P is the target sound source, G1 is the first search site, and G2 is the second search site.

Because of the Beidou/GPS measurement error, the measurement results of the first search site G1 is located at point G (a, b), and the coordinate measurement errors are Δa and Δb. Finally, the target sound source is located at point F. Line PF is the positioning error introduced by Beidou/GPS.

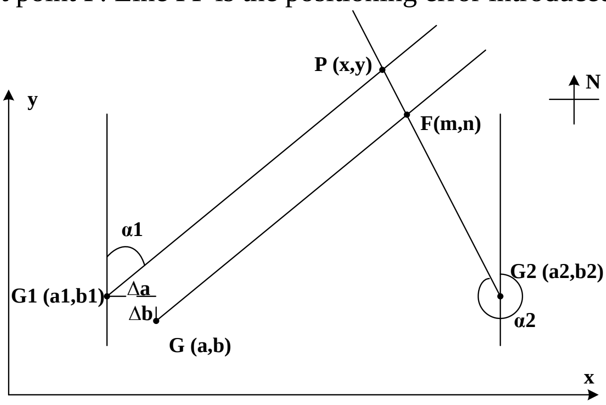

Figure 12. Positioning errors caused by Beidou/GPS system error

As shown in figure 13, PF is the line between two parallel lines PG1 and FG, the distance between the two parallel lines is h, and the positioning accuracy of Beidou/GPS is σ. Considering the values of Δa and Δb, the PF length formula is as follows:

$$\Delta r = \left|\frac{h}{\sin\alpha 3}\right| = \left|\frac{\Delta\alpha * \cos\alpha 1 - \Delta b * \sin\alpha 1}{\sin(2\times\pi - (\alpha 2 - \alpha 1))}\right| = \left|\frac{\Delta\alpha * \cos\alpha 1 - \Delta b * \sin\alpha 1}{\sin(\alpha 2 - \alpha 1)}\right| \qquad (7)$$

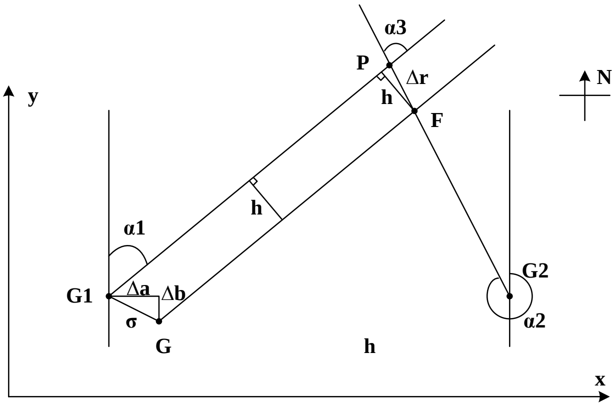

Figure 13. Positioning errors caused by Beidou /GPS system

According to formula (7), the accuracy of Beidou/GPS has a direct impact on the azimuth angle of two detection operation sites. The larger the value of $\sin(\alpha 2 - \alpha 1)$ is, the smaller the positioning error will be. In the process of using the system, we can select reasonable locating sites to make the locating rays perpendicular to each other, that is $\sin\alpha 3 = 1$, to reduce the locating error.
It can be seen from figure 13, h≤σ.
So, the formula (7) can be simplified to:

$$\Delta r \le \sigma \qquad (8)$$

According to formula (8), the resulting positioning error is less than Beidou/GPS positioning accuracy.

3.3. Location error induced by direction measurement error

When the underwater acoustic short baseline array locates the target by the two-direction and cross-location method, the location error caused by direction error is shown in figure 14. In the figure, G1 is the first detection site, G2 is the second detection site, P is the true location, θ is the direction measurement error, and the shadow area is the location error. Point F is the farthest site from point P in the shadow area, PF=δ.

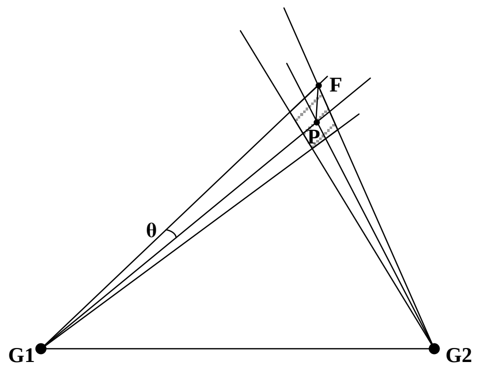

Figure 14. Blurred location area caused by the accuracy of the system direction measurement

The geometric relationship is shown in figure 15.

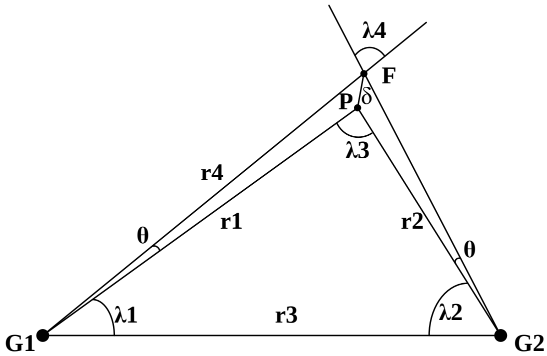

Figure 15. Positioning error caused by the accuracy of direction measurement of the system

According to the geometric relations, the equations can be obtained as follows:

$$\begin{cases} \lambda_1 = \arccos\dfrac{r_1\times r_1 + r_3\times r_3 - r_2\times r_2}{2\times r_1\times r_3} \\ \lambda_2 = \arccos\dfrac{r_2\times r_2 + r_3\times r_3 - r_1\times r_1}{2\times r_2\times r_3} \\ \lambda_3 = \arccos\dfrac{r_1\times r_1 + r_2\times r_2 - r_3\times r_3}{2\times r_1\times r_2} \\ \lambda_4 = \pi - \lambda_1 - \lambda_2 - 2\times\theta \\ r_4 = \dfrac{r_3\times\sin(\lambda_2+\theta)}{\sin\lambda_4} \\ \delta = \sqrt{r_1\times r_1 + r_4\times r_4 - 2\times r_1\times r_4\times\cos\theta} \end{cases} \tag{9}$$

The maximum positioning error is δ.
Among them, r1、r2、r3、λ1、λ2 are measured values.
From the formula (9), we can see that $\sin\lambda_4$ is the largest value and δ is the smallest value. When the angle between two positioning rays (PG1 and PG2) approaches 90 degrees, the positioning error is much smaller. When the two positioning rays are perpendicular to each other, the positioning error is the smallest.
It is assumed that the distance between the two detection sites and the underwater target is 500 meters. The maximum positioning error δ varies with the direction measurement accuracy and the distance between the two detection sites as shown in Table 3.

Table 3. The influence of direction measurement accuracy and the distance of the detection sites on location error

Distance(m) / Relative bearing angle (°)	100	200	300	500	707.1
1°	105.62	47.72	30.80	18.00	12.562
2°	267.58	105.32	65.47	37.17	25.586
3°	547.57	176.28	104.81	57.64	39.11
3.5°	781.25	218.32	126.55	68.41	46.07
4°	1149.22	265.91	149.87	79.56	53.16

When the distance between the two detection sites is 707.1 meters, the two locating rays are perpendicular to each other.

When the system's direction measurement accuracy is 3.5°, Beidou/GPS positioning accuracy is 1 m, the positioning error of the system is 46.07+1=47.07(meters), and the positioning accuracy is less than 10% of the detection distance.

4. Conclusion

In this paper, the error sources of underwater acoustic short baseline array positioning system are quantitatively analyzed in great detail, which provides theoretical basis and technical guidance for the offshore detection and positioning system operations. In this paper, two directions are used to locate the target. In practical operations, more precise positioning results can be obtained by increasing the number of detection sites and crossing multiple directions.

Although the location precision and technical maturity of the underwater short baseline location method are very high, the location precision is easily and greatly influenced by the installation method and the installation platform of the distributed array element. So the further studies of the underwater acoustic short baseline array detection and location system will focus on the improvement of the precision of the underwater acoustic short baseline array detection and location system.

5. References

[1] PHILIP DIPHS D R C. *An Evaluation of USBL and SBL Acoustic Systems and the Optimisation of Methods of Calibration-Part 2*. The Hydrographic Journal, **2003**, p237-238.

[2] Zhang Yu, Ji Xiaoyan, Zhang Dan. *The principle and error analysis of short baseline underwater positioning*. Ship Electronic Engineering, **2017,37(7)**, p41-45.

[3] Mikhail Arkhipov. *An algorithm for Improving the Accuracy of Z-Coordinate Determination for USBL Systems*. WSEAS Transactions on Systems ,**2008,7(7)**, p298-309.

[4] Janos Sallai, Will Hedgecock, Peter Volgyesi, Andras Nadas, Gyorgy Balogh, Akos Ledeczi. *Weapon classification and shooter localization using distributed multichannel acoustic sensors*. Journal of systems architecture, **2011,10(10)**, p869-885.

[5] Tian Tan. *Underwater positioning and navigation technology*. Beijing: National Defense Industry Press, **2007,** p8-10.

[6] Gazzah H. *Optimum Antenna Arrays for Isotropic Direction Finding*. IEEE Transactions on Aerospace and Electronic Systems, **2011,2(2)**, p1482-1489.

[7] KILFOYLE D.B. BAGGEROER A.B. *The state of the art in underwater acoustic telemetry*[J]. IEEE Journal of Oceanic Engineering: A Journal Devoted to the Application of Electrical and Electronics Engineering to the Oceanic Environment, **2000,1(1)**, p4-27.

[8] CHITRE M. *A high-frequency warm shallow water acoustic communications channel model and measurements*.The Journal of the Acoustical Society of America, **2007,5(5)**, p2580-2586.

[9] ILTIS R.A., ANDERSON K.L. *A consistent estimation criterion for multisensor bearings-only tracking*. IEEE Transactions on Aerospace and Electronic Systems, **1996,1(1)**, p108-120.

[10] ANDERSON K.L, ILTIS R.A. *A distributed bearings-only tracking algorithm using reducedsufficient statistics*. IEEE Transactions on Aerospace and Electronic Systems, **1996,1(1)**, p339-349.

IOP Conf. Series: Earth and Environmental Science **369** (2019) 012005 doi:10.1088/1755-1315/369/1/012005

Numerical simulation and analysis of the sink-stability for the deep-sea walking & swimming robot

Wei Wei[1], Xinliang Wang[1], Kang Zhang[1] and Hong Chen[1]

1 Wuhan Second Ship Design & Research Institute, Wuhan 430205, China
E-mail: 15307141325@163.com

Abstract. A brief introduction to the design concept of deep-sea walking & swimming robot is provided in this paper. And based on the computational fluid dynamics (CFD) method, a hydrodynamic numerical simulation model for the robot body is established. Then the flow field under different body inclination conditions and different ocean currents is numerically simulated by ANSYS Fluent, and the curves of resistance, lift and pitching moment with inclination are obtained. At the same time, the stability analysis method for deep-sea walking & swimming robot is established by combining dynamic stability margin method (DSM), and the stability of the walking & swimming robot is analysed. The stability of the tilting activity threshold is obtained under different inflow environments.

1. Introduction

With the increasing demand for energy all over the world and the difficulties for finding resources in land and shallow water, the competition for marine resources has shifted from offshore to deep water. Deep-sea submersible is important Marine engineering equipment for the exploration and development of deep-sea resources. By carrying various electronic devices and mechanical equipment, it can quickly and accurately work in the complex environment of the deep sea for resource exploration, scientific research and special military use.

Autonomous underwater vehicles (AUVs) are typical deep-sea submersibles. They can independently accomplish various tasks such as detection or exploration with low risk, and play an important role in maritime activities. However, with the demand for vehicles with long-range, large-depth and multi-functional characters, Wuhan Second Ship Design & Research Institute proposed a concept of Deep-sea Walking & Swimming Robot that had the ability of both cruising in deep sea and crawling on the sea bed[1]. As shown in Fig. 1, it can realize a wide range of manoeuvres through the propeller very fast, and loading near the working area. Then, it can use multi-feet to accurately move to the working place on the complex seabed. So it can meet the needs of exploration, sampling, and mechanical operations in the deep sea floor. The robot combines the high-efficiency, wide-range characters of the unmanned autonomous vehicle (AUV) and the precise operating capability of the remotely operated vehicle (ROV). It has the characteristics of high stability, low energy consumption and strong environmental adaptability.

It's important for the robot to keep steady in the current environment during the operation. So an analysis of the stability of the robot after it has landed on the seabed called "sink-stability" in this paper is made.

Figure 1. The Deep-sea Walking & Swimming Robot.

2. Numerical method

2.1. Simulation mode and grid generations

In this paper, in order to save computing resources, the simulation is conducted on a simplified model as shown in Fig. 2. The propeller and frame structure are both ignored, and the distance between bottom of the body and ground is 500mm.The The length, width and height of the robot body are 2500mm, B=1500mm, D=1000mm. Six legs are simplified as cylinder, whose diameter is 140mm and the length of two sections is 400mm and 700mm, respectively.

As shown in Fig.3, the dimensions of the calculation domain are -10L<x<25L， -10L<y<10L， -1.2L<z<10L（L is the height of the robot body）， respectively. The unstructured tetrahedral mesh is used for the calculation, and at the area around the interfaces, the grids are well refined. With the study of grid indifference, the final mesh number of the calculation domain is 2.5 million.

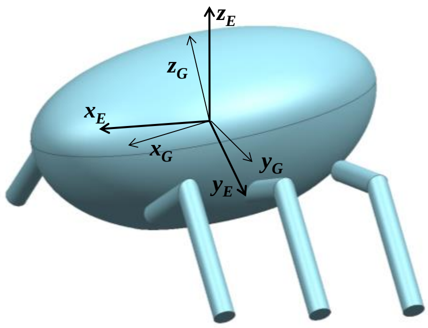

Figure 2. Calculation model.

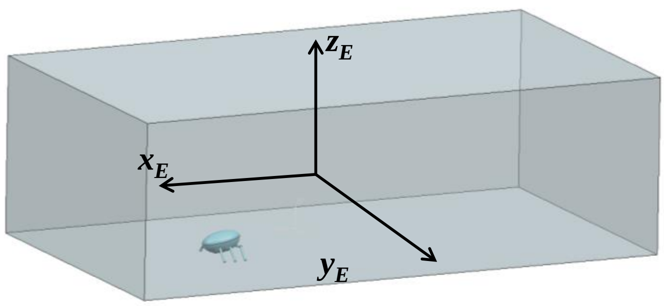

Figure 3. Calculation domain.

2.2. Governing equation

In this paper, the calculations are conducted based on Reynolds Averaged Navier-Stokes equations. The governing equations are as follows [2]:

$$\partial u_i / \partial x_i = 0 \tag{1}$$

$$\frac{\partial u_i}{\partial t} + u_j \frac{\partial u_i}{\partial x_i} = -\frac{1}{\rho}\frac{\partial p}{\partial x_j} + \frac{1}{\rho}\frac{\partial}{\partial x_j}\left(\mu \frac{\partial u_i}{\partial x_j} - \rho \overline{u_i^{'}}\,\overline{u_j^{'}}\right) \tag{2}$$

Where u_i 、 u_j 、 p are time-averaged variables; $\partial\left(-\rho \overline{u_i^{'}}\,\overline{u_j^{'}}\right) / \partial x_j$ is Reynolds stress term; ρ 、 μ respectively are density and hydrodynamic viscosity coefficient.

3. Force analysis in current environment

3.1. Analysis model

The coordinate system of the simulation model was established as shown in Fig. 2. The x_E- y_E- z_E is the reference coordinate system, and the x_G- y_G- z_G is the body coordinate system. In this paper, it is assumed that the centre of buoyancy coincides with the centre of gravity for simplification, and they both at the origin of body coordinate.

As shown in Fig. 4, the force acting on the robot includes: gravity W, buoyancy B, drag force F_D , lift force F_L, and M_h is defined as pitching moment. The angle between x_G and x_E is defined as pitch angle θ, and the clockwise sense as positive. The analysis assumes that the ocean current flows are uniform and constant, considering near-ground effects.

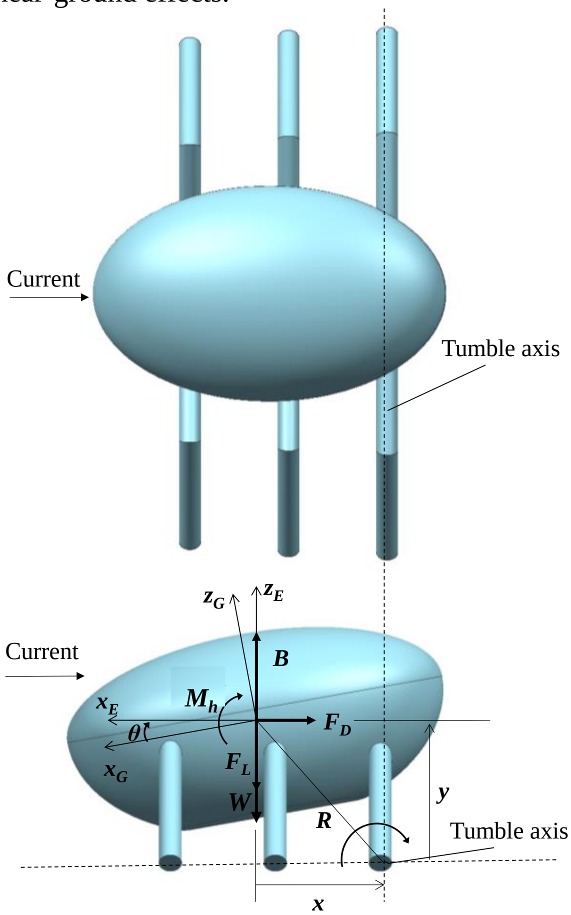

Figure 4. Force diagram.

IOP Conf. Series: Earth and Environmental Science **369** (2019) 012005 doi:10.1088/1755-1315/369/1/012005

3.2. Simulation result

In this paper, the numerical simulations were performed for the force acting on the robot in current environment. The pitch angle of the robot varies from -30 °to 30 °and the current velocity varies from 0 to 1.5m/s.

Fig. 5 shows the simulated flow around the body when the pitch angle is 30 °. And as shown in Fig. 6 when the current velocity is 1m/s, the drag force varies from 329N to 598N, and the lift force as well as the pitching moment has an approximate linear relationship with the pitch angle.

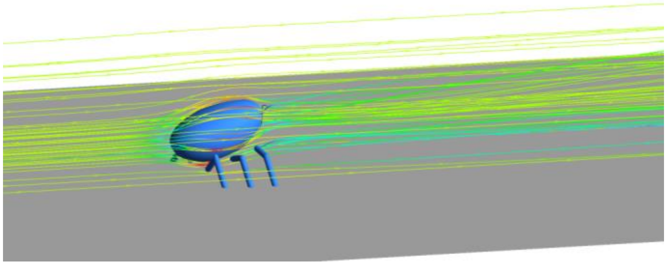

Figure 5. Flow around the robot in current (θ=30 °).

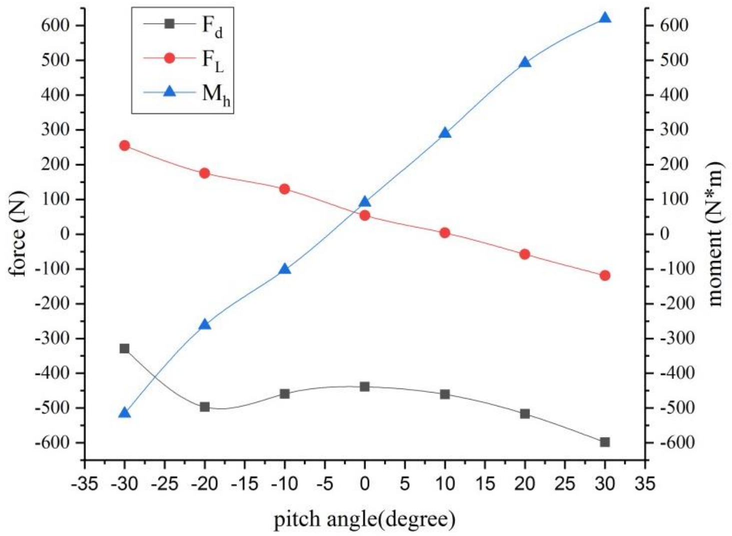

Figure 6. Hydrodynamic force and moment in current(v=1m/s).

4. Stability analysis in current environment

4.1. Stability judgment method

The sink-stability analysis of the deep-sea robot can be conducted based on the research achievements of land multi-foot robots which have been well studied in recent years. The stability of multi-foot robot usually includes static stability and dynamic stability. The study of static stability started earlier and developed more. As early as 1968, R B Mcghee et al. [3] proposed the centre of gravity shadow method, and other static stability methods developed afterwards were all based on it, such as static stability margin method [4], energy stability margin method, [5], normalized energy stability margin method [6] and so on. With the rise of walking robots, especially the rise of bipedal walking robots, the requirements for dynamic stability of robots are getting higher and higher, and the research on dynamic stability is mostly concentrated in this field. For the dynamic stability problem, LIN and SONG [7] proposed the concept of Dynamic Stability Margin (DSM). In this paper, based on the characteristics of the Deep-sea Walking & Swimming robots, the DSM method is used to analyze the stability characteristics of the robot in ocean current disturbance environment.

The Dynamic Stability Margin (DSM) is defined as the minimum moments of each rotating axis in the support polygon. The normalized mathematical expression is as follows.

$$S_{\mathrm{DSM}} = \min_{\mathrm{i}}\left(\frac{M_{\mathrm{i}}}{mg}\right) = \min_{\mathrm{i}}\left(\frac{e_i \cdot \left(F_E \times P_i + M_E\right)}{mg}\right) \tag{3}$$

Where P_i is the position vector from the centre of gravity to the i-th support foot, e_i is a unit vector that revolves around the support polygon in the clockwise sense, F_E and M_E are the resultant force and moment of robot/ground interaction.

When all the moments are positive which means $S_{\mathrm{DSM}} > 0$, the system is stable.

As for the deep-sea robot in this paper, if we assume that the heading of robot is aligned with the current direction, the stability margin of deep-sea walking robot in current can be written as follows, and the notations follow the definition above.

$$S_{\mathrm{DSM}} = \left(\frac{M}{mg}\right) = \left(\frac{\left(F_D + F_L + W + B\right) \times R + M_h}{mg}\right) \tag{4}$$

4.2. Stability in current environment

In this paper, the velocity of the ocean current varies from 0 to 1.5m/s, and the pitch angle of the body varies from -30 °~30 °. The difference between gravity and buoyancy is 500N. It can be seen from the previous analysis that when the stability margin parameter S_{DSM} is positive, the corresponding working condition is stable, and vice versa. And when $S_{\mathrm{DSM}} = 0$, the corresponding angle will be the critical safety pitch angle.

Fig. 7 shows the variation of the stability margin parameter S_{DSM} with the body pitch angle at different inflow speeds when the lateral distance of the tumble axis is 1m. It can be seen from the figure that when the incoming flow velocity is 0 m/s, it is mainly determined by the difference between the weight and the buoyancy. As the inflow velocity increases, the amplitude changes sharply with the angle. When the flow velocity is 1 m/s, the body begins to tip over when θ = -5 °. In addition, it can be known from the curve that when the flow velocity v ⩽ 0.5 m / s, the body is stable in the range of -30 ° ~ 30 ° . When θ ⩾ 6° , the body can remain stable within the flow velocity varies from 0 to 1.5m/s.

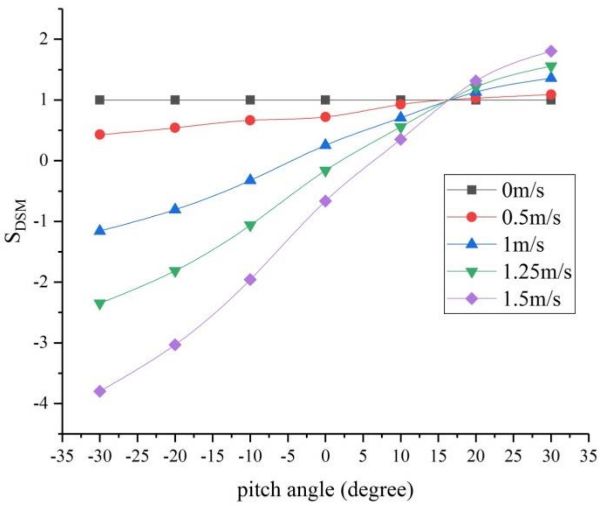

Figure 7. Dynamic stability margin (*x=1m*).

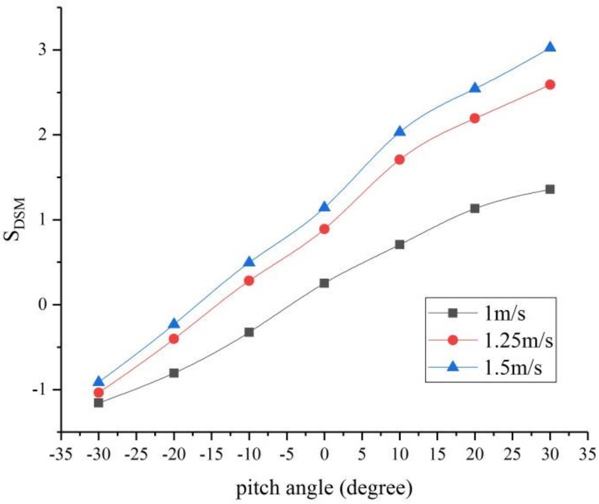

Figure 8. Dynamic stability margin (*v*=1m/s).

Fig. 8 shows the stability margin as a function of the pitch angle of the body when the position of the rear foot (or the tumble axis) is different (the value of x is different). It can be seen from the analysis that as the value of x is larger, the corresponding critical safety pitch angle is larger. When x=1m, the corresponding critical overturning angle is -5 °, and when x=1.5m, the critical overturning angle is -17 °.

It can be seen that, within the allowable range, the more backward the hind foot is, the higher the stability of the body in the ocean current disturbance.

5. Conclusion

In this paper, the force and stability of the Deep-sea Walking and Swimming robot in the ocean current environment are analysed, and the following conclusions are obtained:
(1) When the current velocity is 1m/s, the resistance value varies from 329N to 598N, and the lift force as well as the pitching moment has an approximate linear relationship with the pitch angle.
(2) when the lateral distance between the tumble axis and the centre of gravity is 1m, and the flow velocity $v \leqslant 0.5m/s$, the body is stable with the pitch angle of the body ranging from $-30°$ to $30°$. When the pitch angle $\theta \geqslant 6°$, the body can remain stable within the flow velocity varies from 0 to 1.5m/s.
(3) Within the allowable range, the more backward the rear foot is, the body is more stable in the ocean current disturbance. Therefore, in order to ensure the stability of the robot in the ocean current environment, the distance between the rear foot and the centre of gravity can be increased as much as possible.

6. References

[1] Chen H, Wang X L, Wei W, Liu Z, Ma Z, Zheng C and Tang P P 2018 Concept and Key Technology Analysis of Deep-sea Robots *Chinese Ship Research* **6** p19-26
[2] Jing S R and Zhang M Y 2001 *Fluid Mechanics* (China: Xi'an Jiaotong University Press) p68-72
[3] Mcghee R B and Frank A A 1968 On the stability properties of quadruped creeping gaits *Mathematical Bioscience* **3** p331-351
[4] McGhee R B and Iswandhi G I 1979 Adaptive Locomotion for a Multilegged Robot over Rough Terrain *IEEE Transl. on Systems, Man, and Cybernetics* **4** p176–182
[5] Messuri D A and Klein C A 1985 Automatic body regulation for maintaining stability of a legged vehicle during rough-terrain locomotion *IEEE Journal of Robotics and Automation* **RA-1(3)** p132-141
[6] Hirose S, Tsukagoshi H and Yoneda K 1998 Normalized energy stability margin generalized stability criterion for walking vehicles *Proc. of Int. Conf. Climbing and Walking Robots* **11** p71-76
[7] Lin B S and Song S M 1998 Dynamic modeling stability and energy efficiency of a quadrupedal walking machine *Journal of Robotic System* **1(4)** p657-670

Acknowledgments

The work was supported by the National Key Research and Development Program of China (2016YFC0301700).

Chapter 3:
Ship Engineering

Desalination for drinking water demonstration project: a case study at Sichang Island, Thailand

R Sompop[1], I Takehiro[2], C Petchporn[3], T Fijita[2] and K Nakajima[2]

1 Senior Researcher, Aquatic Resources Research Institute, Chulalongkorn University, Bangkok 10330, Thailand
2 SANSO ELECTRIC CO., LTD. 1-1-1 Aoyamakita, Himeji city, Hyogo, Japan
3Associate Professor, Department of Environmental Engineering, Chulalongkorn University, Bangkok 10330, Thailand
E-mail: rsompop@chula.ac.th

Abstract. "Desalion", a compact and movable SANSO ELECTRIC Company desalination machine was implemented for 617 days and tested at Sichang Marine Science Research Station (Aquatic Resources Research Institute, Chulalongkorn University), Sichang Island, Cholburi Province, Thailand. The utilization ratio of actual working days and effective working days was 76%. 483 tons of pure fresh water was produced for the utilization of 333 people. Fresh pure water and brine water were of WHO standards (2011) and Thailand's drinking water quality standard (maximum allowable concentration). Brine water outlet and seawater inlet salinity experienced a 23.9% changed but suitable for coral and abalone cultured. Apart from its aquatic culturing use, the water from "Desalion" can also be used for agriculture and human consumption considering its 1000 liters per day production capability. This research also founded that "Desalion", with more sample size, can prove to be a greatly useful tool in water production for areas or islands where fresh water access is scarce.

1. Introduction

Desalion of SANSO ELECTRIC Company compact and movable desalination machine is a small water management system recommended by the WHO in providing a safe and secure drinking water, with its small size, light weight and low power consumption, to remoted islands and areas in developing countries where installing pipelines proved to be difficult. The Desalion is capable of producing 1000 litres of purified water per day which can be sufficient for a community of 200 to 300 people. The installation process is simple and easy, and the machine can start working with a push of a button. Additionally, the Desalion could possibly be utilized in commercial uses such as selling purified water. There is also a possibility of agricultural uses by combining the machine with drip farming or other suitable agriculture methods. While producing 1000 litres of fresh water, the Desalion uses 1.4 kWh of energy and emitted 53 dB of average noise level. The Desalion uses 10 tons of seawater to produce 1000 litres or a ton of fresh water. In other words, its recovery rate is 10%. The Desalion also removes boron from seawater, reducing its concentration to the point that it passes the Japan's standard which is less than half of the WHO's. Generally, there are two methods of utilizing the Desalion in remoted areas. First, by bringing seawater to the Desalion-installed site to produce purified water and the second, by installing the Desalion near the sea to produces the water.

Sichang Island, Cholburi Province, Thailand is far from mainland there is no fresh water reservoir. The island composted on carbonate rock with a little ground water pond but not enough from increased people. [1,2]. Local people used rainy storage each house, buy fresh water from mainland

and local Sichang island municipal office distributed fresh water sometime. In 2004 the 250 cubic meter per day desalination plant started [3] but stopped in 2014. In 2016 the new 1,000 cubic meter per day desalination was started in Sichang island [4]. The new desalination plant produced fresh water with some salt contaminated caused heater and pipe line device broken.

Chulalongkorn University, Thailand are researching the influence of concentrated wastewater on marine organisms. A part of that research is a research facility at Sichang island, Chonburi province, Thailand, called Sichang Marine Science Research Station which is remoted from the main land causing fresh water insufficiency. A Desalion was installed at the station with aim to test its performance in real-life situation. The fresh water was utilized and other by product of the purifying process, brine water and seawater with higher concentration was also tested, by using them to grow specific types of plants and for coral and abalone culturing respectively.

2. Methodology

A Desalion was installed at the Sichang Island Research Station, Cholburi province, Thailand (a part of Aquatic Resources Research Institute, Chulalongkorn University) along with a seawater inlet pump and pipelines, storage tanks for seawater and fresh water, fresh water pipelines, brine seawater outlet, and seawater overflow 'Figure 1-2'. Specification of Desalion as indicated in Table 1. The Desalion took in seawater for desalination resulting in three types of water including fresh high-quality water, brine water, and seawater with higher salinity. For the sake of testing its performance and capability, the Desalion was kept running for 24 hours straight every day. Every maintenance was recorded. Several other parameters were monitored for 12 months including water quality and quantity of the fresh water outlet and brine outlet, the status of storage tanks, and the water quality and quantity of the seawater inlet [5,6,7].

Figure 1 "Desalion" test desalination system.

Figure 2 Desalination system at Sichang Marine Science Research Station, Thailand.

Table 1 Specification of "Desalion" SANSO ELECTRIC Company, Japan [8]

Subject	Detail
Desalination performance	Max 0.7 L/min/max 1.0 ton/day
Water quality	Pass Water act Water Quality standard 51 items in Japan
Rated voltage	Device 200-220Volt, or 3K VA/from 380V to 200V
Rated current	Device 5.3A or input transformer 3.2(A)/380V
Power consumption	1,400W
Noise level	53(dB-A)/3m nearly equal to the idling noise of a compact car
Safety protection	Earth leakage breaker, overcurrent of motor, excessive water pressure
Alarm	Insufficient water supply, insufficient purified water discharge, insufficient waste water discharge
Size	W910mm (including valves 1,100mm) *D:610mm*H:1,030mm
Weight	150 kg
Maintenance	Micro filter: every week to every month (depend of the seawater condition: turbidity), High-pressure pump ever year, RO elements: every year; other: every year

3. Results and discussion

Water Quality Monitoring: Fresh water outlet were monitored by volume (litres per day), turbidity (ppm), conductivity (mS), pH, total dissolved solid, hardness, and chloride and after 12 months of operation by Governmental services and private companies authorized for water quality analysis (Table 2-4). Summary of the test operation period as indicated in Table 5. Coral and Abalone tested in brine water storage as shown in 'Figure 3'.

Table 2 SANSO ELECTRIC Company "Desalion" "fresh water pure" quality compare to Thailand Standards.

Parameter	Pure fresh water: Sanso "Desalion" (this project)		Pipe water standard [9]	Drinking Water Quality Standard in Thailand (maximum allowable concentration) [10]
	Provincial Waterworks Authority Region 1 (Cholburi Province) Water quality	Water Analysis Center Company Limited		
Physical:				
-Appearance colour (Pt-Co Unit)	nd[a]	7.4	15	15
-Taste and odour	nd[a]	nd[a]	not observed	no objectionable
-Turbidity (NTU)	0.26	0.36	4	no objectionable
-pH	7.5	-	6.5-8.5	9.2
-Conductivity(mS/cm)	0.212	-		-
Chemical:	2			
-Total dissolved solid (mg/l)	30	<25	600	1,500
-Calcium (mg/l)	2	<1.0		-
-Iron (mg/l)	0.01	-	0.3	1.0
-Manganese (mg/l)	nd[a]	<0.04	0.3	0.5
-Copper (mg/l)	nd[a]	<0.05	2.0	1.5
-Zinc (mg/l)	nd[a]	-	3.0	15.0
-Total hardness as $CaCO_3$ (mg/l)	14	5	300	-
-Total Alkalinity(mg/l)	4	-	-	-
-Sulfate	7.0	<0.20	250	250
-Chloride	5.9	<6	250	600
-Fluoride		-	0.7	1.0
-Nitrate as NO_3 (mg/l)	nd[a]	<0.01	50	-
-Nitrite as NO_2 (mg/l)	nd[a]	-	3	-
-Fluoride (mg/l)	nd[a]	<0.50		-
Toxic substance	-	-	-	no standard
-Inorganic mercury(mg/l)		<0.0005	0.001	-
-Lead (mg/l)		<0.01	0.01	-
-Arsenic (mg/l)		<0.0005	001	-
-Selenium (mg/l)			0.01	
-Chromium (mg/l)		<0.05	0.05	
-Cadmium (mg/l)			0.003	
-Barium (mg/l)		<0.10	0.7	
-Cyanide (mg/l)		<0.05	0.07	
-Aluminum (mg/l)		<0.10		
-Silver (mg/l)		<0.01		
-Phenol (mg/l)		<0.001		0.002

nd[a] = not detectable

Table 3 Summary of water quality from "Desalion": 2017-2018.

	daily volume (litres/day)	Turbidity (ppm)	Temperature (degree Celsius)	Conductivity (mS)	pH	weekly TDS (gm/l)	weekly total hardness	weekly chloride
Fresh water pure	698.3 (425-1,152)	9.8 (4.0-17.0)	30.1 (28.3-31.8)	0.056 (0.015-0.117)	7.9 (7.0-8.3)	0.5 (0.32)	5.6 (5.4-6.0)	5.6 (4.5-5.9)

	Turbidity (ppm)	Temperature (degree Celsius)	Conductivity (mS)	Salinity (ppt)	TDS (g/l)	pH
Fresh water bypass	589.7 (127.0-1,130.0)	30.5 (28.8-32.0)	4.03 (2.65-6.34)	1.9 (1.2-3.4)	1.19 (0.08-2.52)	-
Seawater inlet	-	28.7 (27.5-30.2)	45.4 (14.8-49.8)	28.0 (23.5-29.7)	14.0 (11.2-17.3)	7.9 (7.7-8.0)
Brine water	-	31.1 (29.8-33.1)	58.8 (49.2-71.6)	34.7 (28.3-38.8)	17.8 (14.8-20.0)	7.9 (7.7-8.0)

Table 4 Brine water quality compared to waste water standard for Desalination plant.

	SANSO ELECTRIC Company" Desalion"	Ministry of Natural Resources and Environment: Ministry announcement "Standard of brine water from desalination"[10]
Pumping rate	within standard	not more than 0.1 meter/sec with 9.5 mm. screen
pH	7.9 (7.7-8.0)	6-8.5
Turbidity (NTU)	17.8 (14.8-20.0)	100

Table 5 Summary of the test operation period

Test operation	details
Term	21 July 2017 – 31 March 2019
Total examination days	617 days
Planned stop days	356 days
Effective working days	550 days
Actual working days	420 days
Utilization ratio: (420/550)	76%

Coral tested

Abalone tested

Figure 3 Coral and Abalone tested in brine water storage.

4. Conclusion

The Desalion was running continuously for 550 days with a utilization ratio of 76%. It produced, in total, more than 480 tons of fresh high-quality drinking water for at least 330 peoples, with a utilization rate of 3 litres/person/day as shown in Table 5. The fresh water quality was of WHO standards (2011) and Thailand's drinking water standards (Maximum allowable concentration in Table 2). The brine water was used to grow plants that can withstand brininess in water. Seven type of plants were chosen to be tested including tomato, roselle, holy basil, seed tomato, peppermint, lettuce, and green oak, with all result indicating that they can grow well using brine water from the Desalion compare to normal fresh water. The seawater with higher salinity, its salinity was tested resulting in 34.7 ppt comparing this to the seawater inlet showed an increase of 23.9%. This water was then compared to Thailand's standard of brine water from desalination in Table 4. The seawater with higher salinity was then used for culturing coral and abalone since both organisms thrive in high salinity seawater. The culturing period was 3 months long with a conclusion that both species can survive and grow in this type of water as shown in Figure 3

This research was a collaborative effort of the Aquatic Resources Research Institute, Chulalongkorn University, Thailand and Sanso Company, Japan for the Desalion. The Desalion proved to be a beneficial and effective tool in providing high-quality drinking water with low environmental impact, considering the by-products, brine water and seawater, can be utilized effectively in other areas. In addition, by utilizing Desalions on a broader scale prove valuable for local uses, agricultural uses, and tourism on remoted islands and areas with scarcity of fresh water.

5. References

[1] Naent Ponil, (2003). Fresh water shortage and management: Sichang island case study.
[2] Pisini Suntrivichit, (2006). Studied of Fresh water insufficient on Sichang Island, Cholburi.
[3] http://www.technologymedia.co.th (2016).
[4] http://www.khaochad.com (2016).
[5] APHA, AWWA and WEF (2017). Standard Method for the Examination of Water and Wastewater, 23 ed. American Public Health Association, Washington, DC
[6] J.D.H. Strickland and T.R. Parson (1972). Practical Handbook of Seawater Analysis, 2nd Edition. Fisheries Research Board of Canada, Bulletin no.167
[7] T.R. Parson, Y. Maita and C.M. Lalli (1984) A Manual of Chemical and Biological Methods for Seawater Analysis, Oxford, New York: Pergamon Press.
[8] United Nations Industrial Development Organization (2019) Water Treatment Activity "Desalion" http://www.unido.or.jp/en/technology_db/5317/
[9] World Health Organization (2011). Pipe water standard.
[10] Ministry of Natural Resources and Environment Ministry announcement (2019). "Standard of brine water from desalination"

Acknowledgements

This research was supported by SANSO ELECTRIC CO., LTD. Japan. The authors would like to thank the staff of the Sichang Marine Science Research Station, Cholburi province, Thailand for their assistance, support, and dedication during the experiments. The authors also would like to express their appreciation for all supports from the Aquatic Resources Research Institute, Chulalongkorn University, Thailand and also special great thank to Mr. Montchai Pichitpasutadol, DHANA SIAM CO., LTD. for advice and helpful.

IOP Conf. Series: Earth and Environmental Science **369** (2019) 012007 doi:10.1088/1755-1315/369/1/012007

Study on production of organic acid rust remover from passion fruit fermented by *Aspergillus Niger*

LONG Jiang-xue[1], JIANG Jia-li[1], ZHANG Shi-ming[1], DAI Xiao-feng[1], DONG Xu-jie[2]

1 Environmental Biotechnology (XMUT), Fujian Province University, Xiamen, 361024, China
2 School of Biological Science and Technology, Central South University of Forestry & Technology, Changsha 410004, Hunan, China
E-mail: ljxczl@126.com

Abstract. Organic acid and rust remover based on citric acid were gradually praised by the industry because of its environmental protection and good derusting effect. In this paper, the production cycle of citric acid by *Aspergillus Niger* shaking flask fermentation was studied with Passion Fruit/Shell, and the rust removal effect of the product was preliminarily verified. The cultivation factors included Passion Fruit/Shell 20%+Sucrose 5%, 35 ℃, pH 5.0-5.5,shaking table150 r/min, the fermentation cycle could be completed in 4-5 days ,and the pH in fruit fermentation broth decreased to 2.7. At room temperature, the derusting effect of 1 time diluted fruit fermentation broth equaled that of 3%commercial citric acid , the rust removal time could prolonged properly at low temperature. The resultshad a guiding significance for producing organic rust remover from Passion Fruit by *Aspergillus Niger*.

1. Introduction

Citric acid (CA) is a kind of tricarboxylic acid compound, which is one of the main metabolic products of organisms. It mainly exists in lemon, citrus, pineapple and other fruits, widely used in medicine, chemical industry, cosmetics, etc [1]. It is also an environmental desulfurization adsorbent. In recent years, organic acid environmental rust remover represented by citric acid has become a researc hotspot because it does not contain toxic and harmful substances, environment-friendly, good rust removal andcorrosion inhibition effect [2-4]. For example, the application of scale removal rust in steel wire hot-dip galvanizing production[5] and thermal production operation, the new rust removalsolution for rapid cleaning of stainless steel oxide scale at room temperature [6], and the study of removing heavy metals from soil by leaching with citric acid fermentation broth, etc [7]. Citric acid is mainly extracted from natural plants. There are two main methods of industrial production, synthetic method and biological fermentation method. Now days, liquid submerged fermentation by *Aspergillus niger* is the main method [8-9]. Citric acid is mainly produced by starch fermentation at home and abroad [10-11], but the cost of raw materials and energy are high. It is very important to find cheap substitutes for raw materials to reduce production costs [12]. In recent years, scholars have explored the production of citric acid from biomass cellulose such as *Aspergillus niger* fermentation degradation straw [13-15], apple pomace[16], in order to expand raw materials and reduce industrial costs.

In this paper, citric acid was produced by *Aspergillus Niger* fermentation with abandoned tropical fruit peels (shells) such as Passiflora as raw materials. Appropriate technological conditions and rust remov al effects were explored to provide reference for the development of new raw materials and promote th e green cycle development of local tropical fruit industry.

2. Experimental materials and methods

2.1. Experimental materials

2.1.1 Fermentation materials and equipment
Main reagents: *Aspergillus Niger* strains were purchased from Guangdong Microbial Collection Center. Passion fruit was bought in the agricultural market.
Main equipment: Electronic balance, Vertical pressure steam sterilizer, Ultra-clean worktable, HYG-II rotary constant temperature speed control shaker.

2.1.2 Activation of Aspergillus Niger and preparation of spore suspension
Aspergillus Niger inclined medium, plate medium and liquid seed medium were formulations of PDA medium. The activation of *Aspergillus Niger* and the preparation of spore suspension referenced Sun Jianqiu [17], 10^7 spore suspensions were prepared for reserve.

2.1.3 Basic medium for shaking flask fermentation
The whole Passiflora fruit or shell raw materials were crushed by a crusher to form a basic shaking flask fermentation medium, which contained 20% fruit /shell+5% sucrose+75% water. The initial pH was adjusted to 5.5. Every conical bottle (250 ml) was filled with 100 ml liquid, sterilized 121℃ for 30 minutes with 0.1 MPa and cooled for reserve.

2.1.4 Rust Removal materials
Fermentation broth: Passion fruit fermentation products were filtered through 8 layers of gauze packed in conical bottle sterilization at high temperature, kept in refrigerator.
Commodity standard citric acid solution: 3% (mass) citric acid solution was prepared, pH 2.5-3.0, which was used as standard control.
Fermentation Rust Removal Solution: Dilute the original fermentation liquor into 1, 2 and 3 times of the original liquor for reserve.
Rust iron sheet: 0.5*2*2cm square, provided by the fitter room of the school training center.

2.2. Experimental methods

2.2.1 Determination of fermentation period of passion fruit
After sterile operation on super-clean worktable, 2 ml of activated *Aspergillus Niger* spore suspension was absorbed by sterile pipette and transferred to the prepared fermentation medium. Shaking-bed fermentation was carried out at 30℃ for 5 days at a rotating speed of 150 r/min. The pH value of fermentation broth and the acidity of citric acid in fermentation broth were determined every 12 hours from the 2nd day. Citric acid acidity determination reference Zhou Jing [11]. Fermentation filtrate 1 mL was diluted properly. Phenolphthalein was used as indicator and titrated with standard 0.1429 mol/L NaOH[18]. The acidification degree was evaluated by titrated NaOH volume, and the optimum period of citric acid fermentation by *Aspergillus Niger* was determined.

2.2.2 Effect of nitrogen source on citric acid fermentation
The effects of different nitrogen sources on fermentation culture were investigated. Adding 1.0% ammonium sulfate, urea, peptone and soybean powder to the shake flask fermentation medium of Passion Fruit as exogenous nitrogen source, the other culture conditions were the same as 2.2.1, to determine the best nitrogen source. Subsequent experiments were conducted to prepare fermentation broth under these conditions.

2.2.3 Rust removal test
The rusty iron sheets were weighed and put into 100 mL rust removal liquid at room temperature, 2 sheets in each concentration, and soaked for 0.5-3 h. The quality of iron sheet was measured every 0.5

h, and the effect of rust removal was evaluated according to the weight reduction and appearance. Refrigerate at 4 degrees was used to simulate the rust removal effect at lower temperature.

3. Experimental results and analysis

3.1. Determinate of the fermentation period of CA

CA fermentation period was determined by determining the change of pH value and acidity of fermentation broth during shaking flask fermentation of Passion Fruit. It was found that the pH value of Passiflora hull decreased gradually from 5.5 to 2.7 during the culture of 96 h, and then increased slowly to about 3.0.

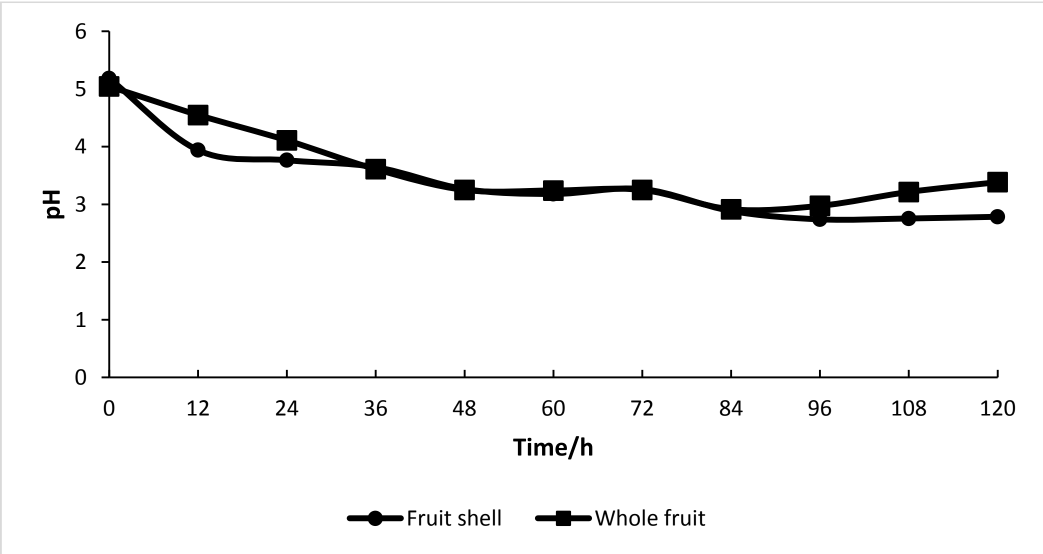

Figure 1 Growth cycle pH curve

The determination of acid production (by NaOH titration) showed that the formation of citric acid was basically consistent with the change of pH value. After 36-96 hours, the organic acids in the culture medium increased gradually and reached the maximum value. After that, the growth rate was slow, indicating that the fermentation had been completed. According to the change of pH value and acid production during fermentation, it showed that the fermentation period of Aspergillus Niger was 96-108 h, and the suitable pH value for citric acid transformation from Passion shell is 2.7-3.0. The fermentation law of Passiflora fruit was similar to that of fruit shell. Because of the sugar content in fruit juice, the transformation of organic acid in the early stage was higher slightly than shell. However, the content of organic acid in the later stage of fermentation decreases rapidly and the corresponding pH value increases gradually, which may be related to the rapid growth of bacteria in the earlier stage and the acceleration of senescence and explanation in the later stage. Considering that the residual Passion Fruit and shell are mostly abandoned and not used, the residual Passion Fruit (shell) could be developed to produce citric acid by fermentation, and 5-10% sugar source supplemented appropriately.

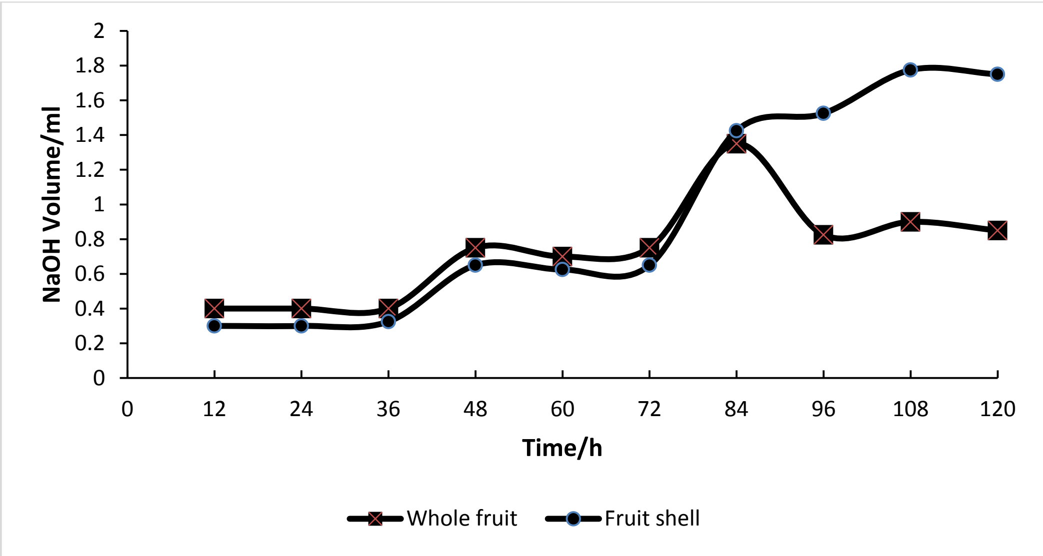

Figure 2 Growth cycle citric acid variation curve

3.2. Comparison of rust removal efficiency of fermentation broth and commercial citric acid

The effect of rust removal was investigated between fermentation broth and standard citric acid solution on iron lumps of different quality (110g, 108g, 112g, 115g).The ratio of rust mass to original mass changes with time was shown in figure 3-4.

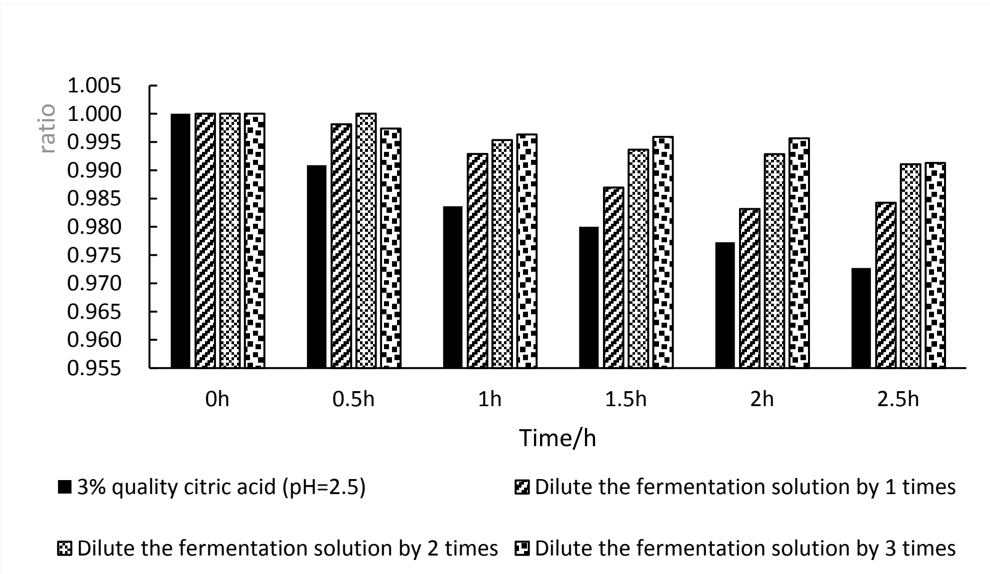

Figure 3 Rust removal at room temperature

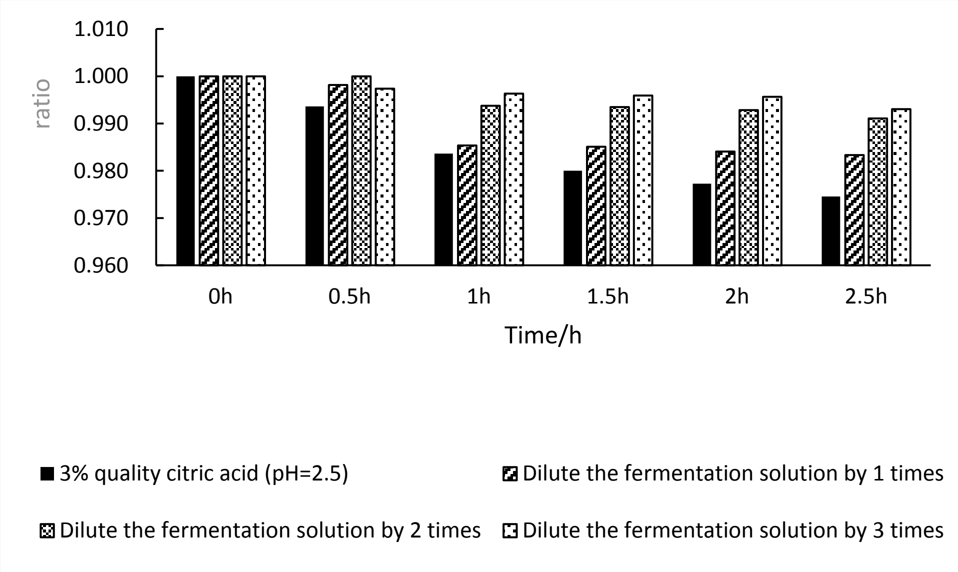

Figure 4 Rust removal at low temperature

It showed (Figure 3) that the quality of iron sheet diluted by 1 times of fermentation broth decreased significantly from 0 h to 1.5 h at room temperature, and tended to be stable after 1.5 h, and its rust removal effect was equivalent to 3% citric acid. The quality of iron flakes in other fermentation broth also decreased, but the decreasing range and speed were lower than that of the former, which may be due to the lower concentration and shorter soaking time. It could conclude that the best time for rust removal was 1-1.5 h. Figure 4 showed that the time of rust removal should prolonged to improve the efficiency of rust removal in winter or at low temperature.

4. Conclusions

In this paper, the production of organic rust remover from Passion Fruit by *Aspergillus Niger* fermentation was studied, and the fermentation process was preliminarily determined. Citric acid fermentation conditions were passion fruit (shell) 20%+sucrose 5%, 35℃, 150r/min. During the fermentation, the pH gradually decreased from 5.5 to 2.7 after cultured 84-96h, and then slowly increased. It indicated the fermentation was completed, and the organic acid accumulated was also the highest. Therefore, the fermentation cycle was generally 4-5d, and the final acid yield was 2.8%. Preliminary evaluation of rust removal effect: Compared with the commercial citric acid standard sample, it was found that the fermentation broth could be used for rust removal without separation and purification, and the effect was obvious.

The effect of 1-fold diluent effect was equivalent to that of 3% commercial citric acid. The best time of rust removal is 1-1.5 h. The time of rust removal should prolong at low temperature to improve the effect of rust removal. By studying, the basic conditions of citric acid fermentation were obtained and the citric acid conversion rate was better. However, how to optimize the citric acid fermentation process and apply it to industrial production needs further exploration and research.

5. References

[1] Zhu Yiren, Wang Jinhua, Zhang Zhenchao, et al. Research progress on extraction methods of fermented citric acid [J]. Fine and Specialized Chemicals, 2003 (14): 18-21.
[2] Zhaojiang. Brief analysis of citric acid chemical cleaning scale and rust removal technology [J]. Regional heating, 2015 (01): 60-62.
[3] Zhao Henghe, Yishouzhi. Research on environmentally friendly rust remover [J]. Electroplating and environmental protection, 2017,37 (06): 35-38.

[4] Chen Zhenzhen, Hu Lei. Development of environmentally friendly cleaning agent for steel rust removal [J]. China detergent industry, 2018, 12 (06): 11-14.
[5] Miao Lixian, Zhang Huijun, Liu Hai, Malin, Xie Yinping, Dou Hongxia. Application of compound hydrochloric acid pickling solution in hot-dip galvanizing of steel wire [J]. Electroplating and finishing, 2006 (07): 8-9.
[6] Yang Xiaolin. A new type of rapid cleaning solution for stainless steel oxide skin at room temperature [J]. Corrosion and protection, 2006 (06): 297-298.
[7] Zhang Hongjiao. Removal of heavy metals from soil by leaching citric acid fermentation broth [D]. Yunnan University for Nationalities, 2017
[8] Gao Nianfa, Yang Feng. Innovation and Development of Citric Acid Fermentation Industry in China [J]. Brewing in China, 2010, 13 (01): 6-8.
[9] Yang Xiaolin, Li Jun, Zhu Fengmei, et al. Advances in metabolomics of Aspergillus Niger [J]. Food Engineering, 2017, 11 (07): 6-10.
[10] Dai Zhenzhen, Zhou Yong, Liu Yuwei, et al. Effects of liquefaction conditions during citric acid fermentation [J]. Journal of Food and Biotechnology, 2011, 21 (03): 5-9.
[11] Zhou Jing, Qin Dan, Zeng Wenjie. Research progress of citric acid fermentation from starchy raw materials [J]. Processing of Agricultural Products (Journal), 2013, 16 (08): 12-15.
[12] BETIKU E, ADESINA O A. Statistical approach to the optimization of citric acid production using filamentous fungus Aspergillusniger grown on sweet potato starch hydrolyzate [J]. Biomass and Bioenergy, 2013, 7 (02) :1-5.
[13] Zhang Jian'an, Zhang Xiaoyong, Han Runlin, Liu Dehua and Li Zuohu. Study on the production of citric acid from cellulase hydrolysate fermented by Aspergillus Niger [J]. Journal of Microbiology, 2001, 21 (3):5-8.
[14] Xie Jun. Study on solid-state fermentation of citric acid with steam explosion straw hemicellulose [D]. 2017.
[15] Meng Xiao. Production of citric acid by Aspergillus niger fermentation from corn straw. East China University of Technology, 2014.
[16] Dhillon G S , Kaur S , Sarma S J , et al. Integrated process for fungal citric acid fermentation using apple processing wastes and sequential extraction of chitosan from waste stream[J]. Industrial Crops & Products, 2013, 50(4):346-351.
[17] Sun Jianqiu, Zangwei, Jiang Saiman, et al. Effects of different fermentation conditions on citric acid production by Aspergillus niger using cornmeal [J]. Chinese condiment, 2008, 12 (02): 1-2.
[18] Shi Yixiang, Liu Zutong. Production of citric acid from cornstarch fermented by Aspergillus Niger [J]. Journal of Tsinghua University (Natural Science Edition), 1998.38 (6): 52-55.

Acknowledgments

This project were funded by :
1. Key Laboratory of Environmental Biotechnology（XMUT）; Fujian Province University.
2. University Student Innovation Training Program（XMUT-2018）.

IOP Conf. Series: Earth and Environmental Science **369** (2019) 012006 doi:10.1088/1755-1315/369/1/012006

Simulation research on mooring stability of oil tankers in Changxing Island Port Area considering open environmental conditions

Jian Huang[1], Xiao Bing[1], Ruoli Shao[1], Yu Liu[1] and Xiangda Li[2,] *

1 The Design Institute of Civil Engineering & Architecture, Dalian University of Technology, Dalian 116023, China

2 State Key Laboratory of Coastal and Offshore Engineering, Dalian University of Technology, Dalian 116024, China

E-mail: 201352026@mail.dlut.edu.cn

Abstract. The contribution of this paper is to study the mooring stability of oil tankers by OPTIMOOR software considering the open environmental conditions in Changxing Island Port Area. Firstly, influence factors on mooring stability is analyzed, which are considered as the inputs in the numerical models. Then, the experimental cases under the combinations of waves, water level, tidal current, and wind are developed. Next, the standard of mooring stability used in this paper is given after comprehensively considering the standards used in Norwegian, German, Japan and British. Finally, by feeding the environmental conditions in Changxing Island Port Area, all the numerical experimental tests are conducted and six motion components of moored ships are obtained. The results show that (1) The water level has little effect on six motion components. (2) Compared with oblique sea and following sea, beam sea has the greatest impact on the mooring stability of oil tankers.

1. Introduction

At present, considerable attention is being given to mooring stability of oil tankers along with the emergence of ultra-large ships and open-sea terminals. Due to the open marine circumstances in Changxing Island Port Area, mooring stability of oil tankers is easily affected by severe natural conditions, such as heavy current, tough wave and strong wind, which can cause huge damage to ships and terminal structure. On the one hand, the failure probability of mooring cables gets higher with the increase of mooring force given the severe conditions, which can cause great harms to ships, especially the large ships. On the other hand, given the poor mooring stability, there is a huge collapsing force of oil tankers to terminal structure, which can give huge economic losses to terminal operators. Therefore, it is urgent to study mooring stability of oil tankers faced with open and severe environmental conditions in Changxing Island Port Area.

For the mooring stability of ships, several researchers have given much attention and studied. For example, Gao et al. analyzed the ship motion, mooring force and impact force for three different mooring cable arrangements involving two alternative mooring points under the combined action of wave and flow [1]. YH Rho et al. performed static and dynamic mooring analyses to evaluate the stability of a spider buoy after disconnection from a turret during cyclone environmental conditions [2]. Shen and Zhou studied the roll motion of a moored ship under the wave and loading conditions by taking a 100000-ton cargo ship as a test ship and analyzed the peak value of the roll motion amplitude [3]. Chen et al. conducted the model test by taking a 3000-ton deck barges as a research object to study the mooring stability of ships, and analyzed the impact factors of the mooring force and the change law of the mooring force [4]. Liu et al. studied the movement law of moored ships at large open terminal under irregular traverse waves through theoretical analysis and physical model test, and gave a complete formula for estimating the movement of moored ships [5]. Zhang et al. proposed a semi-empirical and semi-theoretical calculation formula with higher precision for the motion components of moored ships through theoretical analysis and physical model tests [6]. Sakakibara et al. studied the effect of the asymmetry coefficient of the mooring system between cable elasticity and fender elasticity on the motion components of moored ships using numerical calculations [7]. Liu proposed an estimation formula for the surge, roll and heave movements of moored ships under the action of lateral irregular waves considering the conditions of wave height, wave length, ship load and roll period [8]. Van et al. numerically simulated the motion response and mooring load of a moored LNG in the Withnell Bay in northwestern Australia by using a six-degree-of-freedom model, and proposed an estimation formula for the roll motion of the moored ship [9].

Apart from physical model experiments and mathematical models, some researchers have used the mooring analysis software to study the mooring stability of ships, such as MOSES software [10], MATLAB software [11] and OPTIMOOR software [12-15]. For example, Q Chen established a mooring mathematical model for a 300,000-ton bulk carrier by using the mooring analysis software MOSES, and calculated the ship movement response and cable mooring force of the mooring system under different wave periods, heights and directions [10]. Q Zhang studied the force control system of the mooring cable by using the MATLAB platform, and analyzed the stability balance and cable vibration of the ship mooring [11]. Y Li studied the effects of wave periods, heights and directions on the mooring force and ship movement by OPTIMOOR software, and discussed the mooring response of ships under long-period waves [12]. JF Flory et al. analyzed the influence of mooring cable properties on the stability of 10,000-ton ships under the unfavorable conditions under different properties by OPTIMOOR software [13].

Most of the existing researches have considered the wave characteristics such as wave periods, heights and directions to study the mooring stability of ships through physical model tests and mathematical model tests. Besides, studies by mooring analysis software mainly concentrated on the influence of one factor on the stability of ships. Therefore, to overcoming the limitations of mathematical models, this paper applies OPTIMOOR software used widely to study the mooring stability of ships under complicated natural environments, such as wind, wave and tidal current in Changxing Island Port Area.

2. Method

2.1. Factors on mooring stability

There are many factors affecting the mooring stability of ships, such as the natural characteristics of wind, wave and tidal current. Besides, another factor influencing mooring stability that must be considered is the attributions of ships, such as the tonnages, load and length of ship. A gust of wind, a passing ship or changes in tide and freeboard can cause mooring cable failure and sudden movement of ships. Such an accident can result in costly damage to cargo handling equipment or other nearby structures [13].

Therefore, this paper classifies the factors on mooring stability of ships into five categories: waves, water level, tidal current, wind and the attributions of ships. The following concentrates on the experimental cases of mooring stability considering the combinations of the influence factors.

2.2. Experimental cases

The following experimental cases involve a 300,000-ton oil tanker moored alongside a terminal. The length of the ship is 334 m and the molded depth is 31.5 m. This tanker is used because it is the test ship used for the terminal construction in Changxing Island Port Area. The mooring arrangement which is used in stability analyses is shown in figure 1.

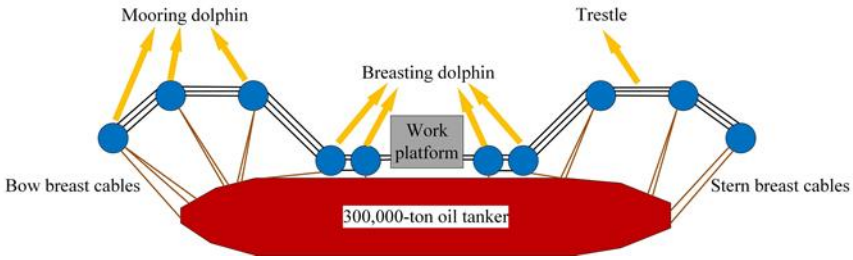

Figure 1. The mooring arrangement of the oil tanker.

Under the condition that ships are fully loaded, mathematical simulation tests are carried out on various test combinations of waves (beam sea, oblique sea and following sea), water level (extreme high-water level, design high-water level and design low-water level), tidal current (flow and edd) and wind (no wind, across-wind and along-wind). The schematic diagram of experimental cases is shown as follows.

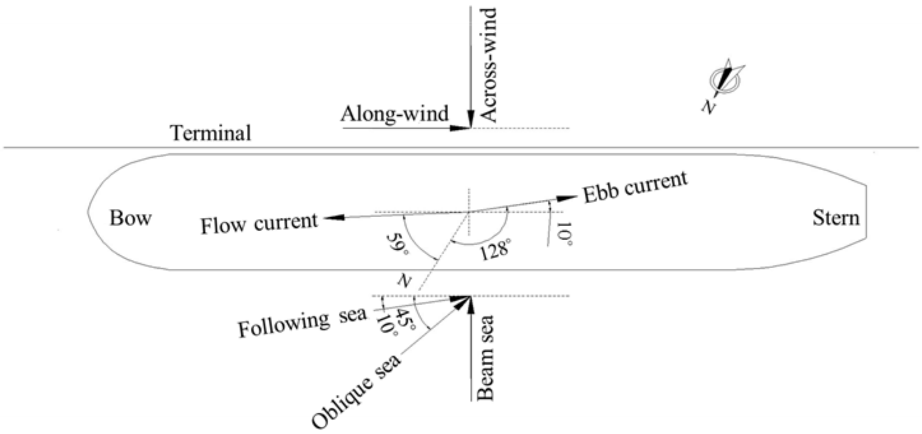

Figure 2. The schematic diagram of experimental cases.

2.3. Standard of mooring stability

Under the action of wave and tide, the motion state of a moored ship can usually be described by six motion components, which are surge, sway, heave, pitch, roll and yaw. In this paper, the six motion components are selected to evaluate the mooring stability of ships. The schematic diagram of six motion components is shown in figure 3.

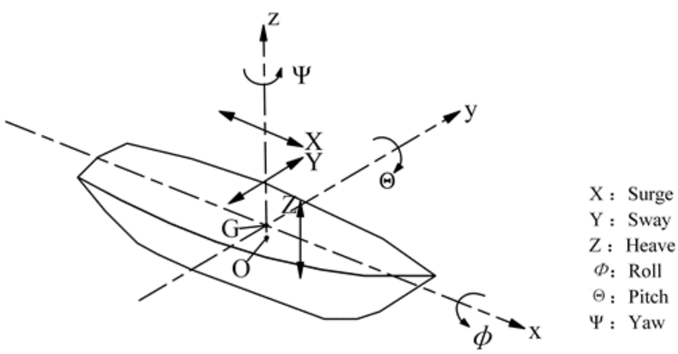

Figure 3. Six motion components of moored ships.

With consideration of the port construction in the real life, this paper refers to the standards of six motion components of moored ships issued in Norwegian, German, Japan and British to determine the standard used in this paper, which are shown in Table 1.

IOP Conf. Series: Earth and Environmental Science **369** (2019) 012006 doi:10.1088/1755-1315/369/1/012006

Table 1. The standard of six motion components of moored ships.

Types of the standard		Six motion components of moored ships					
		Surge (m)	Sway (m)	Heave (m)	Yaw (°)	Pitch (°)	Roll (°)
Standard used in this paper		2.0	2.0	0.5	/	3	4
Norway		±2.3	±1.0	0.5	/	4.0	±3.0
Germany Per Bruun		2.0	±0.5	0.5	1	/	/
Japan	Outer	±1.5	±0.75	±0.5	±2.0	±4.0	±4.0
	Inner	±1.0	±0.75	±0.5	±1.5	±3.0	±3.0
British norms		0.5～2.0	0.5～2.0	/	/	/	/

3. Case study

3.1. Parameter settings

In the mathematical simulation tests, the wave height (H4%) of the beam sea and oblique sea is set as 2.0 m, and the wave height (H4%) of the following sea is set as 2.5 m. Besides, the period of all types of waves is set as 7.0 s. The wind speed of across-wind and along-wind are set as 20.8 m/s to 24.4 m/s. Under the condition of extreme high-water level, only the effect of no wind is considered. Under the conditions of design high-water level and design low-water level, the effects of no wind, across-wind and along-wind are considered. High tides and low tides are considered under all conditions of water level in this paper.

3.2. Results

After conducting all the numerical simulation models, the results of six motion components of moored ships at full load are shown in Tables 2-Table 4. Besides, the contrast between maximum six motion components and standard is shown in Table 5.

Table 2. Six motion components of moored ships subjected to beam sea at full load.

Water level	Tidal	Waves		Six motion components of moored ships					
		$H_{4\%}$ (m)	T (s)	Surge (m)	Sway (m)	Heave (m)	Pitch (°)	Roll (°)	Yaw (°)
Extreme high-water level	Flow	2.0	7.0	0.2	0.4	0.03	0	0.2	0
	Ebb	2.0	7.0	0.4	0.34	0.03	0	0.2	0
Design high-water level	Flow	2.0	7.0	0.2	0.4	0.02	0	0.2	0
	Ebb	2.0	7.0	0.3	0.4	0.02	0	0.2	0
Design low-water level	Flow	2.0	7.0	0.2	0.38	0.03	0	0.2	0
	Ebb	2.0	7.0	0.4	0.38	0.03	0	0.2	0

From the results in Tables 2-Table 5, it can be drawn: (1) The maximum sway of the moored ship at full load in these numerical experiments is 0.4m, and the maximum surge is 0.8m, and the maximum heave is 0.04m, and the maximum value of the roll angle is 0.2 °. (2) The maximum value of sway and roll appears in the case of beam sea, and the maximum surge of the moored ship appears in the condition of design low-water level along with following sea, ebb and along-wind. Other motion components change little with changes in external environmental loads. (3) From the results in Table 5, the mooring stability of oil tankers in Changxing Island Port Area is satisfied according to the standard used in this paper.

Table 3. Six motion components of moored ships subjected to oblique sea at full load.

Water level	Tidal	Wind condition	Waves		Six motion components of moored ships					
			$H_{4\%}$ (m)	T (s)	Surge (m)	Sway (m)	Heave (m)	Pitch (°)	Roll (°)	Yaw (°)
Extreme high-water level	Flow	No wind	2.0	7.5	0.3	0.1	0.04	0	0.1	0
	Ebb	No wind	2.0	7.5	0.4	0.1	0.04	0	0.1	0
Design high-water level	Flow	No wind	2.0	7.5	0.4	0.1	0.04	0	0.1	0
	Ebb	No wind	2.0	7.5	0.4	0.1	0.04	0	0.1	0
Design low-water level	Flow	No wind	2.0	7.5	0.3	0.1	0.04	0	0	0
	Ebb	No wind	2.0	7.5	0.4	0.1	0.04	0	0	0
Design high-water level	Flow	Across-wind	2.0	7.5	0.4	0.1	0.04	0	0.1	0
		Along-wind	2.0	7.5	0.6	0.1	0.04	0	0.1	0
	Ebb	Across-wind	2.0	7.5	0.5	0.1	0.04	0	0.1	0
		Along-wind	2.0	7.5	0.7	0.1	0.04	0	0.1	0
Design low-water level	Flow	Across-wind	2.0	7.5	0.4	0.1	0.04	0	0	0
		Along-wind	2.0	7.5	0.6	0.1	0.04	0	0	0
	Ebb	Across-wind	2.0	7.5	0.5	0.1	0.04	0	0	0
		Along-wind	2.0	7.5	0.8	0.1	0.04	0	0	0

Table 4. Six motion components of moored ships subjected to following sea at full load.

Water level	Tidal	Wind condition	Waves		Six motion components of moored ships					
			$H_{4\%}$ (m)	T (s)	Surge (m)	Sway (m)	Heave (m)	Pitch (°)	Roll (°)	Yaw (°)
Extreme high-water level	Flow	No wind	2.5	7.5	0.3	0	0.02	0	0	0
	Ebb	No wind	2.5	7.5	0.4	0	0.02	0	0	0
Design high-water level	Flow	No wind	2.5	7.5	0.3	0	0.01	0	0	0
	Ebb	No wind	2.5	7.5	0.4	0	0.01	0	0	0
Design low-water level	Flow	No wind	2.5	7.5	0.3	0	0.01	0	0	0
	Ebb	No wind	2.5	7.5	0.4	0	0.01	0	0	0
Design high-water level	Flow	Across-wind	2.5	7.5	0.5	0.1	0.01	0	0	0
		Along-wind	2.5	7.5	0.7	0	0.01	0	0	0
	Ebb	Across-wind	2.5	7.5	0.6	0.1	0.01	0	0	0
		Along-wind	2.5	7.5	0.8	0	0.01	0	0	0
Design low-water level	Flow	Across-wind	2.5	7.5	0.5	0.2	0.01	0	0	0
		Along-wind	2.5	7.5	0.6	0	0.01	0	0	0
	Ebb	Across-wind	2.5	7.5	0.4	0.1	0.01	0	0	0
		Along-wind	2.5	7.5	0.8	0	0.01	0	0	0

Table 5. The contract between maximum six motion components and the standard.

Motion components	Surge (m)	Sway (m)	Heave (m)	Pitch (°)	Roll (°)	Yaw (°)
Maximum values	0.8	0.4	0.04	0	0.2	0
Standard	2.0	2.0	0.5	3	4	0

In addition, in order to validate experimental results, this paper compares the results obtained from the OPTIMOOR test and the physical model test. The experimental cases in the physical model test are same as the cases in the OPTIMOOR test, as shown in section 2.2. After conducting the models, the experimental results from the physical model test are shown in Table 6, consisting of the maximum six motion components of ships subjected to beam sea, oblique sea and following sea at full load.

Table 6. The maximum six motion components of ships at full load from physical model test.

Test conditions of waves	Surge (m)	Sway (m)	Heave (m)	Pitch (°)	Roll (°)	Yaw (°)
Beam sea	0.87	1.08	0.28	0.23	0.70	0.49
Oblique sea	1.07	0.85	0.11	0.40	0.44	0.43
Following sea	1.10	0.77	0.09	0.39	0.40	0.46

As shown in Table 6, the experimental results from the physical model test are larger than the results from the OPTIMOOR test, respectively. This is because wave force is presented as static superposition to wind load, which ignores the excitation effect of wave force to mooring force and results in the inaccuracy of the OPTIMOOR simulation results. Therefore, in the design work of oil terminals, the study of ship mooring stability needs to be correlated with the results from physical model test or the dynamic superposition of wave force and wind force from the OPTIMOOR simulation results.

4. Conclusion

The contribution of this paper is to study the mooring stability of oil tankers by OPTIMOOR software considering the open environmental conditions in Changxing Island Port Area. Firstly, influence factors on the stability of moored ships are analyzed, which are considered as the inputs in the numerical models. Then, the experimental cases under the combinations of waves, water level, tidal current, and wind are developed. Next, the standard of mooring stability used in this paper is given after comprehensively considering the standards used in Norwegian, German, Japan and British. Finally, by feeding the environmental conditions in Changxing Island Port Area, all the numerical experimental tests are conducted and six motion components of moored ships are obtained.

1) The water level has little effect on six motion components.

2) Compared with oblique sea and following sea, beam sea has the greatest impact on motion components of moored ships.

3) The mooring stability of oil tankers in Changxing Island Port Area can be analyzed by OPTIMOOR software and is satisfied according to the standard used in this paper.

The results and proposed method can be applied to study the mooring stability of oil tankers in complicated environments. However, this paper only considers the influence of natural conditions and the contributions of ships on the stability. Future study should consider the characteristics, quality, and arrangement of the mooring cables on the mooring stability.

5. References

[1] Gao F, Zheng B Y, Chen H B and Li Y 2007 Analysis of mooring conditions under different tethering modes *Water Transport Engineering* **3** 48-52.

[2] Rho Y H, Kim K, Jo C H and Kim D Y 2013 Static and dynamic mooring analysis - Stability of floating production storage and offloading (FPSO) risers for extreme environmental conditions *International Journal of Naval Architecture and Ocean Engineering* **5:2** 179-187.

[3] Shen Y S and Zhou Y R 2017 Experimental study on roll motion of a moored ship under different wave and loading conditions *Chinese Journal of Hydrodynamics* **33:3** 364-369.

[4] Chen L, Yang Q F, Yu T and Wang P Y 2017 Model experimental studies of safety of moored ship under landslide surge action *Hydro-Science and Engineering* **1** 80-86.

[5] Liu B J, Sun Z C, Zhang Z M and Yang G P 2008 Research on the amount of mooring of large open dock mooring under the action of transverse waves *Water Transport Engineering* **8** 94-97.

[6] Zhang Z M, Zhou F, Tang G P and Sun Z C 2010 Research for the Moored Ship of Offshore Deepwater Terminal *China Harbour Engineering* **z1** 49-52.

[7] Sakakibara S and Kubo M 2008 Effect of mooring system on moored ship motions and harbour tranquillity *International Journal of Ocean Systems Management* **1:1** 84-99.
[8] Liu B J Study on the Influence of Long-period Waves on Vessel Mooring Stability *Dalian: Dalian University of Technology* 2008.
[9] Van W, Ligteringen H, Van J C and de Waal J C M 2003 Behavior of a Moored LNG Ship in Swell Waves *Journal of Waterway, Port, Coastal, and Ocean Engineering* **129:1** 15-21.
[10] Chen Q Study on mooring characteristics of large ships under long-period waves *Zhoushan: Zhejiang Ocean University* 2014.
[11] Zhang Q 2018 Research on the force control system of the mooring cable of ship *Ship Science and Technology* **40:8A** 190-192.
[12] Li Y Study on the influence of long-period waves on ship mooring stability *Dalian: Dalian University of Technology* 2013.
[13] Flory J F, Banfield S P and Ractliffe A 2014 Computer Mooring Load Analysis to Improve Port Operations and Safety *PORTS ASCE*.
[14] Kong Y N, Liao Z H, Cheng P J and Li Z G 2017 Optimal design for the mooring of FSRU with LNG carrier *Port & Waterway Engineering* **09** 88-93.
[15] Wang L and Yang B 2016 Analysis of mooring at inland harbor under vessel motion based on Optimoor *Port & Waterway Engineering* **10** 57-60.

Acknowledgements
This research was funded by the National Natural Science Foundation of China grant number (No. 51709037 and 51779037). We would also like to thank the Fundamental Research Funds for the Central Universities (No. DUT18RC(4)053) and Doctoral Research Initial Funding in Dalian University of Technology (No. 20170520165) for supporting this research.

Chapter 4:
Utilization of Marine Resources

Exploitation and utilization of marine resources and protection of marine ecology

Huiping Zhong[1]

1 Xiamen Ocean Vocational and Technical College, China
E-mail: jmsxzhong@163.com

Abstract. With the development of society and the gradual enhancement of information science and technology, marine science and technology are gradually strengthened, the marine economy is playing an important part in our national economy. China's marine Energy Resources Total accumulation is very rich, and it is a great wealth, but the development of marine resources is not unlimited. Although it can promote the development of national economy, the sustainable development of marine resources should be considered. As the marine science and technology are growing today, the sustainability of marine resources is also seriously threatened. This paper analyzes the problems that encountered in the exploitation and utilization of marine resources and also in the protection of marine ecology. After expounding the importance of sustainable development of marine resources, the writer puts forward some methods and suggestions on how to make marine resources develop sustainably.

1. Introduction

Marine resources refer to those substances, energy and marine space existing in the marine environment that can be exploited and utilized by people, including marine biological resources, seawater resources, seabed mineral resources, marine renewable energy and marine space resources, etc [1]. The management of marine resources has become extremely complex due to its natural and social attributes. Along with social and economic development and population growth, there is a serious shortage of land resources, especially energy. There is even the emergence of sensational remarks that one who holds control over petroleum energy will have the world under control. By the end of the 20th century, the ocean began to be taken as the direction of resource development under the compelling circumstances. Advances in science and technology as well as the in-depth exploration have gradually highlighted that the oceans contain far more resources than that of land, thereby coastal countries have rapidly launched a large amount of investment for exploitation and utilization. As a series of disasters that cannot be underestimated have been caused by disorderly development, many professionals have carried out detailed research on marine resources development and ecological protection. Since the sustainable development of the ocean means that of human beings, the development of the ocean should be promoted simultaneously with the protection of the marine ecosystem. Nevertheless, the majority of researches have been carried out from one perspective, such as a certain resource or ecological environment, while researches on the development of marine resources and marine ecological protection are expected to be carried out from a systematic perspective. As a huge and organic multivariate dynamic system, the ocean assumes powerful self-repair and purification functions, with a large amount of renewable and relevant resources in it. Hence, sustainable development and ecological protection has to be taken as the primary premise in the exploitation and utilization of marine resources, so as to ensure the sustainable development of mankind.

2. Current situation of exploitation and utilization of marine resources in China

Since ancient times, the exploitation of marine resources has mainly focused on fishing and collecting marine living resources, obtaining salt by evaporating brineand navigating on the sea. In view of the increasing shortage of energy at home and abroad in recent years, as an energy treasury, there are also abundant renewable energy resources in the ocean such as marine wind energy, tidal energy, wave energy, temperature difference energy, salt difference energy except for a large number of mineral energy, which has attracted the attention of energy developers and led the main direction of current energy development to marine energy development. Apart from a variety of energies, the ocean also contains multifarious other resources [2]. With the gradual improvement of scientific and technological level in the exploitation and utilization of marine resources in the world, the economic value of marine resources is becoming increasingly highlighted.

2.1. Overexploitation of marine resources

Since many years ago, the over-exploitation of marine organisms has actually existed in China. In ancient times, the fishing of marine organisms was limited to fishing and shellfish-picking activities, while modern fishing methods are demonstrating increasingly mechanized and on a large-scale. There is also the emergence of highly destructive and predatory ways such as fishing with explosives. Large-scale fishing results in the failure of marine communities to regenerate within the effective cycle, which leads to the sharp reduction of marine species, the deterioration of living conditions, the gradual disappearance of rare species, the significant reduction of large-scale fisheries and the obvious decline or even depletion of fishery resources. In this way, fishermen's lives in the future will be seriously affected.

2.2. Irrational exploitation of marine resources

In recent years, the irrational and disorderly exploitation of marine resources has become increasingly severe in china. For example, failing to strictly conforming to the regulations in the utilization of the ocean, some local governments conduct land reclamation, sea-filling and even block the circulation of sea water, which has caused serious damage to the marine ecosystem. Among them, the most vulnerable are coral reefs, mangroves, casuarina equisetifolia shelterbelts on sandy coasts in the south and wetlands in estuaries, which are parts of marine resources easy to be damaged. In addition, other impacts include the dramatic shortening of coastlines, the dramatic decline in marine life and even the endangerment of some rare species due to their lack of habitat. Whereas, the damage to marine resources caused by such actions as reclamation will take a period of time rather than immediate manifestation, while the exploitation and utilization of resources such as coastal engineering construction and submarine sand extraction will also aggravate the degree of damage to the coastline. The irrational and disorderly utilization of the ocean will cause serious harm to the sustainable development of marine resources.

2.3. Pollution of marine resources due to exploitation and utilization

Petroleum pollution is regarded as the most harmful pollution source in the exploitation and utilization of marine resources. In the process of exploitation, refining and transportation of petroleum and its derivatives, accidental leakage in the sea will form an oil film on the surface of sea water, which will not only prevent sunlight from reaching the seabed but also seriously affect the photosynthesis of animals and plants in the water due to the lack of sunlight so that animals cannot eat, grow and reproduce normally. The harmfulness and toxicity of petroleum and its petrochemical products will also cause corrosion and damage to seawater, marine organisms, marine engineering and even human beings. Pollution of the ocean will destroy the ecological balance of the ocean area, deteriorate the whole marine environment. As a result, a vicious circle will be formed. In view of the variety of potential dangers in the ocean, when improving the utilization rate of marine resources and increasing economic benefits, we should pay due attention to the marine environment, promote low-carbon development, actively cultivate people's awareness of low-carbon life, remind people to reduce the discharge of domestic sewage and change their way of life, so as to achieve the rational exploitation and utilization of marine resources by adhering to the concept of low-carbon development.

In the process of exploiting and utilizing marine resources, another behavior that can cause pollution is mariculture. With the rapid development of the aquaculture industry in the past 30 years, some people in certain areas who merely pursue economic benefits violate relevant regulations and develop aquaculture too intensively, which has led to the increasingly serious self-pollution of aquaculture industry. In order to maximize economic benefits, an increasing number of aquaculture farmers put in excessive amounts of bait and antibiotics, while the aquaculture objects also produce a large number of excreta which will cause serious eutrophication of the water body, thus greatly enhancing the incidence of red tide by facilitating the growth and reproduction of toxic organisms such as red tide in the aquaculture area. As an extremely dangerous phenomenon, except for the harm to the marine environment, marine fisheries and mariculture, serious red tide will also pose threats on human health.

3. Analysis of problems and reasons existing in the exploitation and utilization of marine resources and marine ecology protection

3.1. Analysis of the problems and reasons encountered in the process of overexploitation and overutilization

In order to solve the problem of overfishing, a series of measures have been implemented by the government, including the adoption and formulation of rules on marine fishing relating to overfishing and seasonal fishing, the introduction of regulations on fishing suspension in summer, reproduction and releasing, the enhancement of management of environmental problems around the oceans to ensure the maximum protection of marine resources and the surrounding environment, as well as the constant increase of people's awareness of environmental protection of marine resources and the marine environment by strengthening publicity. Despite the fact that these measures do provide more opportunities for sustainable development of marine organisms, the effect is not as obvious as expected because fishermen are driven by benefits. Those fishermen who live by fishing are most concerned about their actual benefits rather than whether their overfishing will damage the sustainable development of marine resources. The only thing they are sure of is that the more they catch, the more economic benefits they will get. Or simply because of the pressure of life. The less the resources are, the more unscrupulous people will be. Given that the total amounts of marine resources are certain, the more seriously marine resource have been damaged, the more dangerous marine ecology will be.

3.2. Analysis of problems and reasons in exploitation and utilization

It has been found through the survey that for all that the seawater under China's jurisdiction presents slight pollution, the coastal waters demonstrate serious pollution, ecological environment deterioration and frequent natural disasters, which leads to a significant reduction in marine living resources. The major reasons of these phenomena include reclamation of beaches and direct discharge of land-based and sea-based pollutants. In recent decades, the protection of marine resources and the marine environment have been lacking in China. The development of marine economy and the acquisition of wealth from the sea have been emphasized, while the protection of marine resources and marine ecological environment has been neglected. Irrational land reclamation, sea-filling, overfishing and vigorous development of heavy industry aiming at rapid economic growth have resulted in a large number of untreated industrial and domestic sewage which were directly discharged into the sea and caused serious pollution of the sea water in offshore areas, which has seriously affected the normal habitat and reproduction of marine organisms. In serious areas, there has even been a sharp decrease in fishery resources and the abandonment of beach farms, which poses a threat to the natural ecosystem and the living environment of residents.

With the increasingly improvement of living standards and the progress of information as well as science and technology since the reform and opening up, the level of marine science and technology has also been significantly enhanced, which is conducive to people to obtain more considerable economic benefits through the greater exploitation and utilization of marine resources. However, due to immature management and regulations, there are a series of problems arising in the exploitation and utilization of marine resources, such as overexploitation, irrational development and marine pollution, which seriously affects the sustainable development of marine resources. In spite of the existence of traditional concept of local protectionism and pedantic land economy, unlike land resources, marine resources are mobile. On condition that the marine resources of a certain area are over-exploited, irrationally developed or polluted, in addition to the destruction of the marine ecological environment in this region, the ecological environment in other regions will also be harmed to varying degrees, which is regarded to be one of the crucial factors leading to the unstable relationship between the marine areas and regions.

3.3. Analysis of the problems and reasons in the management of the exploitation and utilization of marine resources

The complexity of marine resource management is determined by its natural and social attributes. At present, the planning and management of marine resources in China are carried out in line with their attributes and industries for exploitation and utilization and according to the fields and departments, which is an extension of the management functions of the exploitation departments of various land resources [3]. From the perspective of their own interests, the exploitation departments of various resources ponder over the exploitation and planning of marine resources and believe that this will ensure the comprehensive advantages and potential of marine resources can be fully developed. However, as a dynamic and huge ecosystem different from the terrestrial ecosystem, marine resources of various types are interdependent and interact in the process of exploitation [4].

Faced with the serious impact of a series of problems in the exploitation and utilization of marine resources on their sustainable development, some countermeasures have been adopted by the relevant administrative departments of China. Despite that there was no relevant marine management organization at the beginning of the exploitation and utilization of marine resources, after years of development, the marine management organization has experienced the stages from scratch to integrated management. However, the establishment of relevant administrative bodies and the distribution of related rights are not perfect enough at present. In the management of marine affairs, China's ocean management institutions are gradually found to be lack of departments with high authority and comprehensiveness. In the distribution of management power, the most unreasonable phenomenon existing in the management system of marine resources is the decentralization and overlap of management institutions, which exerts a serious impact on the exploitation and utilization of marine resources and will lead to the vague allocation of management system in the ecological environment protection. When problems arise in marine management, various departments shift blame on each other while the damage to marine resources fail to be fully taken into account, which will inevitably lead to the destruction of the marine resources and the possible impact on the marine ecosystem.

4. Necessity of marine ecological protection

4.1. Prerequisites for the protection of marine ecology and the exploitation of marine resources

As one of the current concepts of economic development, the sustainable development of marine resources through the implementation of marine ecological protection is considered as a low-carbon development model, which is recognized as an essential direction in the development of national economy. With the decline of global forest coverage, the massive consumption of mineral energy and the emission of tremendous harmful gases, the acceleration of air pollution and climate warming, the destruction of the marine environment and the deterioration of the global environment, the new concept of low-carbon development has been put forward by the international community in response to the demand of human survival [5]. The concept of low-carbon economy has been identified as a major and new development direction by the international community. Since marine resources, especially marine renewable resources, are currently the most abundant resources in the world, we are expected to achieve a full understanding of their significance. Considering that the severe destruction of marine ecosystem will be a great challenge to the survival and development of human beings, the exploitation and utilization of marine resources have to be carried out reasonably, which, except for being able to guarantee a favorable living environment for more marine organisms, is also conducive to the effective solution of the problems including resource scarcity and serious environmental pollution. Therefore, the concept of sustainable low-carbon development has to be upheld in the exploitation and utilization of marine resources, while the necessity for marine ecological protection shall be highly emphasized.

4.2. Marine ecological protection is conducive to the promotion of international competitiveness

In developing and utilizing marine resources, we should adhere to the concept of marine ecological protection and establish a low-carbon model of marine development, which is conducive to enhancing international competitiveness. Historically, as the earliest place where life was conceived, the ocean occupies nearly 71% of the earth's total area. Therefore, the protection of marine ecological environment is the most vital link to protect the global ecological environment, while the state of ecological environment maintenance will exert direct impact on the survival and development of human beings. Besides abundant marine organisms, there are also a large number of oil, gas and mineral resources in the huge marine resources, which are closely related to the production and life of human beings. The destruction of marine resources will not only damage the living environment of marine organisms, but also seriously affect human life [6]. With the increasing concern on the research and development of marine resources nowadays, in addition to strengthening the development of new energy sources, people have also carried out a series of studies on ocean currents, thermal gradients and tides, which will affect the researches on new energy sources of human beings. With an in-depth understanding of the significance of marine resources, Li Guoqiang once said that, the limited land resources would be no longer meet the demand of human survival and development in the current situation of large population growth, the importance of marine resources is expected to be fully recognized to achieve human beings’ better survival and a favorable living environment. For all that the exploitation of marine resources is merely in the primary stage and only a small part of the vast marine resources are exploited, the enormous economic wealth has been brought to the state and society. Therefore, the sustainable exploitation and utilization of marine resources on the premise of protecting marine ecology is a low-carbon development model, which will be conducive to the enhancement of China's competitiveness in the international community.

4.3. The only route of social development

Rather than being put forward merely in light of the current situation, the establishment of an ecological concept of marine protection in the exploitation and utilization of marine resources is also a matter of human survival in the future. The sustainable development of marine resources is closely related to the destiny of the whole nation and is considered as the basis of sustainable economic and social development. Promoting the coordinated development of land and sea industries, strengthening the integrated protection of land and sea ecological environment as well as achieving the coordinated and efficient utilization of land and sea resources are the guarantee for the healthy development of society, while we have no right to deprive or impair the rights of future generations to enjoy marine resources. Through strengthening marine education, drawing up national education development plan for marine knowledge and ecological protection as soon as possible, organizing experts and scholars to compile teaching materials and popular readings for marine education at various levels and types, we can enable marine education to enter schools, teaching materials and classrooms, as well as promote universities and research institutions to speed up the construction process of marine education disciplines. The development of marine resources and the protection of marine ecosystem should be promoted jointly through the education of marine resources and the protection of marine environment from early childhood, the persistence of the concept of sustainable development, the adherence of low-carbon development and the cooperation with relevant departments of marine resources.

5. Suggestions on the exploitation and utilization of marine resources and marine ecological protection

It is required that in the development of marine resources and marine ecological protection, we should adhere to the concept of ecological protection in the exploitation and utilization of marine resources. While in developing marine economy obtaining economic benefits through the development of marine economy has to be based on the concern for marine resources and marine ecological environment.

Only when the development of marine resources and the protection of ecosystem are upheld simultaneously can the comprehensive strength and international competitiveness of China be fundamentally enhanced [7].

5.1. Improvement of integrated management mechanism

Apart from the establishment of national marine legal systems and the improvement of relevant comprehensive marine management laws and regulations, the marine environmental quality standards and marine biodiversity protection standards should be continuously improved in the process of marine management. Local marine policies should be established and rigorous training centers might be set up to regularly conduct training for officials lacking management experience in coastal and island areas to enhance the law enforcement capacity of local marine management; Marine-related coordination and management structure should also be established to strengthen the monitoring capacity of marine resources exploitation and utilization as well as the law enforcement and management system of marine resources; A reasonable marine resources detection system should be set up to monitor marine living resources, marine ecosystems and sea level changes in offshore areas in real time, so as to provide timely feedback on changes in the ocean; The evaluation system for the sustainable development of marine resources is proposed to be established, which will enable relevant departments to make decisions on whether to approve the development projects of marine resources by referring to the relevant data in the evaluation system. It is required to assess the situation of the ocean from the whole region and then to formulate a comprehensive plan for the exploitation and utilization of marine resources based on the situation of each region. In addition, the possible impacts of certain man-made or natural disasters on marine resources should also be taken into account so as to achieve the continuous improvement and perfection of an integrated management system.

5.2. Protection of marine living resources

As the key part of the ocean, the protection of marine living resources is considered to be the protection of marine resources to a large extent. It is suggested that plans for the protection of marine living resources should be formulated, cooperation with neighboring countries should be strengthened, integrated management of marine biological resources should be enhanced, diversity of marine resources should be protected, management of marine fishery resources should be strengthened, marine aquaculture resources should be vigorously developed, the convenience of science and technology should be made use of to achieve continuous improvement of the aquaculture level of high-quality varieties, new aquaculture varieties to be continuously cultivated, investment in technology to be increased and high-yield and low-consumption aquaculture technology to be developed [8]. In addition, the protection of marine living resources requires the strengthening of national macro-control, the rational exploitation of marine fishing resources, the reasonable evaluation of the sustainable development of marine fishing for marine resources in the exploitation and utilization of marine resources, as well as the continuous rational adjustment of various laws and regulations in accordance with data provided by the evaluation system. Enhance fishermen's awareness of marine living resources protection. Actively encourage them to participate in the sustainable exploitation and utilization of fishery resources and strengthen the legalization of fishery resources management. Protect certain rare marine natural resources through the establishment of marine nature reserves. Protect marine ecosystems, including biological and ecological areas of great research value, as well as establish special marine conservation areas.

5.3. Protection of marine environment

Aiming at protecting the marine environment, it is firstly required to conduct control over the land pollution, including actively controlling the pollution of land-based pollutants to the marine environment, continuously evaluating the level of marine discharge from coastal sewage outlets, adopting sewage treatment measures to strictly control the sewage discharged into rivers and oceans as well as ensuring that all sewage has been treated before discharging. Minimize the discharge of pollutants which may cause eutrophication or red tide in the sea due to enrichment, encourage farmers to reduce the use of pesticides and fertilizers, prohibit the use of fertilizers and pesticides that may lead to severe pollution to land resources, control the discharge of pollutants and certain pollution activities at sea, require people working at sea to take timely measures to protect the living areas of rare organisms when confronting dangers, protect the living areas of rare organisms, actively assess the impact of the use of oil and gas on sustainable development, strictly prohibit dumping or incineration of dangerous goods at sea, continuously improve the detection system of marine environmental pollution and carry out timely adjustment to the unreasonable systems.

5.4. Strengthening construction of marine science and technology

In order to strengthen the construction of marine environmental scientific research system, it is necessary to conduct in-depth research on marine biology and other disciplines relating to marine protection, continuously develop control technologies for land-based and marine pollutant discharge, improve sewage discharge standards and marine ecological nature protection technologies, real-time monitor the impact of pollutants on the marine environment, strictly control the occurrence mechanism of red tide as well as make prediction. Strengthen the research on marine resources development, actively study the environmental capacity and purification capacity of coastline and island areas to determine the reasonable development scale, layout and carrying capacity for population of the marine industry, real-time monitor the impact of marine exploitation and utilization on marine environmental resources, continuously strengthen the protection of marine nature resources, enhance the technology of desalination and direct utilization of seawater, strengthen the technological development of marine food and drugs, increase the construction of new energy sources and the comprehensive utilization of certain resources and products, as well as achieve more rational and greater exploitation and utilization of marine resources through intensifying the construction and research of marine science and technology.

5.5. Strengthening international cooperation

The protection of marine resources also calls for continuous strengthening of international cooperation, including active cooperation with other countries in scientific research on marine resources, regular training and exchange of technical knowledge with foreign countries, joint formulation of action plans on ecological environment detection and protection with neighboring countries, as well as achieve joint protection and management of marine ecological resources through positive benefits. Achieve common progress in marine resources development and protection with other countries by actively utilizing international aid funds to develop marine science and technology and share information on marine development.

6. Conclusion

From the perspective of sustainable development of marine resources, this paper advocates that the ecological view, future view of sustainable development as well as the responsibility of great powers should be adhered to in the process of marine exploitation and utilization. Except for satisfying the demand of social life and development through appropriate exploitation and utilization of marine resources, the demands of future lives or people of other countries should also be taken into consideration. The exploitation and utilization should be based on the premise that it does not affect the lives and production of future generations or people in other countries. As an irresistible trend of the times and the inevitable requirement of human’s pursuit of a better life, the exploitation of marine resources and the protection of marine ecology are the necessary route to achieve the sustainable development of China's marine economy and the construction of a maritime power, as well as the requirement of strengthening cooperation among coastal countries, promoting the globalization of marine economy and the construction of the community with a shared future for mankind under the "One Belt And One Road" initiative. Covering the production mode, lifestyle and values of human beings, the exploitation of marine resources and the protection of marine ecology should be regarded as an extremely feasible mode of development.

7. References

[1] Xue Shan, Wang Zhao. Protection and Exploitation of Marine Resources based on Sustainable Development[J]. Chinese Fisheries Economics, 2013, 31 (06): 152-156.
[2] Report on Developing Marine Economy and Accelerating the Construction of a Maritime Power,December 24th, 2018
[3] Zhang Fanrong. Discussion on the construction of the relationship model between local governments in regional ocean management [D]. Xiamen University, 2009.
[4] Chen Guosheng, Ye Xiangdong. Sustainable Development and Countermeasures of Marine Resources [D]. Ocean Development and Management, 2009.
[5] Cheng Na. Research on China's Marine Economic Development from the Perspective of Sustainable Development [D]. Jilin University, 2013.
[6] Li Yang. Research on Control of Pollution Damage of Marine Tourism Resources [D]. Resource Economization and Environmental Protection, 2014.
[7] Li Bin. On the construction of marine ecological protection compensation system [D]. Ningbo University, 2017.
[8] Zhou Kai. The studying about the construct of the Bohai Sea synthetical management supervisory-control capability [D].Ocean University of China, 2009.

IOP Conf. Series: Earth and Environmental Science **369** (2019) 012010 doi:10.1088/1755-1315/369/1/012010

Systematic study of renewable energy–resource potential in Pakistan

Qasim Rauf[1], Yanpin Li[1] and Anam Ashraf[1]

1 North China University of Water Resources and Electric Power, Henan, China
E-mail: anamashraf100@yahoo.com

Abstract. Earth does not have an equal distribution of energy sources. Electricity performs a major contribution in the socio-economic improvement and national development of nation. Energy is essential for all financial exercises. In 2008 the government of Pakistan paid almost 9 billion USD to fulfill the energy demand by importing the crude oil. After this Pakistan's national economy effected badly. Now Pakistan is facing and going through its most bad period of energy crisis. The sustainability of the energy sector is directly proportional to the economic sustainability of the country. The important task of this paper is to highlight the perspective of renewable energy in Pakistan. This paper contains the current situation and future plans of renewable resources like Solar, Wind, Hydel, Biogas, Geothermal energy. The total current capacity of operational projects is solar 100 MW, Wind 308 MW, Biogas 145 MW, 98 MW micro hydel. While the many projects are in different stages of the development like solar 856MW, wind 1146 MW, biogas 297 MW and micro hydel 2638 MW. This paper is also presenting the review about the renewable energy resources potential available in the country that is not exploited yet for the steady and reliable energy supply. This paper contains the information regarding the renewable energy which will be helpful for the government as well as for the stake holder of private sector, those who wants to invest in Pakistan for the renewable energy. The renewable energy resources are abundant and have great potentials that shows, Pakistan can minimize the energy gap between demand and supply in the future and overcome the energy crisis. This paper will be helpful for the government as well as the stake holders of national and international level.

1. Introduction

In this era of globalization the demand of energy is increasing rapidly. Energy performs a major role in the advancement of country. The dependency of countries on electricity indicates us that the energy will be the biggest problem in coming years so we must find some alternative sources that fulfill over energy demands. Pakistan is a developing country and requires more energy to fulfill the requirement of households, industrial and agricultural needs. Pakistan is facing the worst problem of energy shortage and going through the periods of energy crisis. The energy crisis in Pakistan is due to the lack of planning for the future development at country level. It will be great referred to reality that the technological and the industrial advancement is heavily depends upon the fossil fuel. The major portion of energy all over the world still relies on the fossil fuel. According to (Odum and Odum 2001), the world is running on 60 % non - renewable resources. "It's expected that worldwide energy demand will be increase by two thirds in 2001-2030 (IEA, 2002a)." These conventional energy resources have not huge reservoirs and these reservoirs are decreasing day by day because demand of energy increasing with the rate of advancement and the rate of population as well. These reservoirs will not last very long. *"It is predicted that fossil fuels can only meet the world's energy demand just for three decades more (IEA, 2002a)."* Because of the excessive use of non-renewable energy resources the climates changes rapidly, which is mainly caused of global warming by the emission of greenhouse gas emission from energy generating systems.

For energy Pakistan uses conventional sources highlighted below.

1.1. Conventional ssources:

a. Thermal Energy
   - Coal
   - Oil
   - Natural Gas
b. Nuclear Energy

1.2. Renewable energy and primary energy consumption in Pakistan

Pakistan has enormous resources of renewable energy that can be used for the generation of electricity. The northern areas of Pakistan have huge ranges of mountains and glaciers that can be used for the hydropower projects of different sizes. Following 1970's oil crisis, the issues from claiming "security of vitality supplies" and "sustainable utilization of vitality sources" need get exceptionally imperative approach issues. Starting with then, the issue of using alternative source of energy becomes very popular and the non-oil producing countries and the developed countries faced the immense supply of oil problem. At that time they created a financial recession in all over the world by raising the oil prices. After the green rising movement the agenda of environmental problem was become dominant.
As far as the fossil fuels are concerned its still important in the world as main energy supplier. The 60% of the total energy comes out from fossil fuels. The utilization of fossil fuels is more than the earth capacity to generate it. So, the reservoirs of oil are depleting out exceptionally quick and it is anticipated that, "the remaining reservoirs can only meet the world's energy demand just three decades more (IEA, 2002a)". In addition, the environmental issue that is caused of non-renewable energy resources is another huge peril with in future. Along with environmental issues, climate alters too made financial and social misfortune. Since of these reasons, the energy generation from renewable resources has been picked up in the energy policy agenda [1].
Pakistan has huge potential and resources of renewable and non renewable energy sources, which are unexplored. So, as a result fossil fuels cannot meet the demand of electricity; the price of per unit is almost 12 to 18 PKR per unit. Moreover, very huge part of the rural areas and villages didn't have the facilities of electricity because either its cost is too high or these areas are too far from the national grid and the country is facing the huge problem of economy because of electricity shortage. If we consider the Pakistan textile industry it is also affected badly.
In current energy supply of country the ratio of Oil is (30%) and gas is (48.5%). Pakistan is full of natural resources, but the resources that are reasonable, affordable, reliable and have shining prospect to be assumed commercially are(Solar (PV, thermal), Water (mega & local macro-micro-hydel), Wind, Wastes/Biomass (animal waste) and Geothermal energy. The conventional resources cannot fulfill the demand of energy in the country. Pakistan is not a developed country and has the issue of economy as well. Therefore, the development is very important in this field to meet the challenges of the country. [2]

1.3. Potential of renewable energy resources and current development status in Pakistan

1.3.1. Solar power

The energy which obtained from the sun radiation is known as Solar Energy. Solar Energy is classified into two categories first one is "**solar photovoltaic (PV)"** and second one is "**solar thermal conversion"**. In solar photovoltaic (PV) the PV cell directly convert radiation into heat. This procedure is not new one. People are using solar radiation for heating, cooking, drying animal skins, clothes, drying crops, evaporating seawater for extracting salt from years. In community level people using PV cell for vaccine refrigeration, heating water, purification and rural electrification. Pakistan government gives the Solar Photovoltaic plate to the students of schools that convert directly sun radiation into electricity. The second type is "**solar thermal conversion"**, In solar thermal conversions; the thermal collectors generate a stream by heating the liquids and works like a standard stream turbine. Solar energy has picked up acknowledgement around the worlds; this innovation is encountering a stunning development. According to European Photovoltaic Industry Association (EPIA)[3], over the last decade, the solar photo voltaic (PV) has seen the most noteworthy development of 28%. According to economic Survey 2017-18 revealed that Pakistan's installed capacity to generate electricity has surged up to 29,573MW by February 2018 which stood at 22,812MW in June 2013, showing the growth of 30 percent [4] We may be racing down the pathway towards a 100% renewable electricity future, but when it comes to heating, cooling and transport, we are coasting along as if we had all the time in the world. Sadly, we don't. [4]"

The total potential of solar power in Pakistan is 2.9 million MW. Pakistan has the 9 hours of sunshine per day is real condition for solar power generation [5]. Pakistan is located in the sunny belt and luckily has high irradiance of sunshine and high insolation level by which can get high advantages of solar technologies. According to the solar mapping survey of National Renewable Energy Laboratory (NREL), USA in collaboration with USAID, Pakistan has ideal conditions for Solar Potential as shown in figure 1.

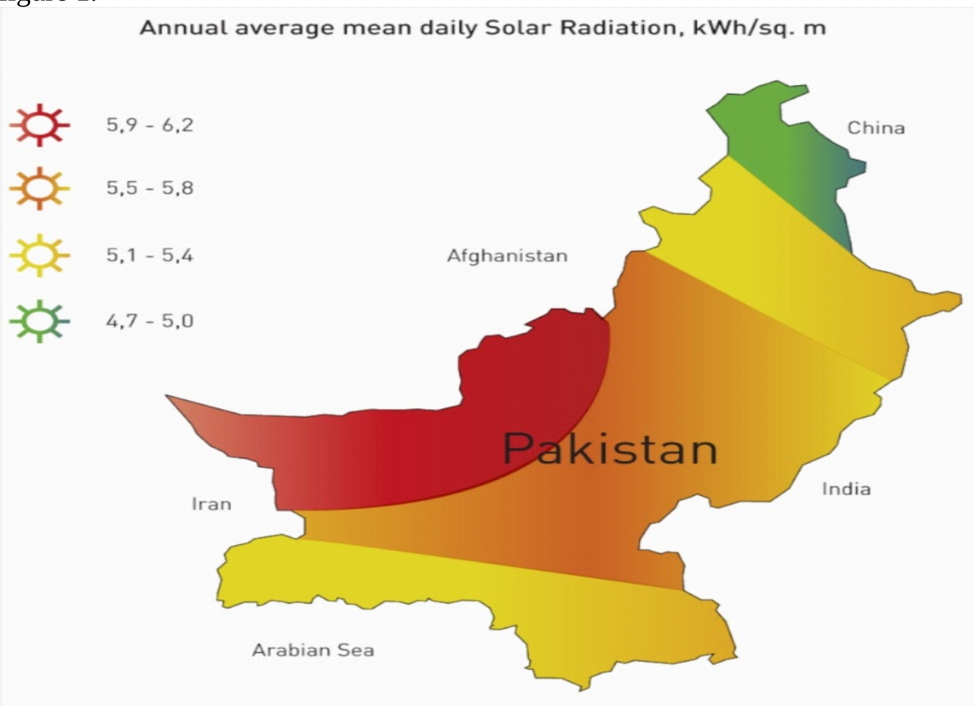

Figure.1. Ideal for Solar Energy [6]

Pakistan can take advantages and improve the condition of people living in rural areas. According to the calculation approx. 40,000 remote villages can be electrified by using the solar energy [7]. Those areas where the installation of transmission lines is expensive solar energy can be used. Solar technologies have broad scope like on grid and off grid applications as mentioned below .

- **Electricity to Villages**

  Those villages that are so far from the grid and it will be very expensive and not feasible to extend the grid toward these areas. These villages are the best candidates for the solar power energy system. These houses are almost 40,000 [7].

- ***Solar Pumps***

  Solar pumps have wide and open market for the investment in Pakistan. Because there is only 22% of people have excess to natural gas.

- **Solar street lights**

Pakistan has total street lights of over 500,000, which used almost 40 MW power. It's a very good that we replace these lights with solar lights for saving the electricity.

- ***Solar fans***

  Solar fan is very helpful and reliable for those who haven't the excess of electricity.

- ***Power project using solar thermal conversion technology***

  Solar thermal conversion technology is pretty similar with the steam turbine. In steam turbine the coal or oil is used in the furnace for making the steam but in solar thermal conversion the sunlight used for the heating the water to make the steam.

Pakistan has five provinces and every province has the huge potential of solar energy. The average irradiance in Pakistan is about 200 to 250 Watt per meter square (W/m^2) per day over a plain surface. The sum is 1.9 to 2.3 MW hour per meter square(MWh/m^2)[8].
In 2003, Pakistan established Alternative Energy Development Board (AEDB) is the sole representing agency of Federal Government [9]. Pakistan governments start so many small and mega projects like this. The mega Project started by Government of Pakistan (GOP) first one of this type, which will produce electricity from photovoltaic (PV) solar on commercial basis. Quaid-i-Azam is the mega project is which based on solar energy, the capacity of this project is to produce the 100MW in start, However this capacity will be increased up to 1000MW with the cooperation of public and private sector [8].Quaid-i-Azam solar plant, look for to attain the socio-financial success and sustainability for the country, for the planet, a higher and for the much better future [9].

1.3.2. Wind power

Wind is created as a result of monster convection streams within the earth's environment, which is driven by the heat energy from sun. It's implies that kinetic energy in wind is a resource of renewable energy, the wind turbines captures the kinetic energy and convert into mechanical energy and used for power generation. Wind is a type of solar energy, so until the sun exists the wind will exist as well. Wind energy contributes in the total electricity production in the country of almost 0.1% [10]. According to the survey China and India have fourth and fifth place in the largest installation of wind turbines. China and India has almost 45,000 MW (megawatt) potential of wind energy and much larger surface area while Pakistan has 50,000 MW (megawatt) wind potential. Pakistan luckily has everything which most of the countries donot have, like the wind speed is very high near Islamabad the wind speed is from 6.2 to 7.4 m/s (between 13.8 and 16.5 miles per hour). The range of wind near Karachi is between 6.2 and 6.9 (between 13.8 and 15.4 miles per hour) [11].
The two province of Pakistan, Balochistan and Sindh have enough potential of wind energy. Because at there exist a corridor between Gharo and KetiBandarthat could alone produce between 40,000 MW to 50,000 MW of electricity. In recent years, the government of Pakistan has completed numerous projects that proves the potential clearly and practically of wind energy in the country. Just the 85 micro winds turbines are installed in Mirpur Sakro which gives electricity to 356 homes, 40 small turbines are installed in Kund Malir which have the capacity to give the electricity to 111 homes. The Alternative Energy Development Board (AEDB) has moreover procured 18,000 acres of land for the establishment of more wind turbines [12]."The Chief Executive Officer of the AEDB, Amjad A. Awan, stated that the total installed wind energy capacity in the country is currently 255.4 MW, but is expected to increase rapidly. Currently 28 projects with a cumulative capacity of 1,396.4 MW are under construction, of which nine have achieved financial closure and 14 are under various stage of project development. Awan did not give details about the balance 1-1.5 GW capacity that the Board expects to be added by 2018[13]."From last few years Pakistan increases the activities in the renewable energy field because the short fall of electricity is increasing day by day. So many European countries are looking for the investment; they announced plans and they are willing to invest in the renewable energy sector. China is the major investor in all sectors of energy in Pakistan[14].
The Alternative Energy Development Board (AEDB) has great efforts and contribution in the development of the energy sector and to minimize the energy crisis of the country. For the collection of data, forty-two stations are installed for wind energy potential data in northern areas at different

heights including the Swat, Dir, Chitral, Gilgit etc. The northern areas are not very suitable and attractive for wind potential energy. In 2007, the yearly Khungi payan power (Dir/NWFP) and Shaheed Gali (AJK) was remained 27.49 W/m2 and 208.19 W/m2 and with highest wind speed of 2.61 m/s and 6.53 m/s respectively [15,16]. These areas are categorized as low potential wind areas with respect to coastal areas of Sindh.The coastal areas of Sindh indicates the high potential of wind, "The annual average of wind speed at 50 m height has given 8.5 m/s, 7.0 m/s, 7.0m/s, 6.7 m/s and 6.6 m/s at Jamshoro, Katibandar, Nooriabad Thatta and Gharo respectively [17]."The Corridor of Wind of the Sindh covers an area of 9700 Sq. Kms. The total potential of Sindh corridor area is 43,000 MW but due to the utilization constraints and some other reasons, the area which is available for the production of the electricity is estimated more than 11000 MW [18]

1.3.3. Geothermal energy

The heat that stored beneath the surface of the solid earth in the form of energy is called geothermal energy. Geothermal has large amount of potential in all the provinces of the Pakistan. However there is no exact evaluation about the potential of this source of energy. Geothermal is still one of unexplored energy resource for the production of electricity. Pakistan can solve the issues of energy crisis at a noteworthy level by using the resource of geothermal resource.

Pakistan exists in the seismic belt, and majority of the hot springs and mud volcanoes exists in this belt of Pakistan [19]. Geothermal energy comprises around the 2% of the renewable energy [20]. The natural resources like solar, wind are unlimited, but these resources are expensive resources and relatively complex control scheme is required to attain energy for grid stations as compared to geothermal energy According to the geologist's survey, the structural study confirms that Pakistan lies on the junction of tectonic plates, that's why it has abundant reservoirs of geothermal energy including high, medium, low temperature to support energy sector at a significant level [21]. The continuous decaying of 20% fossil fuels and 80% radioactive minerals creates heat inside the earth [22].This energy is the best cleanest, reliable, abundant, renewable resource of energy. This resource produces less emission of carbon as compared to oil, gas and coal. The best thing about geothermal energy is the 24 hours availability, while solar can produce electricity in the daylight, wind turbine can produce electricity at coastal areas in the favorable wind speed [23].The setup of geothermal energy is controlled by the geodynamic and tectonic. The fold belts and plates boundaries, including foreland and sub basins, inner deep tensional fracture zones at the anticline axis and the boundaries of graben structures, which considered as heat controlling features [24]. This resource is analysed by four ways namely hydrothermal, geo- pressured, hot rock, dry rock. Due to the flexibility the foremost investigated frame of investigation is hydrothermal resources [25].

1.3.4. Hydrothermal energys

Hot springs or steam springs, geysers or fumaroles are types of hydrothermal energy resources which are continuously flowing in many areas of the Pakistan. The Northern areas of Pakistan namely Chitral, Gilgit, Baltistan and Kashmir have the geothermal resources with the temperature ranging from 80 ℃ to more than 180 ℃. There are many hot springs in all the provinces of Pakistan.

1.3.5. Deep geothermal resources/ enhanced geothermal resources

The geological, tectonics, the active seismic zones and abundant deep oil and gas well with high temperature shows us those deep geothermal resources are available in different areas that could be develop by Enhanced geothermal resources technologies. These resources can produce approx. 30,000 MW electricity [26,27]. Pakistan is producing more than 80% electricity by the fossil fuels (coal, gasoline, oil). While 15% electricity produced by the solar, wind and hydropower resources. Presently the co-produced hot waters from the oil & gas wells are being drained out in dry streams, or re-injected in the wells or evaporated after heating using natural gas.The potential of geothermal energy is huge in Pakistan, the power generation has been estimated 100,000 MW.

1.3.6. Biomass

For the energy security of future and environmental problems is main driving force to increase the utilization of biomass all over the world especially in the developing countries like Pakistan. In the renewable energy the developed countries utilize for the energy production for the feedstock of energy system is waste streams but the Pakistan and the other developing countries are lagging behind and these countries are looking for the correct methods and execution of biomass as an alternative source of renewable energy. The total of global energy nearly 18% of energy comes from the clean energy resources including solar, wind, geothermal, biomass and hydropower [28].The developing nations are confronting the issue of separate energy crisis driving to antagonistic social and long term financial problem [29].From thousands of years the biomass energy has been used as primary source of energy for power generation; IEA states that,"biomass as any organic, decomposable matter derived from plants or animal available on renewable resource basis [30]."Biomass includes wood, agricultural crops, waste and manure and herbaceous [31]. Biomass is mostly used for energy; in 2014 the biomass contributes 10% total global supply of primary energy [32]. In the future the use of biomass energy increases up to reach 3000 TW h by 2050 [33].

Pakistan's 62% of total population lives in the villages and rural areas [34]. The major population of Pakistan's directly or indirectly involves with the agricultural profession. The traditional biomass fuels like fuel woods, cow dung and agriculture residues are the principal source of energy generation in the rural and villages areas[35].Biomass is one of abundant resource which is growing and being used with pace. Till now, the 5357 biogas plants have been installed by the Pakistan Council of Renewable Energy Technology (PCRET) (with a net generation capacity of 12-16 millions m/day) on a cost sharing premise [36]. The Alternating Energy Development Board (AEDB), cooperate with distinctive organization from the USA, Denmark and Germany has evaluated the potential of biomass for power generation in Pakistan. This estimate shows the potential of 1800 MW biogases and 500 MW from waste [37]. So, it's true that considering the quality, quantity and availability of the resources is nothing in front of the current development [38].

1.3.7. Hydro power

Pakistan's Water and Power Development Authority (WAPDA) publish report, Pakistan has potential of hydro electric power is 100,000 megawatt (MW) with identified sites of 59,000 megawatt [39] but annual flow of rivers could store just 13%. In 1960 the approx. 70% of the energy generation came out from hydel electric power [40].The hydel power is already well established worldwide, 87% energy generated from renewable resources comes out from hydel [41].

Pakistan's total capacityof electricity generation is 23,000 megawatt(MW), 6500 megawatt (MW) is produced from the hydro, which is 34% of the total capacity of electricity generation [42]. Pakistan is facing the worst period of energy crisis because the Pakistan's depends upon the fossil fuels. The main reason of energy crisis is due to price fluctuation and over dependence on imported fuels for the thermal power plant.The country's power sector in hydropower was once under pinned in 1991 accounting for 45% of power generation, but this contribution reduce to 28% due to short term planning preferred to thermal power [43]. The public and private sector has installed 300 micro/mini hydroelectric plants in the areas but these plants are not connected with national grid [44]. The Khyber Pakhtunkhwa government took the initiative and installed 1000 micro hydro electric power plants with the support of Asian Development Bank. The expected total capacity is 100 MW [45]These power plants designed to support rural areas and off -grid communities by giving them reliable and affordable electricity. The main Potential sources of hydro power are on the rivers of Indus, Jhelum, Chitral and Swat. Some public sectors projects are under construction, include Golen Gol (106 MW), Neelum-jhelum (969 MW),Dasu (4320 MW) and "Tarbela Dam" extension under the supervision of WAPDA. The Tarbela Dam is located on the river Indus, after fourth extension its capacity will be lift up to 4,888 MW from 3,478 MW. The largest earth filled dam in the world is Tarbela Dam [46].

Moreover,In 2025 Water and Power Development Authority(WAPDA) has planned to generate at least 16,000 MW of electricity from hydel[47].

The total micro hydel potential in the Pakistan is 3010 MW as shown in table 1.

S.No	Area	No. of Potential Sites	Potential Range (MW)	Total Potential (MW)	Remarks
1.	Khyber Pakhtunkhawa	125	0.2 – 32	750	Small / Micro based on Natural Falls Flow
2.	Punjab	300	0.2 – 40	560	Canals
3.	Gilgit – Baltistan	200	0.1 – 38	1300	Natural Falls
4.	Sindh	150	5 – 40	120	Canals Falls
5.	Azad Jammu & Kashmir	40	0.2 – 40	280	Natural Falls
TOTAL				**3010**	

Table 1. Small Hydro Potential in Pakistan [48]

2. Comparison of renewable energy potential for South Asian Countries

Energy is critical directly or indirectly, to the entire process of advancement, development and for the survival of the human being. Energy plays an imperative role in the socio-economic development of the country. South Asian countries are blessed with huge potential of renewable energy. The South Asian countries are Pakistan, India, Bangladesh, Afghanistan, Bhutan, Maldives, Sri Lanka and Nepal. These countries collectively called as SAARC (South Asian Association for Regional Coorporation). SAARC providing the affordable reliable, easily accessible and low to zero carbon electricity in the developing countries, this will be the aim of electricity generation in the next decade [49].South Asian Countries are taking initiative towards the alternating sources of energy to reducing the overdependence on the fossil fuels. These countries have huge gap between energy supply and demand, to overcome the energy demand they must going towards renewable energy sources [50]. Energy Supply is the major challenge on the street to advancement in the South Asian Nations.

2.1. Analysis of electricity consumption of South Asian Countries

2.1.1. Energy consumption of South Asian Countries per capita

Table 2 shows the comparison of energy consumption of South Asian Countries per capita India have the highest consumption of per capita electricity

South Asian country	Per capita electricity consumption in kWh
India	644
Sri Lanka	636.3
Pakistan	457
Afghanistan	119.8
Bangladesh	278.1
Nepal	454.1

Table.2. Total Consumption of energy per capita [51]

2.1.2. Electricity consumption and uses of SAARC

Electricity consumption and uses are showed in below table.

Country	Energy consumed (million tons of oil equivalent)	Fossil fuels (% of total use)	Combustible renewable and waste (% of total use)	Alternative and nuclear energy (% of total use)	Energy produce (million tons of oil equivalent)	Energy Use – Energy production (Mtoe)
India	749.4	72.3	24.7	3	540.9	208
Sri Lanka	10.4	48.7	47.4	3.9	5.3	5.1
Pakistan	84.8	60.9	34.6	4.5	65.1	19.7
Afghanistan	–	–	–	–	–	–
Bangladesh	31.3	71.5	28.2	0.2	26.1	5.2
Nepal	10.4	12.5	84.1	2.7	9	1.4

Table.3. Electricity Consumption and Uses [52]

2.1.3. Dependency of SAARC on fossil fuels

Table 4 shows the how South Asian Countries rely on the fossil fuels for the electricity production. Pakistan and India has overdependence on fossil fuels. Five countries have less than 5% of their total energy in renewable energy.

Country	Electricity production (kWh billion)	Coal (% of total)	Natural gas (% of total)	Oil (% of total)	Hydropower (% of total)	Renewable energy (% of total)	Nuclear power (% of total)
India	1052.3	67.9	10.3	1.2	12.4	5	3.2
Sri Lanka	11.6	8.9	0	50.2	39.7	1.2	0
Pakistan	95.3	0.1	29	35.4	29.9	0	5.5
Afghanistan	–	–	–	–	–	–	–
Bangladesh	44.1	1.8	91.5	4.8	2	0	0
Nepal	3.3	0	0	0.1	99.9	0	0

Table.4. Electricity Production [53]

2.1.4. Renewable energy potential of SAARC

Table 5 shows the Solar, Hydro, Wind Power potential in South Asian Countries. These resources are unlimited if countries use these natural sources and reduce the overdependence on fossil fuels, they can provide the cheapest, reliable and affordable electricity to their nation.

Country	Solar power potential (kWh/m^2/day)	Hydro power potential (MW)	Wind power potential (MW)
India	5.0	150,000	102,778
Sri Lanka	5.0	2,000	24,000
Pakistan	5.3	59,000	131,800
Afghanistan	6.5	25,000	158,000
Bangladesh	5.0	330	–
Nepal	4.0	83,000	–

Table.5. Renewable Energy Potential [54]

3. Agenda of Pakistan Council of Renewable Technology (PCRT)

In May 8, 2001, The Pakistan Council of Renewable Technology (PCRT) was founded by the alliance of National Institute of Silicon Technology (NIST) and Pakistan Council of Appropriate Technology (PCAT) [55]. According to the survey almost 85 to 90 % efforts of PCRT are directed towards the improvement of existing and cost effective renewable energy resources and remaining 10 to 15 % for the new research based concepts and technologies [56].

The main agenda of PCRT is as follows:

1) PCRT is to do research & development in the field of sustainable energy technologies for the county's socio-economic development

2) Promote the existing and new technologies to reduce the gap of energy supply & demand.

3) The environmental polluting resources replace with the clean energy resources

4) To promote the research, develop and spread the energy training services or workshops to those people, who are not familiar with renewable energy, those who are living in rural areas, introduce the new trend of renewable energy among them.

4. Objectives of Pakistan renewable energy society

1) For the country's development, organize the training workshops, seminars, exhibitions and practical projects about the renewable energy.

2) Reduce the poverty in the farther regions implement the different projects of renewable energy.

3) To make great strides and develop the market industry of RE.

4) Public awareness with the help of electronic media like the advertisement etc

5) Make Evaluation and Monitoring Team, who monitors and evaluates the system program & activities that how's going and implemented system successfully

6) PCRT in dominating in research and development of RE, Research institutes can also plays vital role by revised the topics and introduce new technologies.

7) New technologies can be useful source of employment like new technologies needs skilled men, services installation and maintenance & operations.

8) Provide financial incentives to the individual level like India.

5. Purpose of Study

The whole above discussion is about that how much the potential of Pakistan has in the field of renewable energy. There are so many reasons that is why author wants to write and propose the solution. The total population of Pakistan is 201 million [57]. The statistics of Outlook World Energy, at least 27% or 51 million peoples of Pakistan haven't the excess of electricity . Infect, they haven't the basic necessities like clean water, refrigerator etc. Pakistan has total 125,000 Villages and almost 95,000 villages have the excess of electricity and 30,000 villages haven't excess. Even some villages are connected with grid but they have no reliable excess of electricity and they face the load shedding of 10 to 12 hours per day. In Pakistan 50% of the total population living in the rural areas and they are using the traditional biogas technique for the cooking purposes. They used the animals dung, fire woods and agriculture waste as a fuel. The use of animal dung as fuel for cooking inside the houses cause serious health problem. According to the report of WHO [58] death of more than 50,000 premature occur per year in Pakistan because of the inside air pollution. Especially the children and women are affected most. The main purpose of this study is to highlight the renewable energy resources of Pakistan to make them utilize; if the government of Pakistan reduces the over dependency on fossil fuels and policymakers make the policies for betterment of the people future than we can overcome the electricity shortage which is more than 5GW.There is need to be consider the following points :-

1) Try to rely on the existing natural resources of the Renewable energy.
2) Give the awareness to the public, provide financial incentives and organize the training sessions and workshops about the importance of renewable energy. Public investing so much

IOP Conf. Series: Earth and Environmental Science **369** (2019) 012010 doi:10.1088/1755-1315/369/1/012010

on the solid fuels, kerosene oil, batteries, LPG, fire woods ,Gas cylinder etc. They can save that money if they use the solar heater, solar lights, solar fans etc.

3) Pakistan government should give the solar power or biomass power to those rural areas where the excess of grid is not feasible, they are candidates for solar energy.
4) Give the awareness about the small biogas plants and provide the opportunities for development of the future otherwise Pakistan will be in the top 5 countries with highest proportion of people living without the electricity.

6. Conclusion

Pakistan has a huge potential in every sector of renewable energy. Its large potential is lies already in well established hydro power industry. Pakistan has also enormous potential in Solar, Wind, Geothermal and Biomass. The government of Pakistan needs to stop overdependence on fossil fuels and accelerate the development towards the clean energy sources. These sources can provide clean, cheap, reliable and low to zero carbon electricity, which is helpful for the global environment as well. These resources are natural and unlimited. Pakistan is taking several initiatives towards alternative source of energy, Alternating Energy Development Board (AEDB) working hard and trying to reduce the overdependence on fossil fuels but yet huge unexploited potential remains. Pakistan must generate only 10% of energy demand from the renewable resources. If Pakistan use the available renewable resources with proper planning and implement the ideas, the country could have surplus energy to supply and overcome the energy crisis permanently. In future we can extend our research by providing a proper road map for the utilization of renewable energy resources in Pakistan to improve the shortage of electricity in our homeland.

7. References

[1] Ukessays 2015, “Potential of Renewable Energy Sources in Pakistan Environmental Sciences Essay”

[2] http://www.aedb.org/Documents/Policy/REpolicy.pdf. [Accessed on 08.02.18]

[3] Global market outlook for photovoltaic’s 2014-2018, European Photovoltaic Industry Association (EPIA); 05/2014.

[4] https://www.thenews.com.pk/print/309535-country-s-installed-electricity-capacity-increases-by-30pc-to-29-573mw [Accessed on 30/01/19]

[5] Pakistan has 2.9 million MW potential of solar energy,https://tribune.com.pk/story/1357453/going-green-pakistan-1-9mw-solar-energy-potential/ . [Accessed 08-02-2018]

[6] https://www.meeco.net/blog/pakistan-ideal-market-for-solar-energy/ [Accessed on 08/11/18]

[7] « Potential of Renewable Energies in Pakistan « 2015, https://defence.pk/pdf/threads/potential-of-renewable-energies-in-pakistan.379477/ [Accessed 08/02/18]

[8] Khalil, M.S. Renewable Energy in Pakistan: Status and Trends. Pakistan Alternative Energy Development Board, Prime Minister’s Secretariat, [Accessed on 08/18/18]

[9] Term of Reference, Alternative Energy of Development Board, http://www.aedb.org/about-us/terms-of-reference. [accessed on 8/2/18]

[10] "In coal-focused Pakistan, a wind power breeze is blowing", https://www.reuters.com/article/us-pakistan-energy-windpower/in-coal-focused-pakistan-a-wind-power-breeze-is-blowing, [Accessed on 08/05/18]

[11] GLOBE-Net, “India: Renewable Energy Market” http://www.globe-net.ca/market_reports/ , [Accessed on 08/06/18]

[12] Ministry of New and Renewable Energy Sources, “CFA Provided Under Various Renewable Energy Schemes” http://mnes.nic.in/cfa-schemes-programmes.htm, [Accessed on 08/06/18]

[13] “Wind Energy Capacity”, https://cleantechnica.com/2015/11/26/pakistan-add-3-5-gw-wind-energy-capacity-2018/ , [Accessed on 08/06/18]

[14] “Potential of renewable energy in Pakistan” Retrived on 8th august 2018 from https://defence.pk/pdf/threads/potential-of-renewable-energies-in-pakistan.379477

[15] Technical Report no. 07/2008. Pakistan Meteorological Department.Study of Wind Power Potential at Khungipayan. [Accessed on 08/06/18]

[16] Technical Report no. PMD-12/2008.Pakistan Meteorological Department.Study of Wind Power Potential at ShaheedGali, AJK. [Accessed on 08/06/18]

[17] Technical Report no. PMD-07/2007.Pakistan Meteorological Department. Wind Power Potential of Sindh.

[18] "Renewable Energy in Pakistan", https://en.wikipedia.org/wiki/Renewable_energy_in_Pakistan#cite_note-1 ,

[19] Umairyounas**,** Volume 63, September 2016**"**Pakistan geothermal renewable energy potential for electric power generation**",** , [Accessed on 08/07/18]

[20] F.R. Pazheri, M.F. Otham, N.H. Malik. Rev 31 (2014), "A review on global renewable electricity scenario Renew Sustain Energy ", [Accessed on 08/07/18]

[21] Hossein S. 2005, » Energy Scenario in Pakistan. In: Proceedings of the world geothermal congress ». (Antalya, Turkey)[Accessed on 08/07/18]

[22] Government of Pakistan. Pakistan Engineering Council (PEC); 2012. [Online] [Accessed on 08/07/18].

[23] I.B. Fridleifsson, 2001 "Geothermal energy for the benefit of the people", Renew Sustain Energy [Accessed on 08/07/18].

[24] Javed Ahmed 2014, "The Geothermal Energy Potential of Pakistan Clean Sustainable Solution for Our Energy Future", GRC Transactions, [Accessed on 08/08/18]

[25] Wang W, Han Y 2010, The analysis on a potential of saving energy and environmental benefits on heat pump in geothermal heating" , IEEE [online], [Accessed on 08/08/18]

[26] Farah, A. and Dejong, K. A, 1979. Geodynamics of Pakistan. Geological Survey of Pakistan, Quetta. [Accessed on 08/08/18]

[27] Bruce D. Green & R. Gerald Nix, National Renewable Laboratory US D.O.E., Geothermal Resources Estimates for United State. [Accessed on 08/08/18]

[28] Kumar A, Kumar K, Kaushik N, Sharma S, Mishra S. 2010, Renewable energy in India:current status and future potentials. Renew Sustain Energy;14(8):2434e42. [Accessed on 08/0918]

[29] Economic survey of Pakistan, Islamabad. Government of Pakistan Ministry of Finance; 2010, [Accessed on 08/09/18]

[30] International Energy Agency (IEA), Bioenergy, https://www.iea.org/topics/renewables/subtopics/bioenergy, [Accessed on 08/09/18]

[31] zhu L, Huo S, Qin L. A 2015 microalgae-based biodiesel refinery: sustainability concerns and challenges. Int J Green Energy [Accessed on 08/09/18]

[32] International Energy Agency (IEA). IEA Bioenergy annual report; 2014, [Accessed on 08/09/18]

[33] IEA technology roadmap- Bioenergy for heat and power. InternationalEnergy Agency (IEA); 2012, [Accessed on 08/09/18]

[34] The World Bank. Data- Rural Population, http://data.worldbank.org/indicator/SP.RUR.TOTL.ZS [08/09/18]

[35] Butt S, Hartmann I, Lenz V. 2013 Bioenergy potential and consumption in Pakistan. Biomass Bioenergy [Accessed on 08/09/18]

[36] Uddin W, Khan B, Shaukat N, Majid M, Mujitaba G, Mehmood A, Ali S, Younas U, Anwar M, Almeshal A. 2016, Biogas potential for electric power generation in Pakistan: a survey. Renew Sustain Energy [Accessed on 08/09/18]

[37] Ullah K. 2013, Electricity infrastructure in Pakistan: an overview. Int J Energy Inf Commun Accessed on 08/09/18]

[38] Singh P. 2015, Pakistan: DiamerBhasa Dam struck in the funding trap- analysis, Eurasia review March 4th 2015, http://www.eurasiareview.com/04032015-pakistan-diamer-bhasha-dam-stuck-in-funding-trap-analysis [Accessed on 08/09/18].

[39] The Confused Hydel Energy of Pakistan, http://www.pakistaneconomist.com/2018/02/19/confused-hydel-energy-potential-pakistan/ , [Accessed on 08/11/18]

[40] Shah RukhShakeel ,JosuTakala , WaqasShakeel 2016, “Renewable energy sources in power generation in Pakistan, [Accessed on 08/11/18]
[41] Renewables 2013 global status report. REN21 Renewable energy policy network for 21st century; 2013, [Accessed on 08/11/18]
[42] Pakistan energy year book. Hydrocarbons, Development Institute of Pakistan. Ministry of Petroleum and Natural Resources, Government of Pakistan; [Accessed on 08/11/18]
[43] https://www.nepra.org.pk/Policies/Hydel%20Potential%20in%20Pakistan.pdf,[Accessed on 08/11/18]
[44] Integrated energy plan 2009-22.Economic Advisory Council. Government of Pakistan; 2009, [Accessed on 08/11/18]
[45] https://www.hydropower.org/country-profiles/pakistan, [Accessed on 08/11/18]
[46] Water and power development authority, http://www.wapda.gov.pk/, [Accessed on 10/12/18]
[47] Pakistan’s Hydroelectric Power Development, https://www.southasiainvestor.com/2009/04/pakistans-hydroelectric-power.html [Accessed on 05/11/18]
[48] Small Hydro Power Plant, http://www.pres.org.pk/thematic-areas/hydro-energy/[Accessed on 08/11/18]
[49] Cochran J., Miller M., Milligan M., Ela E., Arent D., Bloom A., et. al., 2013. Market evolution: Wholesale electricity market design for 21st century power systems, Technical report for NREL, Colorado, [Accessed on 08/12/18]
[50] T. Salem, E. Kinab 2015,Analysis of building-integrated photovoltaic systems: a case study of commercial buildings under Mediterranean Climate, ProcediaEng, [Accessed on 08/12/18]
[51] S. Ahmed, A. Mahmood, A. Hasan, G.A.S.Sidhu, M.F.U. ButtA 2016, comparative review of China, India and Pakistan renewable energy sectors and sharing opportunities,Renew. Sustain. Energy [Accessed on 08/12/18]
[52] G. Akhmat, K. Zaman 2013, Nuclear energy consumption, commercial energy consumption and economic growth in South Asia: bootstrap panel causality test, Renew. Sustain. Energy , [Accessed on 08/12/18]
[53] K.N. Shukla, K. Sudhakar, S. Rangnekar A 2015, comparative study of exergetic performance of amorphous and polycrystalline solar PV modules,Int. J. Exergy [Accessed on 08/12/18]
[54] S. Liu, X. Meng, C. Tam 2015, Building information modelling based building design optimization for sustainability, Energy Build, [Accessed on 08/12/18]
[55] Pakistan Council of Renewable technology, http://www.pcret.gov.pk/index.html ,[Accessed on 08/30/18]
[56] Pakistan Council of Renewable Technology, http://www.pcret.gov.pk/News.html ,[Accessed on 08/30/18]
[57] World Population Review, http://worldpopulationreview.com/countries/pakistan-population/, [Accessed on 08/11/18]
[58] Sustainable energy for all and Ministry of Finance - Implementation and Economic Reforms Unit (IERU), ‘Pakistan: Rapid Assessment and Gap Analysis’, 2014, 15, http://www.se4all.org/sites/default/files/Pakistan_RAGA_EN_Released.pdf[Accessed on 09/0418]

Chapter 5:
Water Pollution Control

Effect of *Iris pseudacorus* L. on polysaccharide composition and microcystins content of *Microcystis aeruginosa*

G Y Chen[1], Q S Li[1] and M L Zhu[1]

1 College of Environment Science and Engineering, Xiamen University of Technology, Ligong Road 600, Xiamen 361024, China
E-mail: cgy1117@sina.cn

Abstract. The present study aimed to explore the feedback mechanism of *M. aeruginosa* under the stress of *I. pseudacorus* L.. by determining the polysaccharide composition and microcystins (MCs) synthesis and release of *M. aeruginosa* through co-cultivation of *I. pseudacorus* L. and *M. aeruginosa*. The results of our investigation and observation have shown that, under the stress of 20 or 40 g/L of *I. pseudacorus* L., the contents of intracellular and extracellular MC-LR, and the intracellular polysaccharide (IPS), the bound extracellular polysaccharide (bEPS) of *M. aeruginosa* increased at first and then began to decrease gradually afterwards. And the maximum contents were (71.03±10.20) fg/cell, (0.66±0.07) fg/cell, (1.84±0.10) pg/cell, (1.11±0.11) pg/cell and (70.33±8.62) fg/cell, (0.64±0.10) fg/cell, (1.74±0.17) pg/cell, (0.90±0.12) pg/cell. *I. pseudacorus* L. had an adsorption-enrichment effect on MCs.The content of MC-LR in the roots were (8.37±1.58) ng/g and (4.33±1.31) ng/g when *I. pseudacorus* L. was 20 or 40 g/L, respectively.

1. Introduction

In eutrophic water bodies, cyanobacteria "bloom" frequently occur, among which *Microcystis aeruginosa* is the most common dominant population. In the process of growth, *M. aeruginosa* synthesize and secrete two important defensive substances, microcystis (MCs) and polysaccharides (PS), which help them adapt to various unfavorable environments, thus making them dominant in cyanobacteria [1]. At present, more than 90 MCs isoforms have been identified [2]. The synthesis and release of MCs in the cells of *M. aeruginosa* has important biological significance. For example, MCs can not only participate in gene regulation and signal transmission in *M. aeruginosa* cells [3, 4], which helps *M. aeruginosa* resist the stress of H_2O_2 [5], but also inhibit other aquatic plants and algae [6, 7]. PS is a large molecular substance produced by *M. aeruginosa* cells. It is divided into extracellular polysaccharides (EPS) and intracellular polysaccharides (IPS) and it can help *M. aeruginosa* cells form protective barriers to resist ultraviolet radiation, drought, and et al. [8]. And, EPS can promote the aggregation of algae cells in groups, thus helping to form their competitive advantage to a certain extent [9]. The existence of MCs also has an impact on the synthesis of PS. Studies have shown that, the presence of MCs of appropriate concentrations can activate some polysaccharide synthesis genes and promote the synthesis of PS in algae cells [10].

At present, the restoration of aquatic plants is an important biological measure to control water eutrophication and cyanobacteria bloom [11]. *Iris pseudacorus* L., an ornamental emerged plant with a clear effect of purification, can allelopathically inhibits algae [12]. Therefore, *I. pseudacorus* L. has a broad application prospects in the prevention and control of water eutrophication. Studies have shown that, under co-cultivation, the photosynthetic system and anti-oxidase system of *M. aeruginosa* would be affected significantly by *I. pseudacorus* L. [12, 13].

In this study, the content and composition changes of the defensive substances MCs and PS of *M. aeruginosa* were studied when *M. aeruginosa* was co-cultivated with *I. pseudacorus* L.. The production and release of MCs and PS and the absorption of MCs by *I. pseudacorus* L. was analyzed to explore the feedback mechanism of *M. aeruginosa* under the stress of *I. pseudacorus* L., and provide theoretical basis for further elucidation of the allelopathic interaction between *I. pseudacorus* L. and *M. aeruginosa*.

2. Materials and methods

2.1. Plants pre-cultivation

I. pseudacorus L. plants with 20 cm long top shoots were purchased from a local flower market (Xiamen, Fujian, China). They were washed with distilled water firstly and then washed with sterile water three times. And then, they were pre-cultivated for 5 days with BG-11 nutritional solution[14]. *M. aeruginosa* (FACHB-905) was obtained from the Freshwater Algae Culture Collection at the Institute of Hydrobiology, Chinese Academy of Sciences, and was cultured with BG-11 nutrient solution for 1 week to expand in MGC-450BPY-2 intelligent light incubator, with the culture conditions were constant temperature and illumination (25±1 ℃, 2000 lx) and light to dark ratio 12 h/12 h.

2.2. Experiment design

The well-grown *I. pseudacorus* L. plants were selected to be implanted in the glass cylinder with 2 L of BG-11 nutrient solution. The final biomass were set to 20 g/L (fresh weight) and 40 g/L (fresh weight). Then, *M. aeruginosa* was inoculated, and the final densities were 1.0×10^7 cells/mL which was set based on the abundance of microcystis in the water of Meiliang Bay and Zhushan Bay in Taihu Lake [15]. At the same time, the group without *I. pseudacorus* L. plants was treated as the control group. There were three replicates for each group. Then, the glass cylinders were put in MGC-450BPY-2 intelligent light incubator for 15 days, and samples were obtained every 3 days. The density of *M. aeruginosa* and the contents of intracellular and extracellular MCs and PS were determined. At the end of the experiment, the contents of MCs in the roots were measured.

2.3. Determination of M. aeruginosa Densities

Algal solution was shaken uniformly. 5 mL of algal solution was obtained and then was fixed using 10 μL formaldehyde. *M. aeruginosa* densities were determined using hemocytometer. Each sample was repeated 3 times.

2.4. Determination of PS contents

Algal solution was shaken uniformly and then 10 mL of algal solution was obtained. The algal precipitate was obtained by centrifugation at 10, 000 × g for 20 min at 4 ℃. 10 mL deionized water was added to the algal precipitate and the pH value was modulated to 10 using NaOH solution. The mixture was shaken during a 5-hours water bath at 45℃. The supernatant was obtained for the assay of the bound extracellular polysaccharide (bEPS) by centrifugation at 10, 000 × g for 20 min at 4 ℃. The concentration of bEPS was determined by sulfuric acid-anthrone method. The average bEPS content in each algae was calculated according to the algae densities. 0.5 mg / L NaOH solution was added to the second algae precipitation. After a boiling water bath for 10 min, trichloroacetic acid was added to precipitate the pigment and protein. The supernatant was obtained for the assay of the intracellular polysaccharide (IPS) by centrifugation at 10, 000 × g for 20 min at 4 ℃ [16].

2.5. Determination of MCs contents

Extraction of extracellular MCs: 15 mL of algal solution was obtained, and subsequently centrifuged at 10000 g for 20 min. The MC-LR in the supernatant was loaded onto solid-phase extraction cartridges (Poly-sery HLB, 6 mL/500 mg, CNW), and then was eluted with methanol.

Extraction of intracellular MCs: The algal residue, repeatedly being frozen and thawed, was shaken for 3 h in a thermostatic oscillator after adding 10 mL 75% methanol and subsequently centrifuged at 10000 g for 20 min. The supernatant was collected into the 500 mL glass beaker. The residue was extracted 3 times. The total supernatant was diluted to 250 mL by adding deionized water. The MC-LR in the supernatant was loaded onto solid-phase extraction cartridges (Poly-sery HLB, 6 mL/500 mg, CNW), and then was eluted with methanol.
Extraction of MCs from plant roots: The root was cleaned with deionized water 3 times. 1.0 g root was ground in a chilled mortar in 4 mL of 75% methanol, and subsequently treated by ultrasonic fragmentation. The mixture was shaken for 3 h in a thermostatic oscillator after adding 6 mL 75% methanol and subsequently centrifuged at 10000 g for 20 min. The supernatant was collected into the 500 mL glass beaker. The residue was extracted 3 times. The total supernatant was diluted to 250 mL by adding deionized water. The MC-LR in the supernatant was loaded onto solid-phase extraction cartridges (Poly-sery HLB, 6 mL/500 mg, CNW), and then was eluted with methanol.
Determination of MCs: The MC-LR was analyzed using enzyme linked immunoassay kit (detection limit 20 ng/L) (ShangHai HengYuan Biological Technology Co., Ltd, China), on a SpectraMax M2 multimode plate readers (Molecular Devices, USA).
All the data were analyzed with SPSS 15.0 for Windows (SPSS Inc., Chicago, USA) and described as mean $\pm$ SD. The illustrations were performed with SigmaPlot 10.0 (Systat Sofware, Inc., California, USA).

3. Results and discussion

3.1. Effect of I. pseudacorus L. on IPS and bEPS contents of M. aeruginosa

As shown in Fig. 1, The IPS and bEPS contents of M. aeruginosa co-cultivated with 20 g/L I. pseudacorus L. showed a trend of first rising and then declining, with a maximum of (1.84 $\pm$ 0.10) pg/cell and(1.11 $\pm$ 0.11) pg/cell, which were 1.12 and 1.98 times more than them of the control group during the same period. The contents of IPS and bEPS of M. aeruginosa co-cultivated with 40 g/L I. pseudacorus L. also showed a tendency to rise first and then decline, with the maximum values of (1.74 $\pm$ 0.17) pg/cell and (0.90 $\pm$ 0.12) pg/cell, respectively, which were 1.34 and 1.61 times more than them of the control group for the same period.

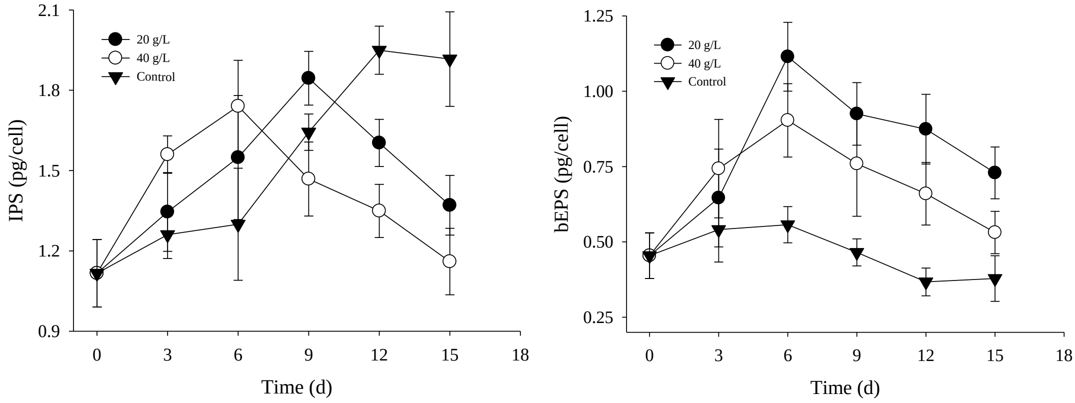

Figure 1 IPS and bEPS contents of *M. aeruginosa* co-cultivated with different *I. pseudacorus* L. biomass

The results showed that, the contents of IPS in M. aeruginosa cells co-cultivated with 20 g/L or 40 g/L of I. pseudacorus L. were 1.19 and 1.34 times more than them of the control group on day 6, which indicated that the production of PS in M. aeruginosa cells co-cultivated with I. pseudacorus L. was promoted significantly sin the early stages of cultivation. Some previous studies have proved that, the photosynthetic activity and some enzymes activities in M. aeruginosa cells co-cultivated with I. pseudacorus L. were also promoted in the early stages of cultivation [12, 13]. Therefore, it can be believed that, in the early stages of cultivation, the allelopathy effect of I. pseudacorus L. on M.

aeruginosa stimulated the defense system in M. aeruginosa cells, and the ability of PS synthesis in M. aeruginosa cells increased significantly. However, the contents of IPS in M. aeruginosa cells co-cultivated with 40 g/L of I. pseudacorus L. were reduced by 39.6% compared with the control group on day 15, which indicated that, with the extension of the cultivation time, I. pseudacorus L. showed allelopathy stress on M. aeruginosa and the production of PS in M. aeruginosa cells was inhibited significantly.

bEPS plays a very important role in the formation of M. aeruginosa colonies [17]. In our experiment, the contents of bEPS in M. aeruginosa cells co-cultivated with 20 g/L or 40 g/L of I. pseudacorus L. were 1.98 and 1.61 times more than them of the control group on day 6, indicating that in the early stages of cultivation, bEPS contents increased significantly. Some previous studies have shown that, the photoelectron transmission rates and photosynthesis efficiency in the colonial M. aeruginosa cells were higher than them in the unicellular cells [18]. Therefore, in the early stages of cultivation, the bEPS contents increased owing to the mass synthesis and secretion of PS in M. aeruginosa cells, which would promote the formation of M. aeruginosa colonies, thus maintaining a higher growth rate to adapt to the allelopathy effect of I. pseudacorus L.. However, with the extension of the cultivation time, I. pseudacorus L. showed allelopathy stress on M. aeruginosa cells. The content of bEPS was significantly reduced, which was not conducive to the formation of M. aeruginosa colonies, thus resulting in a decrease in the ability of M. aeruginosa to resist I. pseudacorus L. stress. Previous studies have showed that, the oxidation damage of M. aeruginosa cells co-cultivated with I. pseudacorus L. was serious [12], chlorophyll decomposition and photosynthetic activity has also dropped sharply [13].

3.2. Effect of I. pseudacorus L. on the synthesis and release of MCs from M. aeruginosa

As shown in Fig. 2, the contents of intracellular and extracellular MC-LR in M. aeruginosa cells co-cultivated with 20 g/L of I. pseudacorus L. showed a trend of first rising and then declining, with a maximum values of (71.03±10.20) fg/cell and (0.66±0.07) fg/cell, which were 2.39 and 1.99 times more than them of the control group during the same period. The contents of intracellular and extracellular MC-LR in M. aeruginosa cells co-cultivated with 40 g/L of I. pseudacorus L. also showed a trend of first rising and then declining, with a maximum values of (70.33±8.62) fg/cell and (0.64±0.10) fg/cell, which were 2.09 and 2.34 times more than them of the control group during the same period (Fig. 2). The results indicated that, M. aeruginosa cells could synthesize more MCs in the early stage of cultivation in order to adapt to the allelopathy impact of I. pseudacorus L.. Previous studies have also showed that, Lemna japonica could significantly increase the contents of intracellular and extracellular MCs in M. aeruginosa cells [19]. MCs play an important role in the resistance of M. aeruginosa to adverse environment and the acquisition of competitive advantage [1]. Therefore, under the allelopathy stress of I. pseudacorus L., M. aeruginosa cells responded to this environmental change by synthesizing and releasing more MCs. The higher the plant contents were, the more significant the excitating effect was.

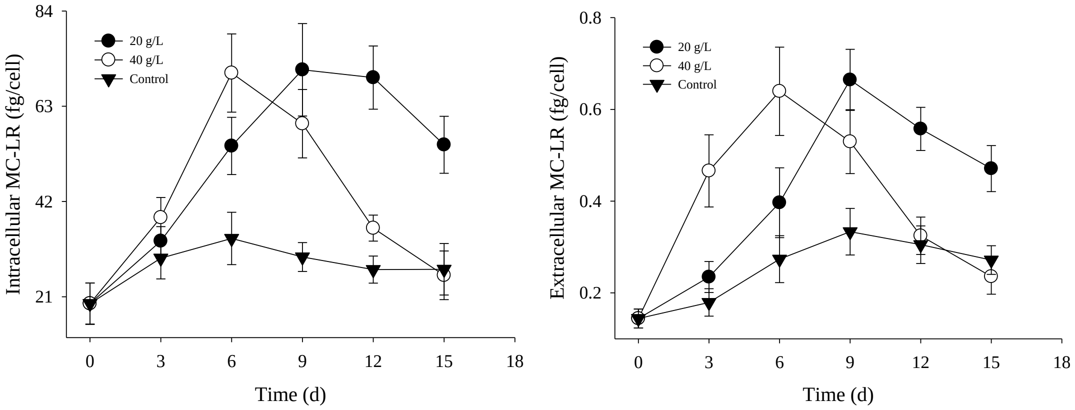

Figure 2 Intracellular and extracellular MC-LR contents of *M. aeruginosa* co-cultivated with different *I. pseudacorus* L. biomass

The study also showed that, the change trend of MC-LR contents was consistent with that of PS contents in M. aeruginosa cells at the early stage of cultivation. For example, the contents of IPS, bEPS and intracellular MC-LR in M. aeruginosa cells co-cultivated with 40 g/L of I. pseudacorus L. reached the maximum values on the day 6, which was owing to the presence of appropriate concentrations of MCs activating some polysaccharide synthesis genes and promoting the synthesis of PS[10]. However, the contents of MC-LR decreased gradually with the extension of cultivation time, which was owing to that, under the continuously allelopathy stress of I. pseudacorus L., various physicochemical properties and photosynthetic system of M. aeruginosa were severely affected [12, 13], thus inhibiting the synthesis of MCs. In addition, when the allelopathy stress is intensified, the dead M. aeruginosa cells increased [12], and the intracellular MCs will be released in large quantities [20], resulting in a sharp decrease in the content of intracellular MCs.

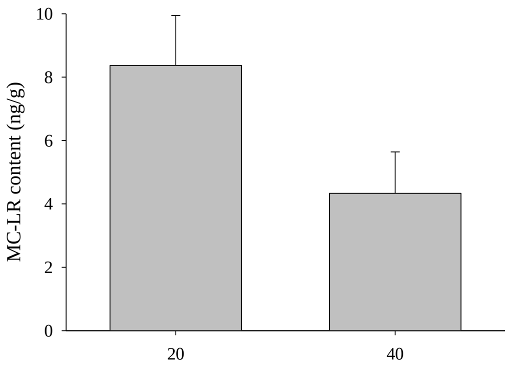

Figure 3 MC-LR contents in the roots of *I. pseudacorus* L. co-cultivated with *M. aeruginosa*

The changes in the content of extracellular MCs depend on a variety of factors, including the release of intracellular MCs, adsorption of plants, and natural degradation. The physicochemical properties of MCs are relatively stable. The cultivation conditions are consistent throughout the cultivation process, and the cultivation time was short. Therefore, the reduction in MCs owing to natural degradation is basically negligible. The release of large amount of intracellular will cause a sharp increase in the content of extracellular MCs [21], which was not consistent with our research that the extracellular MC-LR content decreased gradually. The extracellular MC-LR contents of M. aeruginosa cells co-cultivated with 20 or 40 g/L of I. pseudacorus L. were only (0.47 $\pm$ 0.05) fg/cell and(0.24 $\pm$ 0.04) fg/cell on day 15, respectively. Therefore, the adsorption by I. pseudacorus L. was an important reason for the significant reduction of extracellular MC-LR content. Our results showed that, at the end of the experiment, the MC-LR contents were (8.37 $\pm$ 1.58) ng/g and (4.33$\pm$1.31) ng/g in the roots of 20 and 40 g/L of I. pseudacorus L. respectively (Fig .3). Studies have shown that, many aquatic plants could absorpt MCs. For example, Vallisneria natans seedlings could absorb MC-RR and concentrated the MC-RR in the roots [22]. The average concentration of MCs in Eichhornia crassipes was (5. 95 $\pm$ 0.76) ng/g[23], and the amount of MCs accumulated in Lemna gibba can reach 2. 24 μg/g [24].
The effects of plants on the content of extracellular MCs in M. aeruginosa cells vary with the change in the plant contents. The content of extracellular MC-LR of M. aeruginosa cells co-cultivated with 20 g/L of I. pseudacorus L. still maintained a high concentration on the day 15, which was 1.74 times more than that of the control group during the same period. However, the content of extracellular MC-LR of M. aeruginosa cells co-cultivated with 40 g/L of I. pseudacorus L. maintained a low concentration on the day 15, which was 86.8% of that in the control group during the same period. That was because that, the higher the content of plant was, the stronger the allelopathic stress was at the later stage of the cultivation, thus reducing the synthesis of MCs. Although the death of algae cells and the increase in cell membrane permeability would lead to an increase in the release of MCs, the total MC-LR absorbed by plant would also increase, thus leading to a large decrease in the concentration of extracellular MCs.

4. Conclusions

In the early stages of cultivation, *M. aeruginosa* adapted to the allelopathy of *I. pseudacorus* L. through two strategies. Firstly, *M. aeruginosa* cells synthesized and secreted a large amount of PS, leading to an increase in the content of bEPS, which would promote the formation of *M. aeruginosa* colonies. Secondly, *M. aeruginosa* cells produced and released plenty of MCs to respond to this environmental change. The higher the plant contents were, the more significant the excitating effect was. However, with the extension of the cultivation time, *I. pseudacorus* L. showed allelopathic stress on *M. aeruginosa* cells, thus inhibiting the synthesis of PS and MCs. The content of bEPS was significantly reduced, which was not conducive to the formation of *M. aeruginosa* colonies, thus resulting in a decrease in the ability of *M. aeruginosa* to resist *I. pseudacorus* L. stress. And, the adsorption by *I. pseudacorus* L. was one of the main reasons for the significant reduction of the extracellular MC-LR content.

5. References

[1] Yan H, Zhang SJ, Li C, Liu L and Zhang TT 2014 *J. Hyg. Res.* **43** 290 (in Chinese)
[2] Pantelić D, Svirčev Z, Simeunović J, Vidović M and Trajković I 2013 *Chemosphere* **91** 421
[3] Dittmann E, Erhard M, Kaebernick M, Scheler C, Neilan BA, von Döhren H and Börner T 2001 *Microbiology* **147** 3113
[4] Zilliges Y, Kehr JC, Mikkat S, Bouchier C, Marsac NT de, Boerner T and Dittmann E. 2008 *J. Bacteriol.* **190** 2871
[5] Ding Y, Gan NQ, Zheng LL and Song LR 2013 *Acta Hydrobiol. Sinica* **37** 515 (in Chinese)
[6] Máthé C, Beyer D and Erdődi F 2009 *Aquat. Toxicol.* **92** 122
[7] Hu ZQ, Liu YD, Li DH and Dauta A 2005 *Hydrobiologia* **534** 23
[8] Ren XX, Jiang H, Leng X and An SQ 2013 *Chin. J. Ecol.* **32** 762 (in Chinese)
[9] Zhang YQ, Yang GJ, Qin BQ, Zhou J, Xu HP, Wang Y and Wu YL 2014 *J. Lake Sci.* **26** 559 (in Chinese)
[10] Gan NQ, Xiao Y, Zhu L, Wu ZX, Liu J, Hu CL and Song LR 2012 *Environ. Microbiol.* **14** 730
[11] Yuan SF, Wang WD, Dong HY, Qaing ZM, Li S, Wang ZQ, Yang JZ and Yin CQ 2013 *Acta Scien. Circum.* **33** 1475 (in Chinese)
[12] Chen GY and Tang K 2014 *Chin. J. Environ. Eng.* **8** 465 (in Chinese)
[13] Chen GY, Li QS, Xie PY and Chen YH 2015 *Chin. J. Environ. Eng.* **9** 4145 (in Chinese)
[14] Stanier RY, Kunisawa R and Mandel M 1971 *Bacteriol. Rev.* **35** 171
[15] Li DM, Kong FX, Yu Y, Zhang M and Shi XL 2011 *Acta Scien. Circum.* **31** 292 (in Chinese)
[16] Yang Z, Kong FX, Shi XL, Zhang M, Xing P and Cao H 2008 *J. Phycol.* **44** 716
[17] Dai XX, Zhu W and Li M 2013 *J. Lake Sci.* **25** 277 (in Chinese)
[18] Wu ZX and Song LR 2008 *Phycologia* **47** 98
[19] Jang MH, Ha K and Takamura N 2007 *Toxicon* **49** 727
[20] Daly RI, Ho L and Brookes JD 2007. *Environ. Sci. Technol.* **41** 4447
[21] Fang L, Liu WQ, Zhao NJ, Duan JB, Wang ZG, Xiao X, Zhang YJ, Liu J, Yin GF and Shi CY 2013 *J. Saf. Environ.* **13** 6 (in Chinese)
[22] Yin LY, Huang JQ, Li DH and Liu YD 2005 *Environ. Toxicol.* **20** 308
[23] Zhou Q, Han SQ, Song W and Liu GF 2014 *Environ. Sci.* **35** 597 (in Chinese)
[24] Saqrane S, Ei ghazali I, Ouahid Y, Ei Hassni M, Ei Hadrami I, Bouarab L, del Campo FF, Oudra B and Vasconcelos V 2007 *Aquat. Toxicol.* **83** 284

Acknowledgments

This work was financially supported by the Natural Science Foundation of Fujian Province of China (2017J01491) and the Technology Project of Xiamen Municipal Construction Bureau (XJK2018-1-2).

IOP Conf. Series: Earth and Environmental Science **369** (2019) 012011 doi:10.1088/1755-1315/369/1/012011

Degradation of Diclofenac Sodium in Microbial fuel cells

Y C Wu[1], H Y Fu[1], H Wen[1], F D Chen[1], Z N Dai[1] and A L Yang[1]

1 College of Environmental Science and Engineering, Xiamen University of Technology, Xiamen 361024, China
E-mail: ycwu@xmut.edu.cn

Abstract. Diclofenac sodium is an extensively consumed non-steroidal anti-inflammatory drug for certain non-rheumatic diseases and frequently detected at surface water. This work we studied the degradation process of diclofenac sodium in an anodic chambers of microbial fuel cells. It was found that biodegradation of diclofenac sodium could be achieved in the microbial fuel cells, and the removal rate of diclofenac sodium was accelerated after bioelectrochemical activity microorganism acclimation. The highest removal rate can reach up to 30.73% after 2 weeks of operation. The results also showed that weak acid (pH=5.5) condition favour the degradation of diclofenac sodium, while low temperature condition inhibited its degradation. This work provided a new way to remove diclofenac sodium from wastewater.

1. Introduction

Owing to the wide application of non-steroidal anti-inflammatory drugs (NSAIDs), large amounts of NSAIDs were discharged to the environment. NSAIDs are the groups of emerging contaminants of extreme environmental concern [1, 2]. Diclofenac Sodium is one such synthetic NSAIDs, mostly used in medical care as an analgesic, antiarthritic and antirheumatic [3]. Global usage of diclofenac sodium exceeds 900 tons per year, and about 15% of diclofenac sodium is excreted as unchanged after human consumption [4]. Extensive usage and stable chemical structure make diclofenac sodium a recalcitrant stable environmental pollutant. Diclofenac sodium is always detected at surface water and also in drinking water, which causes a great threat to the environment and human health [5].

Removal of diclofenac sodium has always been an important aspect of research due to the increasing awareness about the environment. Bagal and Gogate [6] have reported degradation of diclofenac sodium using combined processes based on heterogeneous photocatalysis and hydrodynamic cavitation. Sutarn and Rathod [4] have assisted enzymatic degradation of diclofenac sodium using ultrasound. Recently, advanced oxidation processes used to degrade of diclofenac sodium have widely reported [7-10]. However, high operational costs and slower removal kinetics along with hazardous by-products hinder the application of these techniques.

Microbial fuel cells (MFCs) provide new ways for electricity generation and pollutant degradation through metabolism of electrochemically active microorganisms [11]. Our previous study revealed that high degradation of sulfamethoxazole is achievable using MFCs [12]. In the present study, we explore the possibilities and effect factors of diclofenac sodium degraded by MFCs.

2. Methods and materials

2.1 Chemicals

Diclofenac sodiumwas purchased from Aladdin Industrial Corporation. Methanol and formic acid (HPLC grade) were purchased from Fisher.

2.2 Microbial inoculum and reactor operation

Two-chamber glass MFC reactors were used in this study. The working volumes of anodic and cathodic chambers are all 100 mL. The anode and cathode are all made of graphite felt (6 cm length × 6 cm width × 1.0 cm thickness, Haoshi Carbon Fiber Co., Ltd., China) connected with titanium wire. Anodic and cathodic chambers were separated by a cation exchange membrane (10.0 cm^2, Zhejiang Qianqiu Group Co., Ltd., China). The Anodic chamber was inoculated with anaerobic sludge and potassium ferricyanide (50 mM, pH 7.0) as an electron acceptor filled in the cathodic chamber. The voltages of the reactors were recorded at 5 min intervals by a digital multi-meter.

2.3 Determination of diclofenac sodium

Chromatography was performed with an HPLC (LC-20A, Shimadzu, Japan) system at a flow rate of 220 μL min^{-1} on a C18 column (4.6×250 mm, 5 μm). Methanol and 0.1% formic acid solution were used as the mobile phase.

3. Results and discussion

3.1 Reactor start up and operation

Microbes in the biofilm attached to anode play a key role in contaminants biodegradation and electricity of MFCs. Figure 1 shows one output voltage cycle of the MFCs fed with NaAc (control) and diclofenac sodium with an external resistance of 1000 Ω. As shown in Figure 1, after two months of operation, the output voltages of the reactors fed with NaAc and diclofenac sodium was in a steady state. BESs are fueled by sodium acetate and diclofenac sodium, and output voltage increases with the addition of fuel and decreases with fuel consumption. A stable output voltage of MFCs with sodium acetate as the substrate reached 0.57 V, while the diclofenac sodium fuelled MFCs platform voltage is just about 0.30 V, which may be related to the microorganisms growth in the biofilm attached to the anode which prefer to use sodium acetate as a substrate for electricity generation.

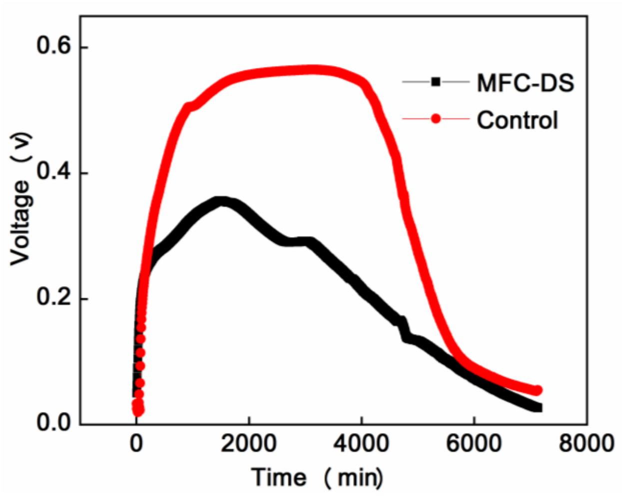

Figure 1. Voltage output of MFC with sodium acetate (control) and diclofenac sodium (MFC-DS) as substrate.

3.2 Standard curve drawing

Different concentrations of diclofenac sodium were determined by HPLC. Taking the peak area as the abscissa and the diclofenac sodium concentration as the ordinate to draw the standard curve (Figure 2). The relationship between diclofenac sodium concentration (C, mg/L) and peak area（x）is shown as

C = 0.00004x - 0.1396, and R^2 is 0.99997, indicating that the peak area has a good linear relationship with diclofenac sodium concentration.

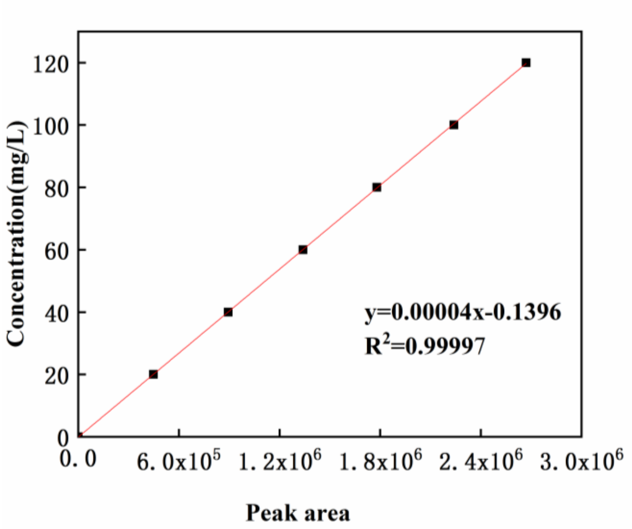

Figure 2. Standard curve of diclofenac sodium concentration

3.3 Effect of initial concentration on diclofenac sodium degradation

The initial diclofenac sodium affects the growth of microorganisms on the surface of the anode, which in turn affects the biodegradation of diclofenac sodium by MFCs. The removal rate of diclofenac sodium at different initial concentrations is shown in Figure 3. The concentration of diclofenac sodium in anode chamber gradually decreases with the treatment time. After two weeks of treatment, the removal rates were 15.33% and 9.16% for the initial concentrations of 50 mg/L and 60 mg/L, respectively. While the removal rate was only 4.96% for initial concentrations of 70 mg/L. High concentrations of diclofenac sodium with a lower removal rate may be due to the high concentration of diclofenac sodium which inhibits the growth and metabolism of microorganisms in the anode biofilm.

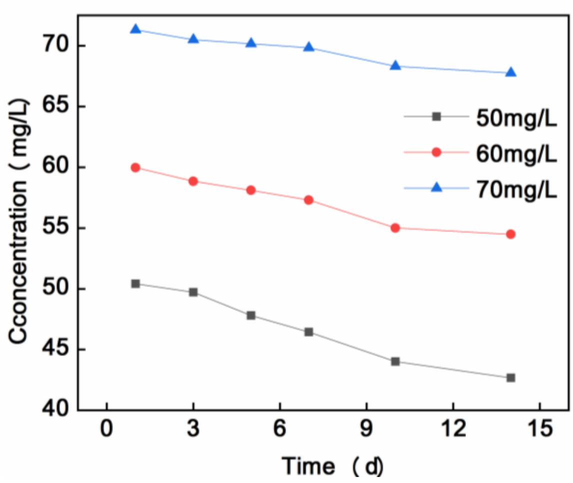

Figure 3. Effect of initial concentration on diclofenac sodium degradation.

3.4 Effect of pH on diclofenac sodium degradation

pH is an important factor affecting the growth of microorganisms. To investigate the effect of pH on diclofenac sodium degradation, the pH of the anolyte in MFCs was adjusted to 5.5, 7.0 and 8.5. As shown in Figure 4, the degradation rate of acid in diclofenac sodium gradually decreased with the increase of pH. After 14 days of treatment, in the case where the anode solution is weakly acidic (pH=5.5), the concentration of diclofenac sodium is reduced from 59.68 mg/L to 41.43 mg/L, and the removal rate is up to 30.73%; however, the removal rate is only 7.16% under neutral condition (pH=7.0), the removal rate dropped to 3.28% under weak alkaline conditions.

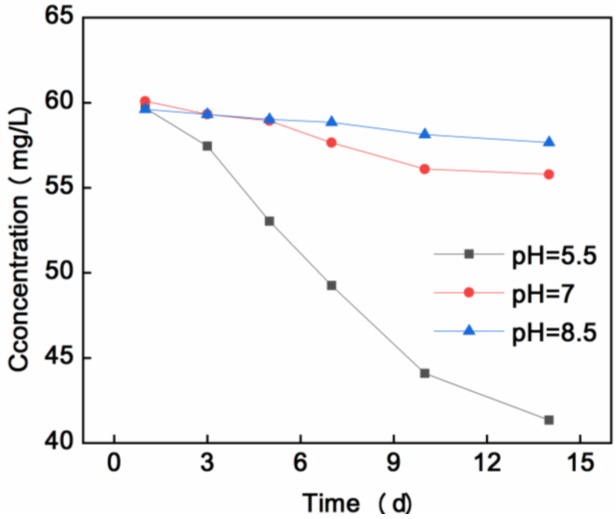

Figure 4. Effect of pH on diclofenac sodium degradation

3.5 Effect of temperature on diclofenac sodium degradation

Temperature is another important factor affecting microbial growth. We have studied the degradation efficiency of diclofenac sodium in MFCs at normal temperature (28℃) and low temperature (4℃). As shown in Figure 4, after 14 days of treatment, the concentration of diclofenac sodium is reduced from 59.98 to 54.48 mg/L at normal temperature, while there is almost no degradation of diclofenac sodium in the anode chamber when MFCs are operating at low temperatures.

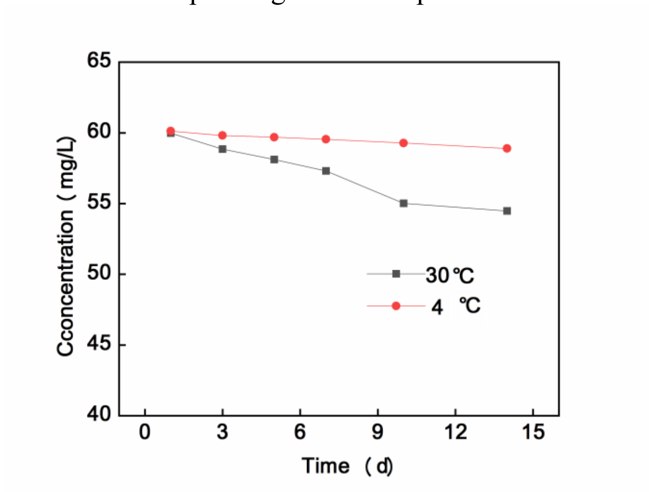

Figure 5. Effect of temperature on diclofenac sodium degradation

4. Conclusions

This study investigated the possibility of utilizing MFCs to degrade diclofenac sodium. It was found that the ability of MFCs to degrade diclofenac sodium was accelerated in the conditions of weak acid, high initial concentration and low treatment temperature decrease removal rate of diclofenac sodium. This study offers a feasible low cost and energy recovery choice for the elimination of diclofenac sodium in wastewater.

5. References

[1] Kummerer K, Alexy R, Huttig J and Scholl A. Standardized tests fail to assess the effects of antibiotics on environmental bacteria, 2004 *Water Res* **38** 2111-2116.
[2] Hirsch R, Ternes T, Haberer K and Kratz KL. Occurrence of antibiotics in the aquatic environment, 1999 *Sci Total Environ* **225** 109-118.
[3] Zhang N, Liu G, Liu H, Wang Y, He Z and Wang G. Diclofenac photodegradation under simulated sunlight: effect of different forms of nitrogen and kinetics, 2011 *J Hazard Mater* **192** 411–418.
[4] Sutar RS and Rathod VK. Ultrasound assisted enzymatic degradation of Diclofenac Sodium: Optimization of Process Parameters and Kinetics6, 2016 Journal of *Water Process Engineering* **9** 1-6.
[5] Andreozzi R, Rafaele M and Paxeus N. Pharmaceuticals in STP effluents and their solar photo degradation in aquatic environment, 2003 *Chemosphere* **50** 1319-1330.
[6] Bagal MV and Gogate PR. Degradation of diclofenac sodium using combined processes based on hydrodynamic cavitation and heterogeneous photo catalysis, 2014 *Ultrason Sonochem* **21** 1035-1043.
[7] Vogna D, Marotta R, Napolitano A, Andreozzi R and Ischia M. Advanced oxidation of the pharmaceutical drug diclofenac with UV/H2O2 and ozone, 2004 *Water Res* **38** 414-422.
[8] Ravina M, Campanella L and Kiwi J. Accelerated mineralization of the drug diclofenac via Fenton reactions in a concentric photo-reactor, 2002 *Water Res* **36** 3553–3560.
[9] Perez-Estrada LA, Malato S, Gernjak W, Aguera A, Thurman M, Ferrer I and Fernandez-Alba AR. Photo-Fenton degradation of diclofenac: identification of main intermediates and degradation pathway, 2005 *Environ Sci Technol* **39** 8300-8306.
[10] Naddeo V, Belgiorno V, Kassinos D, Mantzavinos D and Meric S. Ultrasonic degradation, mineralisation and detoxification of diclofenac in water: optimisation of operating parameters, 2010 *Ultrason Sonochem* **17** 179-185.
[11] Liu H, Ramnarayanan R and Logan BE. Production of electricity during wastewater treatment using a single chamber microbial fuel cell, 2004 *Environ Sci Technol* **38** 2281-2285.
[12] Wang L, Wu Y, Zheng Y, Liu L and Zhao F. Efficient degradation of sulfamethoxazole and the response of microbial communities in microbial fuel cells. 2015 *RSC Adv*, **5** 56430-56437.

Acknowledgements
This work was supported by Xiamen Science and Technology Plan Guidance Project (3502Z20179029) and Scientific Climbing Plan of Xiamen University of Technology (XPDKQ18032).

Author Index